Offshore Crew and Cargo Transfer Limits:

Efficient Utilization of Safe Time

by Mitchell Anderson, P.Eng.

A Thesis submitted to the School of Graduate Studies in partial fulfillment of the

requirements for the degree of

Master of Ocean and Naval Architectural Engineering

Faculty of Engineering and Applied Science

Memorial University of Newfoundland

October 2024

St. John's, Newfoundland and Labrador

Abstract

There have recently been significant petroleum discoveries in the Flemish Pass region of offshore Newfoundland, and their development is an active topic of conversation and research. The Flemish Pass region is further offshore than the currently producing oil installations in the province, and it is in a region characterized by higher winds, higher waves, deeper water, pack ice, and reduced visibility. Typical crew transfer operations in the province are conducted with helicopters, but the Flemish Pass poses some unique challenges in terms of visibility and range for the current helicopter fleet. Marine crew transfer with the current FROG-6 capsule H_s limitation of 4.0 m could make operability drop as low as 10% in the winter months based on public-domain environmental data. As such, improved efficiency in marine crew transfer is sorely needed. This thesis poses the question: can the limits for crane-based transfer methods be improved, if the problem is studied in more detail? This thesis has considered the specific ship and the specific environmental conditions, in terms wind speed and wave height, heading, and peak period. A secondary question is: even if the limits for routine crew transfer remain unchanged, is it possible to safely and practically complete crew transfer operations in seastates above the typical limits for emergency situations? A potential flow analysis is conducted on 6 representative OSV hull forms using ShipMo3D. Time domain analyses are conducted to compare anticipated deck velocities with the operating limits of a commonly-used crew transfer capsule, the FROG-6. It is determined that there is significant variation between the wave height that causes a limit exceedance, depending on the size of the ship, its heading relative to the waves, and its loading condition (GM).

Through analysis of the time between limit exceedances, it is discovered that there is significant "safe time" in between limit exceedances, even in extremely rough sea-states. Filtering out the "safe times" with duration less than 10 minutes, there is still significant "useable time" in all the simulations, i.e. there are significant windows of time with benign vessel motions during which crew transfers can be conducted – even in extreme seas. This thesis concludes that: firstly, that operating limits for crew transfer could be reconfigured to account for differences in ship size/loading condition, and wave period/heading. Secondly, that the "safe time" in between limit exceedances could well be utilized for non-routine crew transfer operations, when supported by the appropriate procedures and motion monitoring/prediction systems.

General Summary

Crane-based marine crew transfer refers to the lift of a personnel-carrying capsule between an Offshore Supply Vessel (OSV) and an Offshore Installation. Traditionally, for the FROG-6 personnel capsule, a flat significant wave height limit of 4.0 m has been used as a cut-off point, beyond which crew transfer operations are not completed. This thesis presents a justification to expand these limits on a case-by-case basis, by considering different ship sizes, wave heights, wave periods, and the incoming wave direction in detail. Ship motions are simulated for a range of representative OSVs, and compared against the deck velocity limits for the FROG-6. The results are compared against the specific environmental conditions in the Flemish Pass region, to determine what percentage of time is "operable" based on the specific deck velocity limits of the capsule. The amount of time between extreme motion events is also analyzed, and it is determined that there is significant "safe time" to complete crew transfer operations in between limit exceedances. This finding could be of particular use when combined with new technologies for predicting vessel motions in real-time, to conduct emergency crew transfers in extreme sea-states.

<u>Acknowledgments</u>

Co-Authorship Statement

This thesis is an expansion of the preliminary work presented in the paper *Assessment of Current Offshore Supply Vessel Capabilities for Crew Transfer Operations in the Flemish Pass*, OMAE2018-78014 [11]. Published in the Proceedings of the ASME 2018 37th International Conference on Ocean, Offshore and Arctic Engineering – OMAE 2018.

This content is in Section 2.1, 2.2.1, and 3.3.1.

For the paper, the contributions are as follows:

a) **Design and Identification of the Research Topic:** Dr. David Molyneux

b) **Practical Aspects of the Research:** Mr. Mitchell Anderson

c) **Data Analysis:** Mr. Mitchell Anderson

d) **Manuscript Preparation:** Mr. Mitchell Anderson, with guidance from Dr. David Molyneux

For the thesis, all work was completed by Mr. Mitchell Anderson, with guidance from Dr. David Molyneux

Table of Contents

Table of Figures

List of Nomenclature

Offshore Supply Vessel   OSV

Response Amplitude Operator   RAO

Degrees of Freedom   DOF

Gravity Based Structure   GBS

Transverse Metacentric Height GM_t

Centre of Gravity   C.G.

Significant Wave Height H_s

Peak Spectral Period T_p

Block Coefficient C_b

Ship Heading β

Computational Fluid Dynamics   CFD

1.0   <u>Introduction</u>

1.1   Scope

This thesis presents an argument for improving the environmental limits for crew transfer in offshore NL on a case-by-case basis. This argument is developed through potential flow, zero speed seakeeping analyses for a range of OSV hull forms using ShipMo3D, and subsequent analysis of the peak deck velocities experienced on the working deck, and the "safe time" that exists between those peaks. An independent analysis of the effect of wind speed on operating limits is also presented; at this time, the wind is considered independent of the waves, and interactions/superposition between wind & wave forcing are not considered in detail. Current effects are considered to be negligible and are thus not directly considered. The use of potential flow simulation through ShipMo3D was extremely practical, as the low run times allowed for simulation of many different sea states across a range of hull forms without the need for large CPU clusters or impractical amounts of time.

This being said, the following shortcomings of this paper are noted below, and at some point further study / simulation should be completed to explore their effects:

1. Viscosity, most importantly its impact on OSV roll resistance.

2. Other wave spectra (including multi-directional waves)

3. Lifting from a floating platform, i.e. considering the crane tip and swing velocities directly in the analysis

4. Hydrodynamic interaction forces between OSV and the platform

5. Ship motions caused or exacerbated by onboard machinery such as the OSV crane.

6. Current Forces

7. Superposition of the above effects, rather than treating the wind and wave forcing separately.

1.2 Background and Literature Review

1.2.1 Newfoundland & Labrador Offshore Oil and Gas Industry

The offshore oil and gas industry in the province of Newfoundland and Labrador currently consists of four producing oil platforms (Hibernia, Terra Nova, White Rose, and Hebron) located in the Grand Banks region. This region is approximately 185 NM offshore, and is a very harsh ocean environment, especially so in the winter. High waves, winds, fog, and pack ice present challenges to the operating Offshore Supply Vessel (OSV) fleet. In the summer months the wave heights and wind speeds are more favourable, but there is an increase in fog, resulting in reduced visibility for helicopter operations.

Recently, a promising new oil field was discovered in the Flemish Pass region, North-East of the currently producing platforms. This region is further offshore, at approximately 270 NM [1], is located in much deeper water, and experiences even rougher sea conditions than the Grand Banks. Together, these facts indicate than some analysis must be conducted to verify whether or not the current OSV fleet will be sufficient for operations in the Flemish Pass region. Helicopters are currently used for

2

routine crew transfer operations in the Grand Banks, but the Flemish Pass is beyond the range of existing helicopters with a full complement of passengers, as more fuel must be carried. For the fields that are currently in production, OSVs are often used for personnel transfer when weather prevents flying, or there are too many passengers for helicopters to handle. Transfer between OSV and platform is accomplished using a crane-lifted purpose-built capsule, such as the FROG-6, which has been shown to be safer than other crane-based methods [7], [8].

1.2.2   Marine Crew and Cargo Transfer

As highlighted above, there are concerns about the feasibility of helicopter crew transfer for the Flemish Pass region. In addition to the visibility and range concerns due to the foggy conditions and distance from shore, there is also the perception of risk after the fatal Cougar helicopter crash that shook the local offshore industry in 2009 [16], [17] .

Modern marine crew transfer methods can largely be split into 2 categories:

1. Crane-based methods (E.g. FROG capsules)
2. Walk to work systems

a) Crane Based Methods

Marine crew transfer has been taking place since the start of the offshore oil industry in Gulf of Mexico during the 1950's. Historically methods were very "ad-hoc", and not much investment was made in making them safe or efficient. The main traditional methods for marine crew transfer were "rope swing" and "basket transfer". The "rope

swing" method is exactly as it sounds; the crew member would use a rope to swing between the supply vessel and the platform. This approach has a lot of inherent risk and requires a skilled and daring crewmember to achieve it safely.

Figure 1-1: Rope Swing Crew Transfer [19]

The earliest "basket transfers" were achieved using a collapsible net [14]. With a collapsible net, crane wire tension must be maintained at all times, with personnel in a standing position, holding onto the outside of the net. If the net is laid on deck without crane tension, it will collapse.

Figure 1-2: Collapsible Net Crew Transfer [20]

As an improvement to this method, the rigid basket was developed. In a traditional rigid basket transfer, personnel are still unsecured, and are still required to be standing, but there is less "split-second" thinking required to clear the area as the rigid basket will not collapse. Considerable work has been done to develop the next step in this evolution – the rigid capsule. With this approach, crewmembers are able to sit comfortably and securely inside of a rigid capsule, with shock absorbers to protect the occupants from any unintended impacts. The FROG series of capsules is one example of this technology. The FROG capsule is also buoyant and self-righting, in the unlikely event that the capsule ends up overboard.

Figure 1-3: Rigid Basket Crew Transfer [14]

Figure 1-4: FROG Capsule Crew Transfer [9]

b) Walk to Work Systems

The simplest walk to work system is a "surfer" vessel; in this method, a small vessel docks into a "surfer" receptacle and the crew simply walk onto the platform. This method can only be used safely in benign marine environments, where the motion of the surfer vessel relative to the platform is insignificant.

Figure 1-5: Surfer Vessel Crew Transfer [14]

Walk to work systems, in simplest terms, generally consist of a motion-compensated platform that allows the crewmember to walk between the OSV and the platform. There is quite a variety of these systems, and they vary in terms of complexity. For example,

Uptime and Offshore Solutions have developed heave-compensated gangways. Ampelmann have developed a fully motion-compensated gangway that accounts for relative motions in all 6 degrees of freedom (DOF). The main advantage of these systems is that once they are set up, the actual crew transfer operation is exceedingly simple. As the name suggests, the crew member can quite literally "walk to work". There are however several drawbacks. Motion compensated systems are generally quite expensive and complex mechanically. These systems take up valuable real-estate on the working deck of an OSV, and therefore there is risk of damage to the system when conducting other routine OSV operations. As a more complex system, and one exposed to potential damage, the maintenance costs are certainly greater than for crane-based methods. For a walk to work system, the OSV also has to be close enough to the platform to make the physical connection, which increases the risk of vessel-vessel collisions more than for a crane based transfer. This makes these systems generally more attractive for smaller installations, in more benign environments.

Figure 1-6: Uptime International Motion-Compensated Gangway [18]

Figure 1-7: Ampelmann Motion Compensated-Gangway [14]

As such, walk to work systems are not currently in use in Newfoundland's offshore industry, nor are they very commonly used in other "harsh environment" regions, such as the North Sea, so there is not much of a track record. The walk to work systems have also generally been used for transfer to rigid platforms, while the proposed developments in the Flemish Pass region will certainly be some kind of floating installation due to the water depth.

Crane based methods also have the advantage that they use simple equipment that is already available and require no modification to OSV or offshore platform. Operating wave heights for motion compensated systems are typically the same, or lower than crane-based systems. Considering the points above, the focus of this thesis is on marine crew transfer with a rigid capsule method, as there are less barriers to entry for the local offshore industry.

The "ad-hoc" nature of traditional marine crew transfer methods has created a perception that they are risky activities, and crew transfer by helicopter is the rational, modern choice. To investigate this, DNVGL and Reflex Marine present a comparison of fatality risk for crane based marine crew transfer and transfer by helicopter [7]. They found the individual risk of fatality per transfer for helicopter to be $2.4\text{x}10^{-6}$, with the fatality risk of crane-based transfer significantly lower at $2.2\text{x}10^{-7}$. While more data collection is needed to increase the confidence of these risk assessments, this points towards marine crew transfer being inherently safer than transfer by helicopter. Reflex Marine, also presents a risk assessment [8] showing marine crew transfer is potentially more safe than helicopter

transfer. There are potentially more incidents from marine crew transfer, but they are usually minor, as opposed to helicopter crashes, which more often result in fatalities.

Reflex Marine developed the FROG crew transfer capsule to reduce the risks associated with marine crew transfer even further. Considering most incidents in crew transfer occur due to "human factors" and split-second events that are difficult to avoid entirely (such as pendulum swing due to dynamic motion between OSV and crane, etc.), the idea is to create a capsule that can protect the occupants from impacts. This allows the operator to conduct crew transfer at or above limits where crane operations would typically be shut down – which is especially important in an emergency situation. The FROG capsule is also better than conventional basket transfer as it is an inherently stable and rigid device – the crane operator can pay out extra line to account for vessel motions and sit the capsule on deck. Traditional basket crew transfer was associated with many relatively minor injuries – and could only move 3-4 passengers at a time. With the FROG-9 capsule, large quantities of people can be moved in a short duration, with protection from impact loads from the side and the vessel deck.

Further testing was completed of the FROG-9 capsule on the "CrewZer" class vessel – Seacor Cheetah [9]. It was determined that this system can reduce costs by 30% compared to helicopter transfer, and has also improved safety. 21,000 personnel were transferred in the first year of service with 0 incidents. Seacor Cheetah has a very stable deck due to its twin hull design, and a large open working deck for transfer operations. Purpose-built high-speed passenger vessels work much better for marine crew transfer

than ad-hoc approaches with OSVs. This thesis focusses on marine crew transfer conducted from OSVs; OSVs spend a lot of time on "standby" for the local offshore industry and have to transit back and forth from field to shore for resupply and refuelling, so it makes sense to use them for marine crew transfer as they have a lot of down time. That being said, dedicated personnel transfer vessels will certainly beat OSVs in terms of efficiency and comfort of marine crew transfer and is an option that should be further researched.

In the current geopolitical landscape, it is of increasing importance for the oil and gas industry to be as efficient as possible. There are many valid concerns about sustainability in the energy industry, and as a society we are attempting an unprecedented energy transition, as we look to make up more of our power needs with renewable energy generation. While this is certainly a worthwhile ambition, the energy demand of society grows with each passing year. In addition, countries are aiming to have more energy security, that is, the ability to meet their power demands without needing to import energy from other nations. The current war in Ukraine is a stark reminder of why that is an important strategy. Many countries import Russian oil and gas products, and when sanctions and other restrictions are imposed it makes the flow of petroleum more costly. In this context, it is of the utmost importance for current oil and gas operations to be as efficient as possible.

1.2.3   Crew Transfer Operating Limits

OSVs are a rapidly evolving, technically sophisticated class of ship, used to perform a variety of tasks for the offshore oil and gas industry. While OSVs in the past have generally been quite small (L ~ 70.0 m), the current trend seems to show an increase in OSV size, with some modern OSVs exceeding 90.0 m length [2]. However, the current in-practice limit for cargo and crew transfer to a fixed platform offshore is a significant wave height (H_s) less than 4.0 m [3], [4], regardless of the ship being used.

Previous work by this research group has shown that when using the H_s = 4.0 m flat limit on the Grand Banks and Flemish Pass, the operational fraction (percentage of time that crew transfer operations are possible) during the month of January could drop as low as 10% [1]. This would severely limit personnel transfer operations in the winter to the point that they may well be impracticable.

There is not much previous research on how to determine operating limits for OSV based personnel transfer. Several industry-based studies for standards of practice exist [7],[8],[14], but there has not been much published scientific research on the topic. There are numerous well-established methods for predicting ship motion (e.g. Shipmo3D, Orcaflex, etc.) but very little has been published on methods of predicting limits for crew transfer. As illustrated by the points above, increased efficiency for crane-based crew transfer in harsh environments must be achieved for successful year-round operations in the Flemish Pass region. Motion-compensated offshore crane technology (including active heave compensation and constant tension implementations) is an active area of

study [13], and any improvements in this area will also likely result in increased efficiency of crane-based crew transfer methods over time.

This thesis investigates whether the time available for crane-based crew transfer methods can be improved if the problem is studied in more detail by considering the specific ship and the environment, such as wave spectra and wind speeds, while remaining within the design limits of the Frog-6 capsule for accelerations and velocities. This thesis also investigates the amount of time between exceedance limits for the crew transfer capsule to determine if it is possible to safely and practically complete crew transfer operations in sea states above the nominal limits?

The concept of useable safe time in a conventionally "inoperable" sea-state is backed up by real-world data and emerging technologies. Ref. [10] outlines field test results from a real-time ship motion prediction system through the use of radar for observing the incoming waves. This technology makes use of a simple interface to display to OSV crew a green, orange, or red light – to determine how much safe time is left to perform a crew transfer or other motion-sensitive operation. This system has promising results [10], and is only the beginning of real-time vessel motion prediction systems. It makes use of standard navigation radar, which presents obvious economic advantages since companies do not have to invest in additional hardware. However, it appears that wave observability with radar has increased efficiency with vertical (VV) polarization, as opposed to the horizontal (HH) polarization of standard navigation radar. Prediction of ship performance in actual sea states is a longstanding, constantly evolving area of research. Modelling of

ship performance can now be compared in real-time with the results from on-board

monitoring systems, and the efficacy of these systems is constantly improving [15]. As

these technologies are investigated further and efficiency improves, it seems likely that

crew transfer operations in harsh conditions will become more and more common as time

goes on.

2.0   Methodology - Motion Calculations

The following subsections provide an overview of the methodology used to compare the simulated OSV motion responses against the operating limits of the FROG-6 capsule. The analysis is comprised of 3 separate sections:

- **Section 2.1 – ShipMo3D Analysis:**

Zero-speed seakeeping analyses for a series of hull sizes representative of the range of OSVs currently operating in the Grand Banks region were completed using the potential flow panel code software ShipMo3D. Frequency domain results from these simulations are presented in Section 3.2. Time histories were then developed for a range of seastates, as further discussed in the proceeding sections.

- **Section 2.2.1 – 20 Minute Simulations – Operability Contours**

Through the use of a Matlab script for post-processing, 20 minute time histories were analyzed to determine if velocity limits for the FROG-6 capsule were exceeded during the simulation time. Next, using public domain MetOcean data published by Nalcor Energy [5], case-specific operational fractions for each season can be determined using the newly defined limits. These results and associated discussion are presented in Section 3.3.1.

- **Section 2.2.2 – 8 Hour Simulations – 'Safe Time' Analysis**

The analysis described in Section 2.2.1 is based solely on the peak values of deck velocities that occur at a given location over the 20 minute simulation duration. Further analysis was completed on a selection of conditions that had a limit exceedance in the 20 minute simulation, by simulating 8 hours of time and analyzing the distribution of times between limit exceedances across different ship sizes and sea states. The 'safe time'

results are presented and discussed in Section 3.3.2. It is noted that it is not likely for a seastate to remain static for 8 hours. The 8 hour simulations are considered to be mathematical constructs developed to determine statistics on the percentage of safe time within a collection of stationary 20 minute seastates.

2.1   ShipMo3D Analysis

The analysis was completed on a series of 6 geometrically similar OSV hull forms, which were developed using a "vertical bow" type OSV that was generated as previous work in the larger research project [6] as a basis. Using DELFTship, the initial hull was first scaled along the X-axis to lengths of 70.0, 80.0 and 90.0 m. Next, the hulls were scaled along the Y-axis to maximum breadths typical of each respective length [2]. Finally, the Lackenby Transformation Method was applied to the hulls to achieve two different Block Coefficients (Cb = 0.65 and 0.79). The 6 developed hulls are believed to adequately represent the range of sizes of OSV currently operating in the Grand Banks region. The purpose of selecting 2 series of hull forms was to determine if longer and/or heavier ships resulted in more operable time when compared to shorter and lighter ships. The principal particulars for the developed hulls are shown in Table 2-1 below.

Table 2-1: Principal Particulars of OSV Hulls

Name	Length (m)	Breadth (m)	Draft (m)	C_b	Displacement (MT)
Small Light	70.0	17.0	5.6	0.65	4,207
Small Heavy	70.0	17.0	5.6	0.79	5,273
Medium Light	80.0	19.5	6.4	0.65	6,302
Medium Heavy	80.0	19.5	6.4	0.79	7,900
Large Light	90.0	22.0	7.2	0.65	8,999
Large Heavy	90.0	22.0	7.2	0.79	11,280

Lines plans for the "Medium / Light" and "Medium / Heavy" OSVs are shown in Figure

2-1 and Figure 2-2 below, respectively.
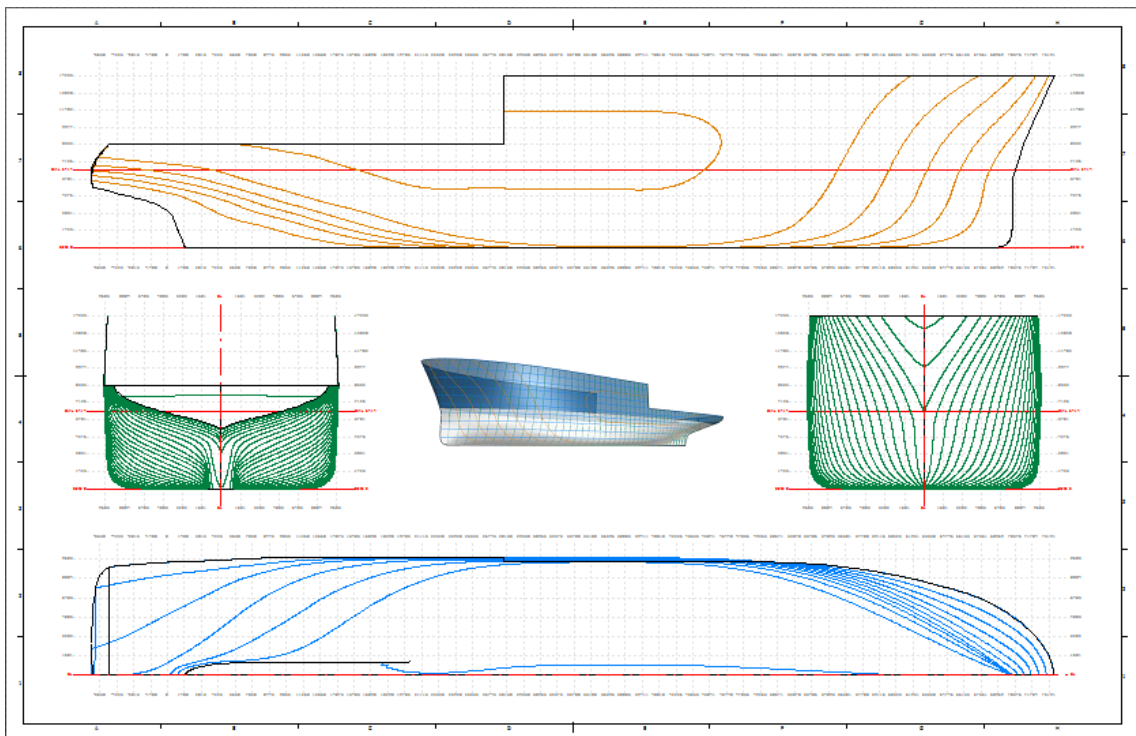
Figure 2-1: Lines Plan for "Medium / Light" Hull Form
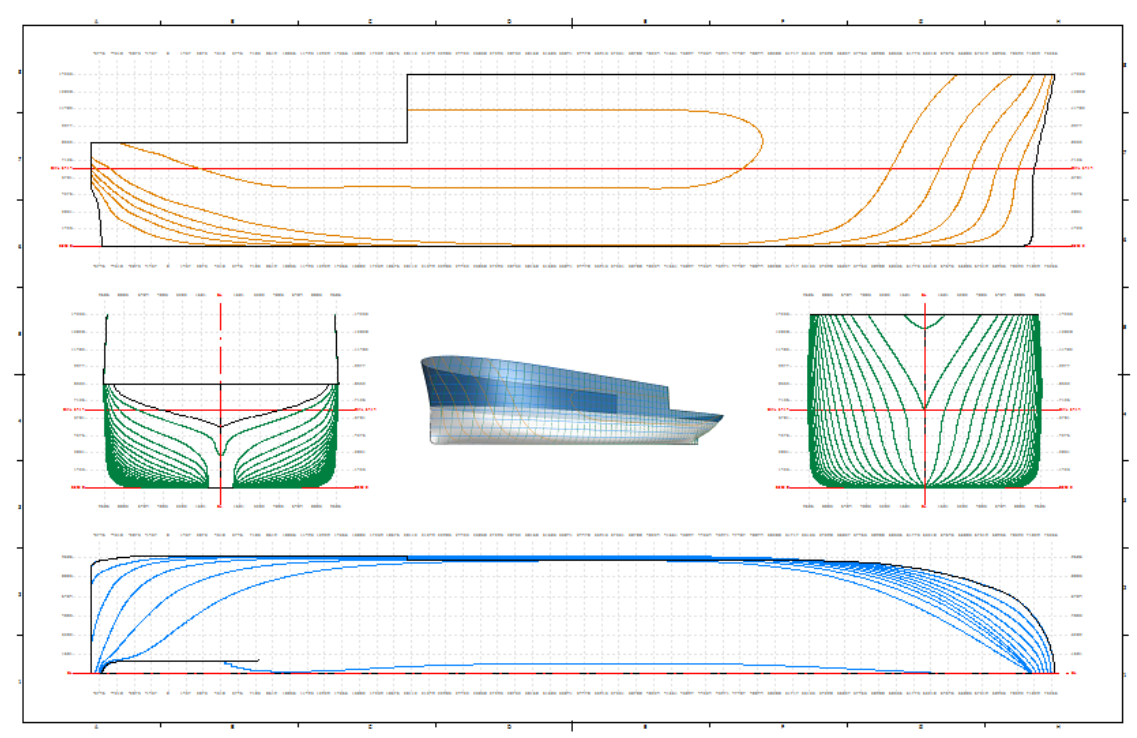
Figure 2-2: Lines Plan for "Medium / Heavy" Hull Form

Once the geometry scaling was complete, the NURBS surfaces were exported from DELFTship to Rhinoceros 3D, where they were converted to mesh entities and saved using the .igs format, to allow for import to ShipMo3D. The starboard side of each hull was also removed, as ShipMo3D's "Panel Hull" application mirrors the input geometry across the centreline.

Since ShipMo3D is a potential flow-based code, some viscous damping had to be added in order to damp the roll response of the OSV to reasonable levels. To achieve this, pairs of bilge keels were added to each ship. ShipMo3D makes use of an oscillating plate model for determination of roll damping due to bilge keels. A sensitivity study was completed on roll motion to determine a depth for the bilge keels based on industry

experience/engineering judgement. The resulting depths were 1.31 m, 1.50 m, and 1.69 m

for the small, medium, and large OSVs, respectively. The difference in depth of the bilge

keels was determined through linear scaling with length. This reduced peak roll responses

in beam seas to maxima of 10.6 °/m, 7.8 °/m, and 6.0 °/m for the small, medium and large

OSVs, respectively.

Using ShipMo3D, zero-speed added mass and damping coefficients, and subsequently

Response Amplitude Operator (RAO) curves were calculated for all 6 hull forms, in all 6

Degrees of Freedom (DOF). The RAO curves were generated for relative sea directions

evenly spaced between 0° (Head Seas) and 180° (Following Seas), in increments of 15°.

For all ships, the calculations were completed using $GM_t = 2.0$ m and 2.75 m. A higher

GM of 3.5 m was also considered for the 90 m long OSVs. The frequency domain results

are presented and discussed in Section 3.2.

All environmental data used for the following seakeeping analyses was taken from the

study MetOcean Climate Study Offshore Newfoundland & Labrador – Cell Report – Cell

337 [5]. This report contains monthly tables showing the probability of occurrence of a

given sea-state (H_s and T_p) in the Flemish Pass region over the given month. For the

purposes of this analysis, cumulative probability distributions for two distinct seasons

were used: Summer (May, June, July and August), and Winter (November, December,

January, February). These tables can be seen in Appendix B.

2.2 Matlab Analysis – Time Domain Simulations

2.2.1 20 Minute Simulations - Operability Contours

Next, using the "TimeSeriesfromRAOs" application within ShipMo3D, 20 minute time histories of OSV motions were calculated across a range of wave heights and peak periods within the probability distributions for each season. The ITTC guidelines for seakeeping experiments recommend a lower limit of 50 encounters for a seakeeping experiment, 100 encounters as "the standard", and anything over 200 encounters as excellent practice [12]. Considering this, a 20 minute simulation time was chosen, to achieve a sufficient number of encounters while maintaining computational efficiency. For the shortest considered wave period of 6.0 s, this results in 200 encounters. For the longest considered wave period of 18.0 s, this results in 66 encounters. This is considered sufficient for the initial time-domain simulations described in this section. Note that certain sea-states that cause a FROG-6 deck velocity limit exceedance are selected for further, longer duration analysis, as described in Section 2.2.2 below.

The following three headings were used: 0° (Head Seas), 45° (Bow Quartering, and 90° (Beam Seas). Note that the ShipMo3D coordinate system has head seas at 180°, and following seas as 0°. This convention was reversed for this study, for simplicity, since most of the studied results are associated with weathervaning towards head seas. For all results and discussion presented below, 0° represents head seas. A unidirectional JONSWAP spectrum with a peak enhancement factor of 3.3 was used to represent individual points within the probability distribution. Table 2-2 below shows the combinations of wave heights and peak periods that were used in the analysis. Note that

as shown in the environmental data in Appendix B, there are no data points with an H_s

over 5.0 m when the peak period is 6.0 s. Therefore for $T_p = 6.0$ s, the highest H_s analyzed

is 5.0 m.

Table 2-2: Sea-States for Operability Contours

T_p (s):	6.0	7.5	11.5	15.5	18.0
H_s (m):	3.0	3.0	3.0	3.0	3.0
	4.0	4.0	4.0	4.0	4.0
	5.0	5.0	5.0	5.0	5.0
	-	6.0	6.0	6.0	6.0

In common practice, crew transfer operations from OSV to a Gravity Based Structure

(GBS) offshore Newfoundland and Labrador are generally limited to sea-states with

significant wave height less than 4.0 m, regardless of the OSV size, loading condition, or

relative sea direction, unless a specific hazard analysis is conducted for the planned lift, to

show that it is safe [3], [4].

The FROG-6 user manual [3] presents a table of recommended sea states based on

significant and maximum wave heights, as well as the type of platform to which the

transfer is occurring (e.g. fixed platform, semi-sub, FPSO, or other vessel). However,

these are conservative limits as they do not consider mitigating factors such as: OSV size,

the effect of various hull shapes and parameters, active and passive roll damping systems,

etc. There are specific limits on vertical and horizontal impact velocity magnitude for the

FROG-6 personnel capsule in the FROG-6 user manual, which are defined as [3]:

- A maximum permissible lateral velocity of 2.0 m/s.

- A maximum permissible vertical velocity of 4.0 m/s.

In order to simplify the analysis, only the motion of the OSV is considered; it is assumed that the crew transfer is being made to a GBS with a platform-side crane. It is therefore assumed that crane tip velocity is zero, and any swing velocity is negligible. Therefore, the deck velocity of the OSV is considered equivalent to the maximum impact velocity that could be experienced by the capsule.

Since deck velocity can vary greatly depending on the size of the ship and the relative sea direction, in order to evaluate whether or not the FROG-6 capsule can be used in a given condition, deck velocities must be evaluated at that location, to see if both the lateral and vertical velocities are less than their respective limits. Since ShipMo3D outputs time domain motions as 6 DOF motions about the local rigid body frame, a MATLAB script (Presented in Appendix A) was developed to convert these motions to deck velocities at a given point. Each point is described by a positon vector <X,Y,Z> relative to the OSV's Centre of Gravity (C.G.). Velocities for 8 points along the deck were calculated, however the focus of this analysis is placed on two points: The first point is directly above the C.G., as this is the point at the working deck level with the most benign vessel motions, and as such is the ideal point for crew transfer from a vessel motions perspective. The second point was a "target landing" location directly in the middle of the working deck. This point still has relatively favourable motions as it's on the centreline of the ship, when compared to the edges of the working deck. The middle of the working deck is generally used for lifting sensitive or valuable cargo, due to the decreased risk of impacting the

bulwarks, superstructure, or other items should the load start to swing. Both of these points had to "pass" the operability checks for a given condition to be deemed operable.

The ShipMo3D time domain output consists of the following variables and their associated velocities (Denoted 'VariableName_vel'), at each time-step:

- t (s) = Time passed since start of simulation.

- X_f (m) = X position in global coordinates of the C.G. (North +).

- Y_f (m) = Y position in global coordinates of the C.G.   (East +).

- Heave (m) = Vertical displacement from the starting position (Up +).

- Roll (°) = Angle of roll from starting position (Port Up +)

- Pitch (°) = Angle of pitch from starting position (Bow Down +)

- Heading, β (°) = OSV's heading in global coordinates (North = 0°).

At each deck point (for each time step), the MATLAB script decomposes each of the 6 DOF motions into a velocity vector with the following three components:

- V_x: Positive towards the bow.

- V_y: Positive towards starboard.

- V_z: Positive up.

The first step in this process is to transform each deck point from ship-fixed to global coordinates, in order to properly identify lateral and vertical velocity components. This is done using the following transformation equation:

- $<X,Y,Z> = [R_x][R_y]<X_0,Y_0,Z_0>$

Where $[R_x]$ and $[R_y]$ are the following transformation matrices:

- $[R_x] =$

1	0	0
0	cos(-Roll)	sin(-Roll)
0	sin(-Roll)	cos(-Roll)

- $[R_y] =$

cos(Pitch)	0	sin(Pitch)
0	1	0
-sin(Pitch)	0	cos(Pitch)

Next, the radii of rotation about the OSV C.G. for each of the rotational DOFs are found, as follows:

- $R_{Roll} = (Y^2 + Z^2)^{0.5}$

- $R_{Pitch} = (X^2 + Z^2)^{0.5}$

- $R_{Yaw} = (X^2 + Y^2)^{0.5}$

At each time step, the angles between each respective point's position vector and the global principal coordinate axes are found using the following definitions:

- $\Phi = \arctan(Z/X)$ for X > 0, Z > 0

- $\Phi = 0°$ for X > 0, Z = 0

- $\Phi = -\arctan(-Z/X)$ for X > 0, Z < 0

- $\Phi = 90°$ for X = 0, Z > 0

- $\Phi = 0°$ for X = 0, Z = 0

- $\Phi = 270°$ for X = 0, Z < 0

- $\Phi = \arctan(Z/X)$ for X < 0, Z > 0

- $\Phi = 180°$ for $X < 0, Z = 0$

- $\Phi = 180° + \arctan(-Z/-X)$ for $X < 0, Z < 0$

- $\Theta = \arctan(Z/Y)$ for $Y > 0, Z > 0$

- $\Theta = 0°$ for $Y > 0, Z = 0$

- $\Theta = -\arctan(-Z/Y)$ for $Y > 0, Z < 0$

- $\Theta = 90°$ for $Y = 0, Z > 0$

- $\Theta = 0°$ for $Y = 0, Z = 0$

- $\Theta = 270°$ for $Y = 0, Z < 0$

- $\Theta = \arctan(Z/Y)$ for $Y < 0, Z > 0$

- $\Theta = 180°$ for $Y < 0, Z = 0$

- $\Theta = 180° + \arctan(-Z/-Y)$ for $Y < 0, Z < 0$

- $\Psi = \arctan(Y/X)$ for $X > 0, Y > 0$

- $\Psi = 0°$ for $X > 0, Y = 0$

- $\Psi = -\arctan(-Y/X)$ for $X > 0, Y < 0$

- $\Psi = 90°$ for $X = 0, Y > 0$

- $\Psi = 0°$ for $X = 0, Y = 0$

- $\Psi = 270°$ for $X = 0, Y < 0$

- $\Psi = \arctan(Y/X)$ for $X < 0, Y > 0$

- $\Psi = 180°$ for $X < 0, Y = 0$

- $\Psi = 180° + \arctan(-Y/-X)$ for $X < 0, Y < 0$

Next, the contributions to V_x and V_y from the lateral translational motions are found. Since X_{f}_vel represents the change in North-South position with time, it contributes to the OSV's surge motion through the cosine of the heading angle, and to the sway motion through the sine of the heading angle. Conversely, since Y_{f}_vel represents the change in East-West position with time, it contributes to the OSV's sway motion through the cosine of the heading angle, and to the surge motion through the sine of the heading angle:

- Surge = $X_{f}\_vel * \cos(\beta) + Y_{f}\_vel * \sin(\beta)$

- Sway = $-X_{f}\_vel * \sin(\beta) + Y_{f}\_vel * \cos(\beta)$

Finally, combining everything:

- V_x = Surge + (Pitch_vel * R_{Pitch} * $\sin(\Phi)$) – (Heading_vel * R_{Yaw} * $\sin(\Psi)$)

- V_y = Sway + (Roll_vel * R_{Roll} * $\sin(\Theta)$) + (Heading_vel * R_{Yaw} * $\cos(\Psi)$)

- V_z = Heave – (Roll_vel * R_{Roll} * $\cos(\Theta)$) – (Pitch_vel * R_{Pitch} * $\cos(\Phi)$)

The vertical velocity magnitude is V_z, and a lateral velocity magnitude can be obtained simply using the following equation:

- Lateral Magnitude = $(V_x{}^2 + V_y{}^2)^{0.5}$

Once all the ShipMo3D results had been processed through the MATLAB script, each time history was checked to see if the target locations had deck velocities less than the FROG-6 velocity limits over the 20 minute simulation period. If this was the case, then that particular combination of OSV, GM_t, heading, H_s, and T_p were considered "operable". Conversely, if either velocity limit was exceeded at any point during the 20

minute time interval, then that condition was considered inoperable. Then, linear interpolation was used to define exact H_s limits for a given T_p. From here, linear interpolation was again used between the evaluated periods to develop operability contours for each condition. Examples of such contours for both winter and summer seasons are located in Section 3.3.1.

Note: The highest H_s that was allowable for an "operable" condition is 6.0 m, regardless of the output from the calculations. This is done for the following two reasons:

I.   As the wave form and OSV response become increasingly non-linear with increased wave height, there is uncertainty in the accuracy of ShipMo3D's output motions in waves higher than 6.0 m.

II.   When significant wave heights are greater than 6.0 m, the wind limit (20 m/s) is likely to be exceeded, and so cargo / crew transfer cannot occur, regardless of calculated deck velocities. See Section 3.3.2 for further details.

The following step in the analysis was to simply sum all the time fractions that seastates occurred, where the limits were not exceeded, resulting in a percentage of time that a given OSV / loading condition would be able to operate in a given season.

2.2.2 8 Hour Simulations - 'Safe Time' Analysis

The operability contour approach described above only considers if a limit exceedance occurs during the 20 minute simulation time; it gives us no information on the number of

limit exceedances, nor how much time is actually useable for crew and cargo transfer

operations in between limit exceedances. A selection of seastate/OSV/loading condition

combinations are selected to be run for a much longer simulation time (8 hours). The

cases considered for the longer time simulations are summarized in Table 2-3 below.

Further justification of the selection of these cases is presented in Sections 3.3.1 and

3.3.2.

Table 2-3: 8 Hour Simulation Matrix

GM (m)	Hs (m)	Tp (s)	Heading
2.00	5.0	6.0	Beam Seas
		7.5	Beam Seas
		11.5	Beam Seas
	6.0	7.5	Beam Seas
		11.5	Beam Seas & Bow Quartering
		15.5	Beam Seas
	8.0	12.5	Head Seas & Bow Quartering
2.75	4.0	6.0	Beam Seas
		7.5	Beam Seas
	5.0	6.0	Beam Seas
		7.5	Beam Seas
		11.5	Beam Seas
	6.0	7.5	Bow Quartering
		11.5	Beam Seas & Bow Quartering
		15.5	Beam Seas
	8.0	12.5	Head Seas & Bow Quartering

8 hour simulations were completed for all ships for the conditions presented above.

Another Matlab script (Presented in Appendix A) was developed to analyze the time

between limit exceedances over these 8 hour simulations. Any time such that the deck

velocities are below the limits is considered "safe time". However, it is possible that the

time between limit exceedances is too short to safely complete a crew transfer operation.

Hence, the concept of "useable time" is defined as a time between limit exceedances of at least 10 minutes. It is assumed that this is a sufficient amount of time to complete a transfer operation. For these simulations, only the "target landing" location is considered, in the middle of the OSV working deck. This is based on the assumption that when attempting any crew transfer operations in extreme weather, the capsule take-off/landing location will be as far from any obstructions as possible, to reduce the risk of any impacts. Results for these long time simulations are presented and discussed in Section 3.3.2.

3.0 Results and Discussion

3.1 Roll Natural Frequency

Natural roll frequencies for all 6 OSVs and 3 GM values considered are presented below

in Table 3-1. First, the roll radius of gyration (k), is assumed to be:

- $k_{roll} = 0.35 * B \ (m)$

Then, the natural roll frequency is given by:

- $\omega = \dfrac{\sqrt{GM*g}}{k_{roll}} \ (\dfrac{rad}{s})$

The natural roll period can then be determined by:

- $T = \dfrac{1}{\omega} * \dfrac{2\pi rad}{1cycle} \ (s)$

Table 3-1: Natural Roll Frequencies

Vessel:	Small-Light		Small-Heavy		Medium-Light		Medium-Heavy		Large-Light			Large-Heavy		
GM (m):	2.00	2.75	2.00	2.75	2.00	2.75	2.00	2.75	2.00	2.75	3.50	2.00	2.75	3.50
Beam (m):	17.00				19.50				22.00					
k_roll (m):	5.95				6.83				7.70					
Natural Frequency (rad/s):	0.74	0.87	0.74	0.87	0.65	0.76	0.65	0.76	0.58	0.67	0.76	0.58	0.67	0.76
Natural Roll Period (s):	8.44	7.20	8.44	7.20	9.68	8.26	9.68	8.26	10.92	9.32	8.26	10.92	9.32	8.26

These natural frequencies are relevant in discussing the peaks in OSV response in the

RAO curves presented in Section 3.2 below.

3.2 Frequency Domain Results

Sections 3.2.1 through 3.2.3 below present some representative RAO curves, for discussion of the effect of various parameters on the OSV response. 13 incoming wave directions are considered in the ShipMo3D analysis, ranging from 0° *(head seas)* to 180° *(following seas)* in 15° increments. To reduce the sheer amount of data presented, 3 representative headings are studied in detail. Considering that OSVs generally attempt to weathervane towards head seas when completing offshore lifting operations, the following cases are chosen:

1. **Head Seas (0°)**: Ideal heading for crew/cargo transfer offshore.
2. **Bow Quartering (45°)**: Represents the reality that it is not always possible to weathervane 100% effectively, for operational and field layout reasons. E.g., transfer may need to be completed on one side of a fixed platform, OSV crane may not be able to reach the landing area unless positioned beam towards the platform, etc.
3. **Beam Seas (90°)**: Represents a worst-case for OSV motions, as the limiting deck velocity is generally governed by roll motions.

The complete set of RAO curves are not included due to the shear amount of data; they are available upon request.

3.2.1 Frequency Domain Results – Head Seas (0°)

Figure 3-1 through Figure 3-3 below present the RAO results across all OSVs with GM fixed at 2.0 m, and a head seas seastate.
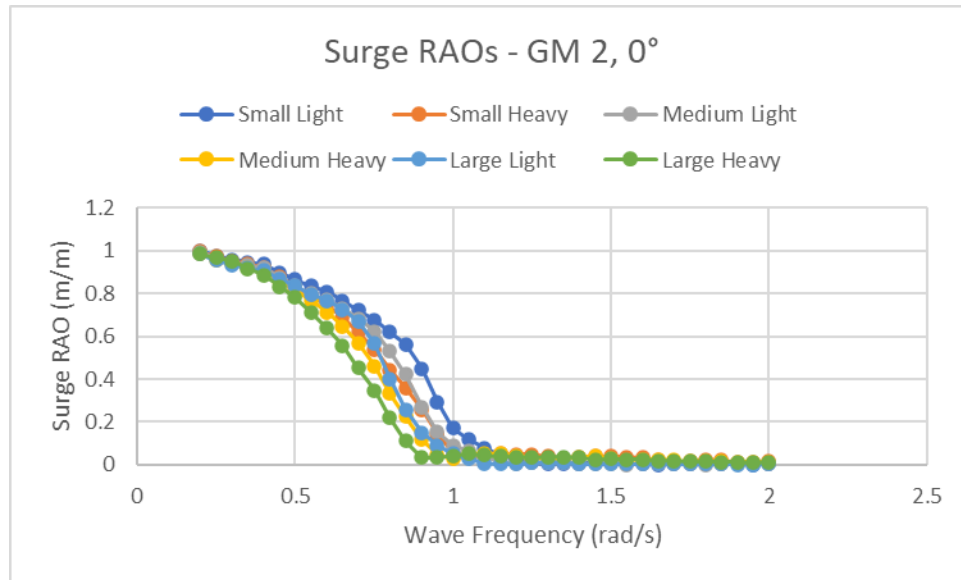
Figure 3-1: Surge RAOs by OSV, Head Seas, GM = 2.0 m

The surge RAOs above generally show the expected trend; the worst-case motions occur in the smallest OSV (Small-Light), and the lowest amplitude motions occur in the largest OSV (Large-Heavy). It is clear from this plot that increasing OSV size is associated with a decrease in surge response. The second point to note is that surge response trends towards 0 with an increase in incoming wave frequency. The frequency at which the surge response becomes negligible increases with OSV size. For example, the Small-Light OSV sees a surge response of nearly 0.2 at a wave frequency of 1 rad/s, while the larger OSV responses are near 0 at this frequency.

The sway RAO plot in head seas is a trivial plot (i.e. an all 0 response), as expected since the OSV and seastate are fully symmetrical in ShipMo3D. As such, it is not presented.
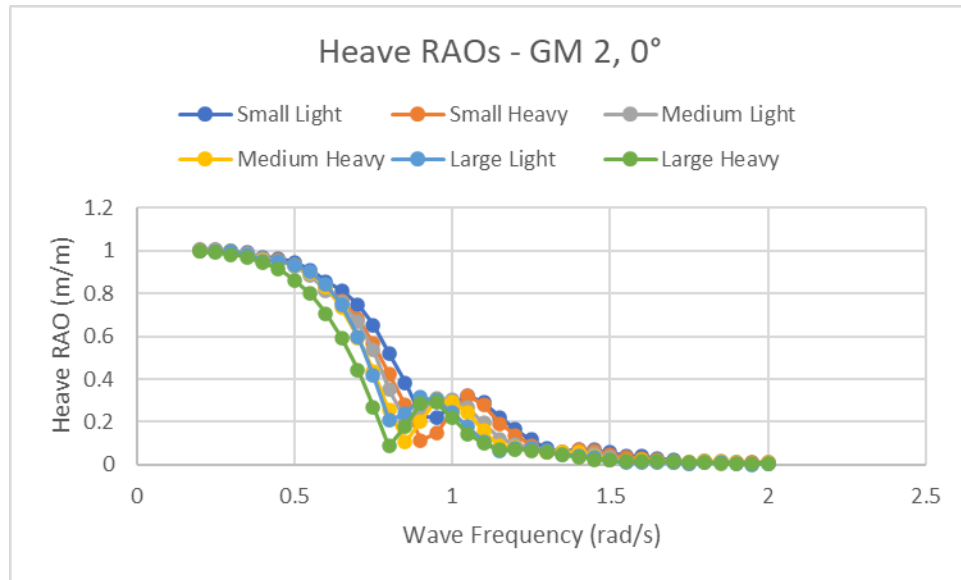
Figure 3-2: Heave RAOs by OSV, Head Seas, GM = 2.0 m

The heave RAOs in head seas show a similar trend as discussed for the surge RAOs above. The magnitude of maximum heave response decreases with an increase in OSV size, and the peak heave response is at a lower wave frequency for the larger OSVs, than for the smaller OSVs.

As with the sway RAOs, the roll plot in head seas is a trivial, all 0 plot, due to the symmetry of the geometry and incoming waves. As such, it is not presented.
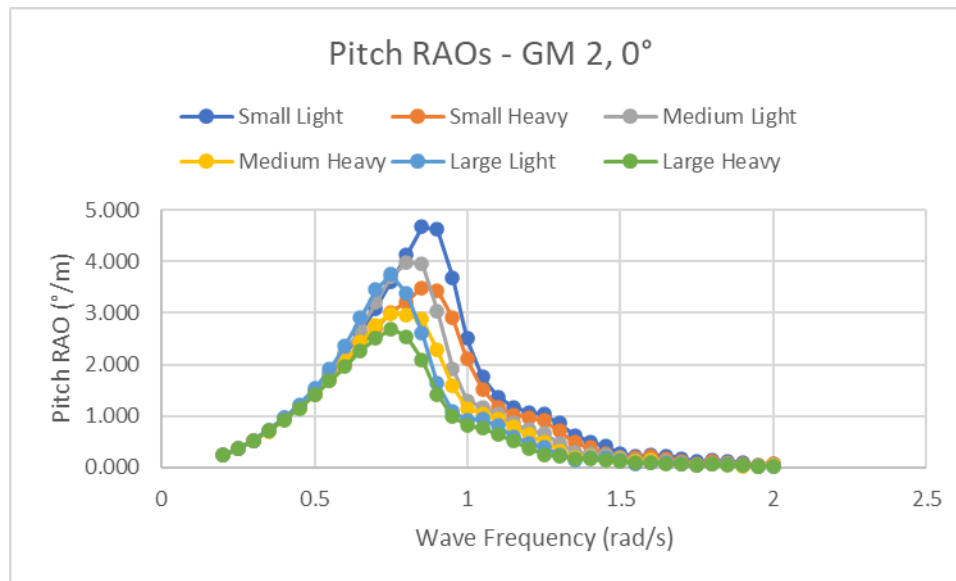
Figure 3-3: Pitch RAOs by OSV, Head Seas, GM = 2.0 m

The pitch RAOs in head seas show a similar trend as discussed for the surge and heave RAOs above. The magnitude of maximum pitch response decreases with an increase in OSV size, and the peak pitch response is at a lower wave frequency for the larger OSVs, than for the smaller OSVs.

As with the sway and roll RAOs, the yaw plot in head seas is a trivial, all 0 plot, due to the symmetry of the geometry and incoming waves. As such, it is not presented.

3.2.2 Frequency Domain Results – Bow Quartering (45°)
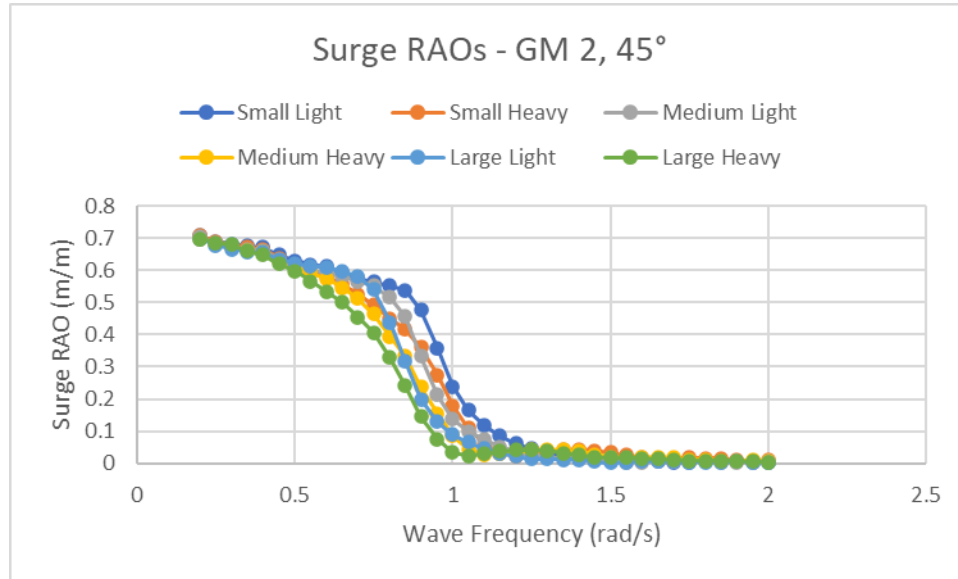
Figure 3-4: Surge RAOs by OSV, Bow Quartering, GM = 2.0 m
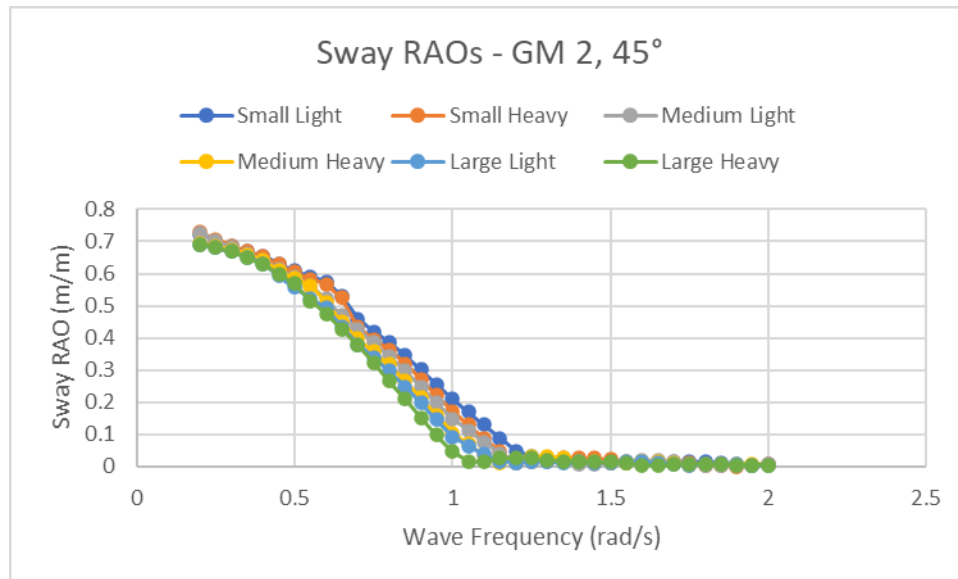
Figure 3-5: Sway RAOs by OSV, Bow Quartering, GM = 2.0 m
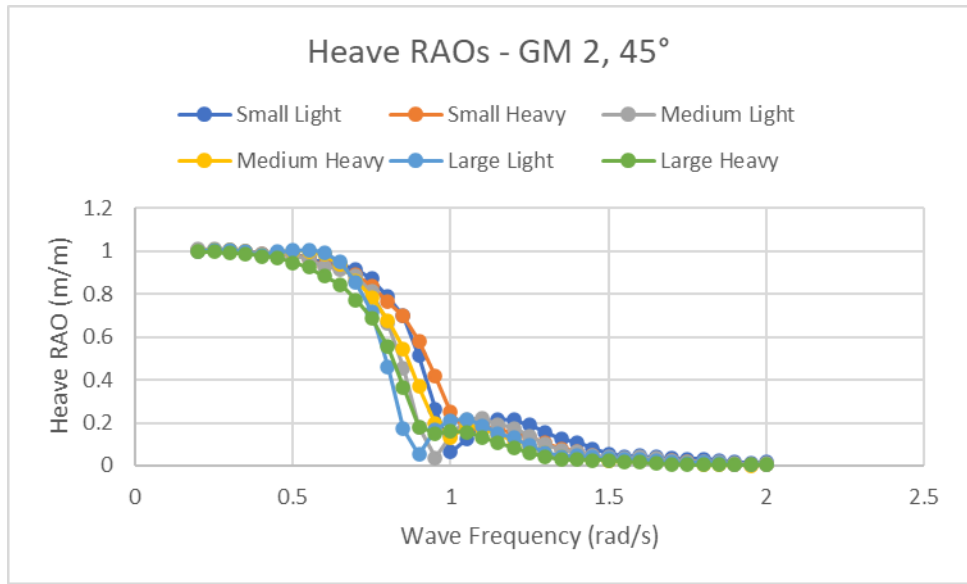
Figure 3-6: Heave RAOs by OSV, Bow Quartering, GM = 2.0 m
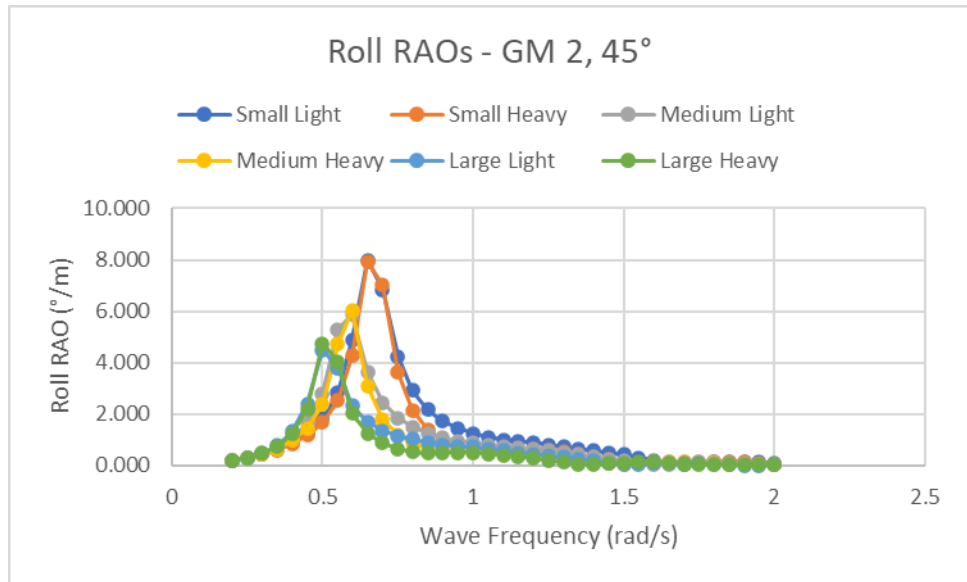
Figure 3-7: Roll RAOs by OSV, Bow Quartering, GM = 2.0 m
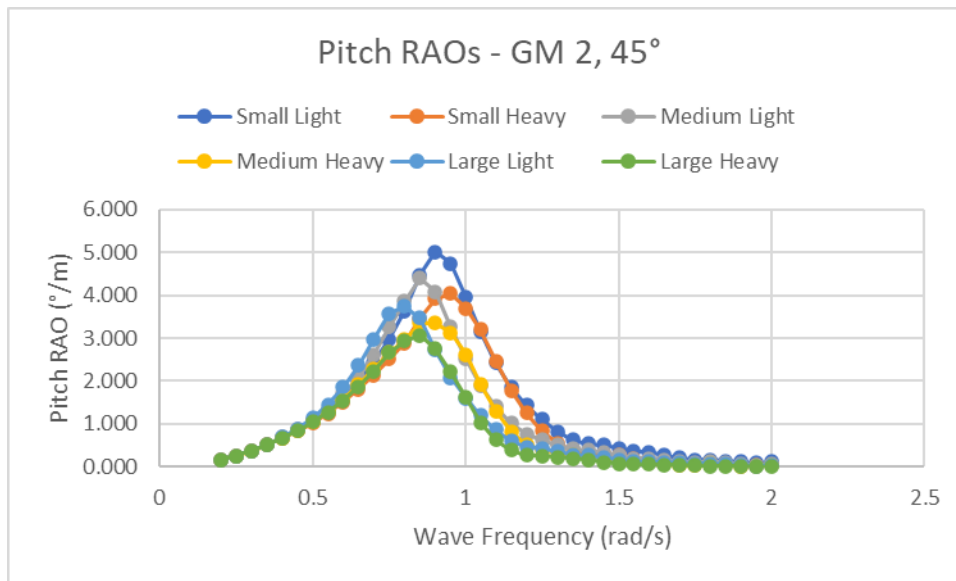
Figure 3-8: Pitch RAOs by OSV, Bow Quartering, GM = 2.0 m
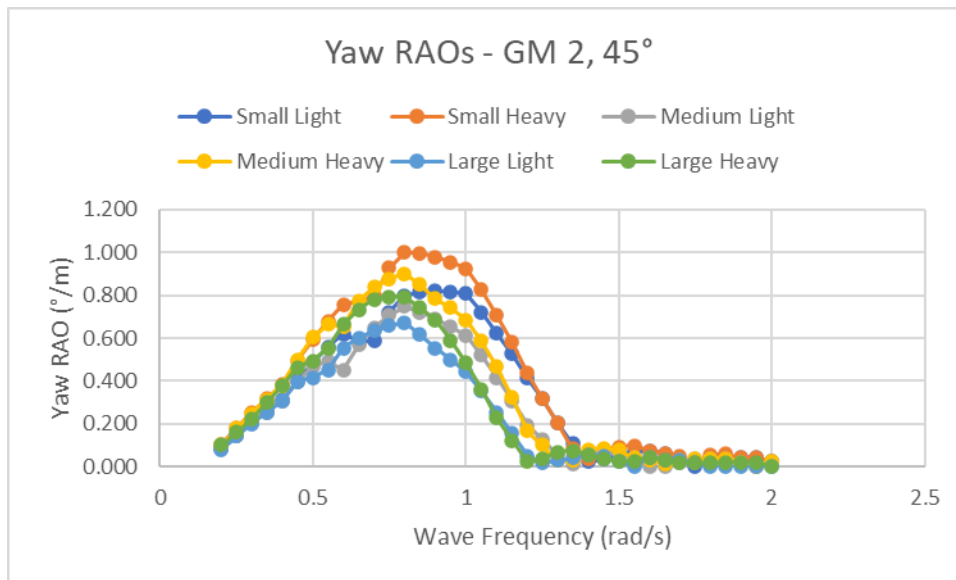
Figure 3-9: Yaw RAOs by OSV, Bow Quartering, GM = 2.0 m

The RAOs in bow quartering seas generally show the expected trend, that is, the largest vessel response is generally for the smallest OSV, and vice versa. Further discussion on these results is presented in Section 3.2.3 below.

3.2.3 Frequency Domain Results – Beam Seas (90°)
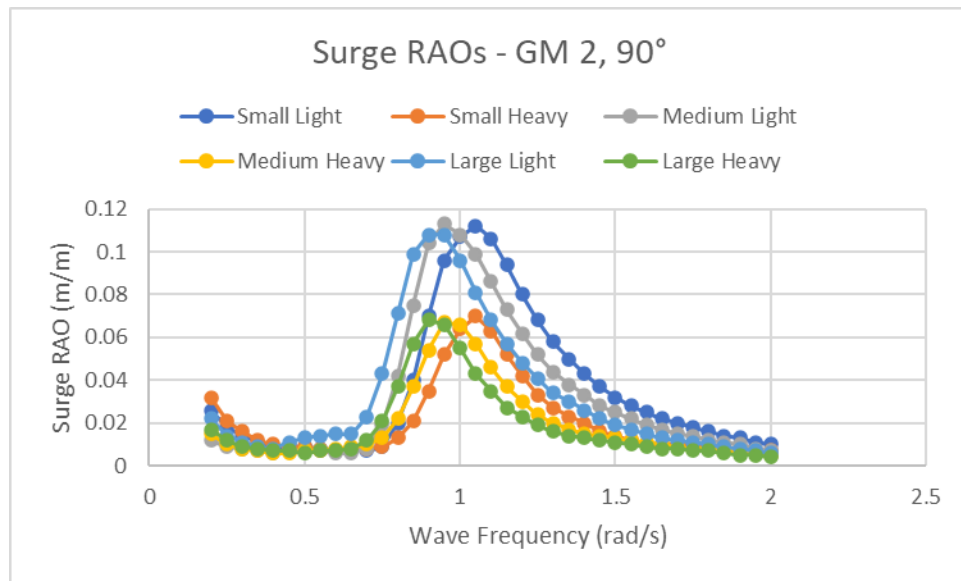
Figure 3-10: Surge RAOs by OSV, Beam Seas, GM = 2.0 m
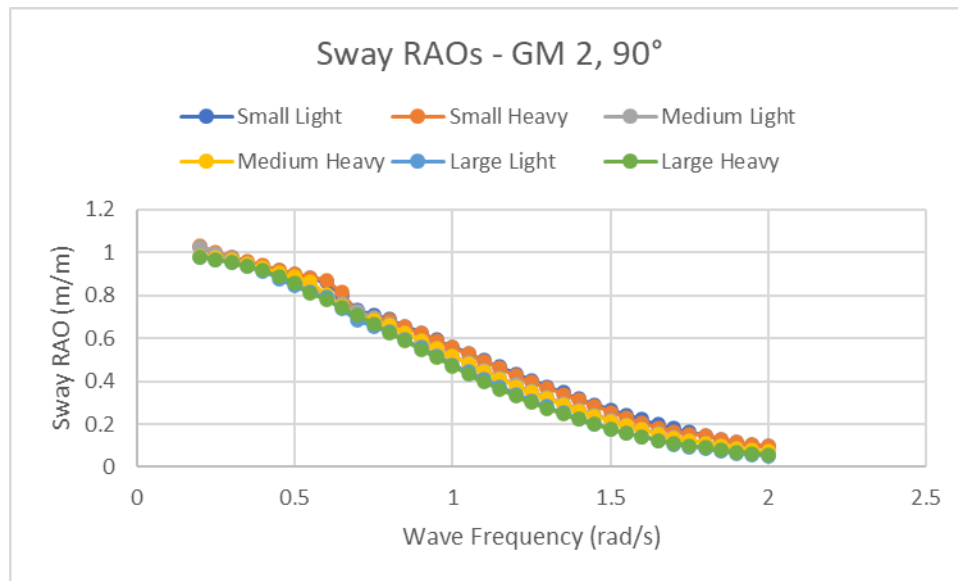
Figure 3-11: Sway RAOs by OSV, Beam Seas, GM = 2.0 m
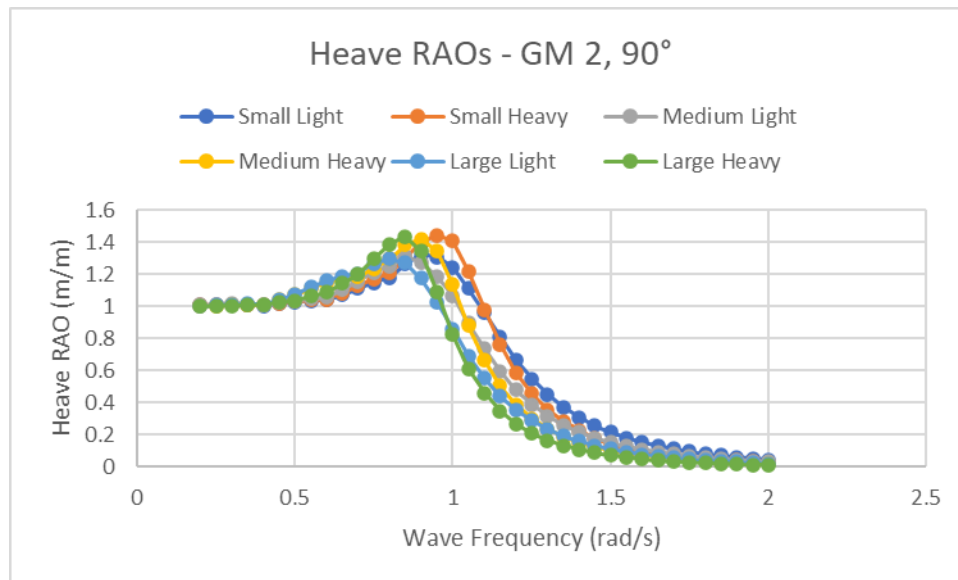
Figure 3-12: Heave RAOs by OSV, Beam Seas, GM = 2.0 m
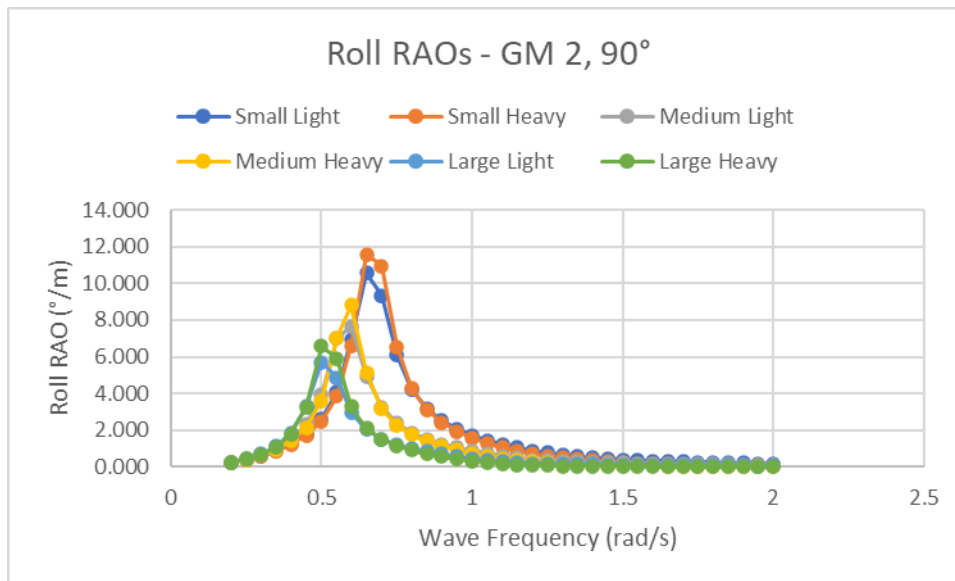
Figure 3-13: Roll RAOs by OSV, Beam Seas, GM = 2.0 m
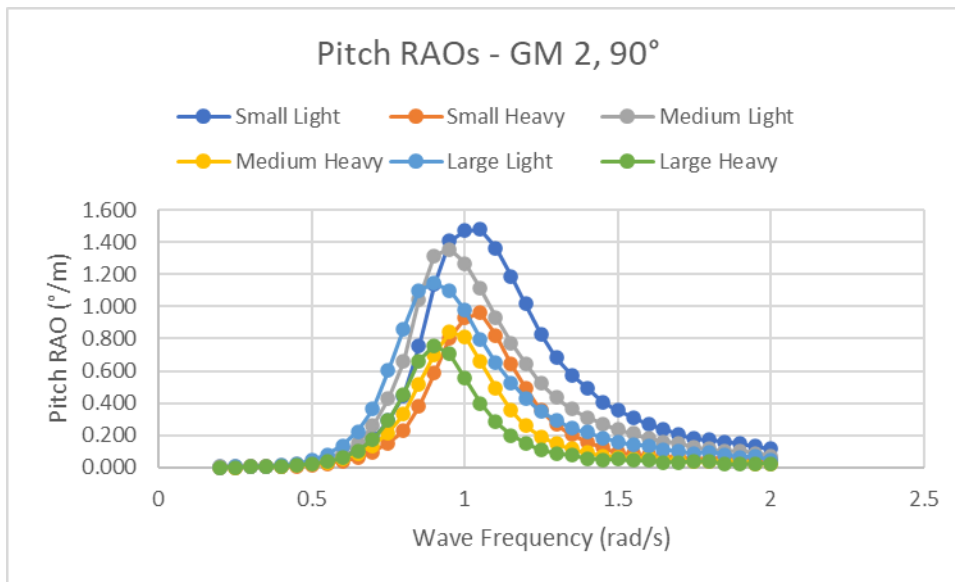
Figure 3-14: Pitch RAOs by OSV, Beam Seas, GM = 2.0 m
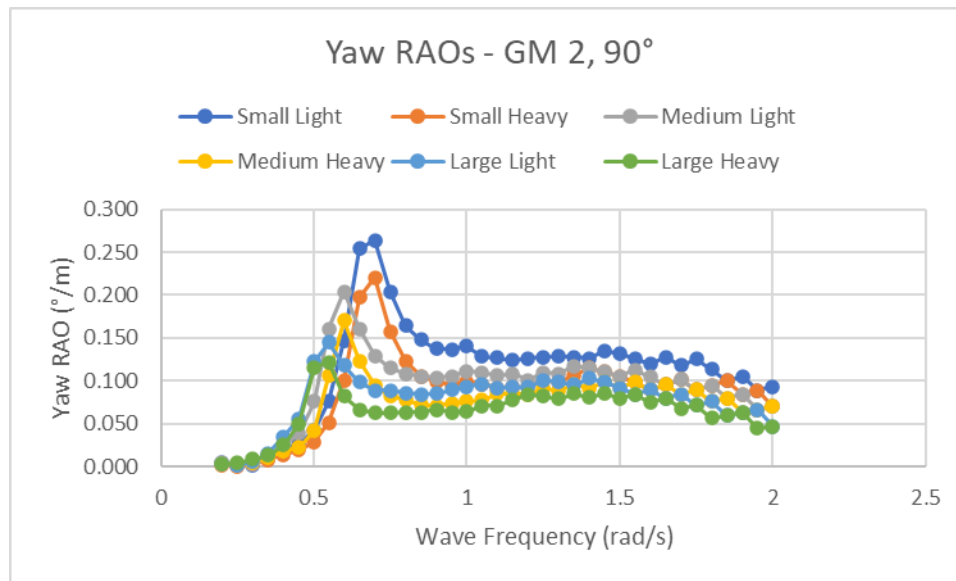
Figure 3-15: Yaw RAOs by OSV, Beam Seas, GM = 2.0 m

The figures presented in Section 3.2.1 through 3.2.3 above generally follow the expected trend with respect to OSV size. In most cases, the maximum peak response for a given loading condition is associated with the "small-light" OSV, and the minimum peak response is associated with the "large-heavy" OSV. This is most noticeable and significant for the pitch and roll RAOs than for the other degrees of freedom. As shown in Figure 3-8, the peak pitch response is approximately 5 degrees/m for the small-light OSV and approximately 3 degrees/m for the large-heavy OSV, in bow quartering seas.

For roll motion, the difference is even more drastic; Figure 3-13 show a peak response of nearly 12 degrees/m for the "small-heavy" OSV, and under 6 degrees/m for the "large-light" OSV. The roll natural frequencies presented in Table 3-1 above can be directly observed as the roll motion response peaks in Figure 3-7 and Figure 3-13. The "small"

42

OSVs have peak roll response at approximately 0.75 rad/s, the "medium" OSVs at approximately 0.65 rad/s, and the large OSVs at approximately 0.6 rad/s. This validates the simulation software against the first principles used to determine these natural frequencies.

Interestingly, the roll motion response is generally worse for the "heavy" OSVs than the "light" OSVs. This effect is less pronounced than the effect of OSV length, such that the "large" OSVs both have lower responses than the "medium" OSVs, which in turn have lower responses than the "small" OSVs. This indicates that the fuller hull forms are not ideal from the perspective of controlling roll motions, at least not for the simulated range of OSV sizes and loading conditions. Since the roll response is generally so much larger than the other degrees of freedom it is the governing DOF for exceedance of the FROG-6 deck velocity limits. This explains why, in Table 3-6 below, we see a decreased operational percentage for the "large-heavy" OSV when compared to the "large-light" OSV, despite the fact that in other degrees of freedom the OSV with the larger displacement generally has a lower amplitude response.

3.2.4   Frequency Domain Results – Aft Incoming Waves

Figure 3-16 through Figure 3-24 below present a selection of RAO plots for waves impacting the aft half of the OSV. No time domain analysis was completed for these headings; these RAOs are presented for completeness, and a comparison between these results and those for the head seas and bow quartering cases is discussed below. Note that

all trivial RAO plots are omitted from this section, for example, sway RAOs in following seas.
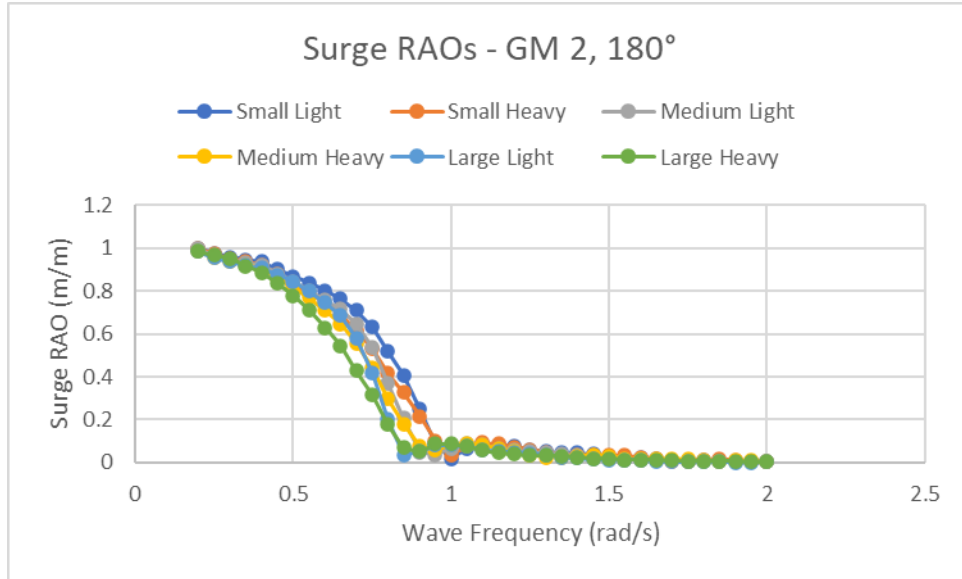
Figure 3-16: Surge RAOs by OSV, Following Seas, GM = 2.0 m
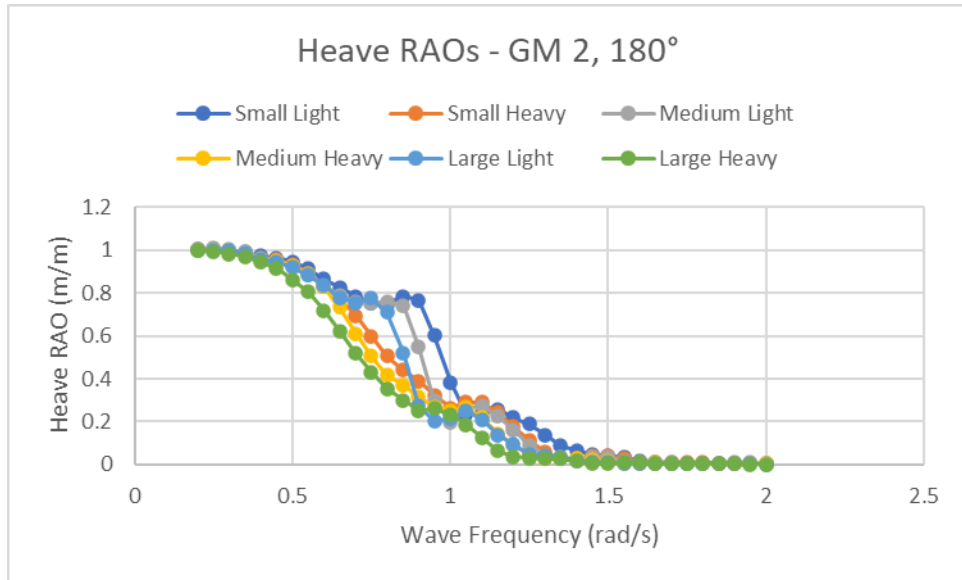
Figure 3-17: Heave RAOs by OSV, Following Seas, GM = 2.0 m
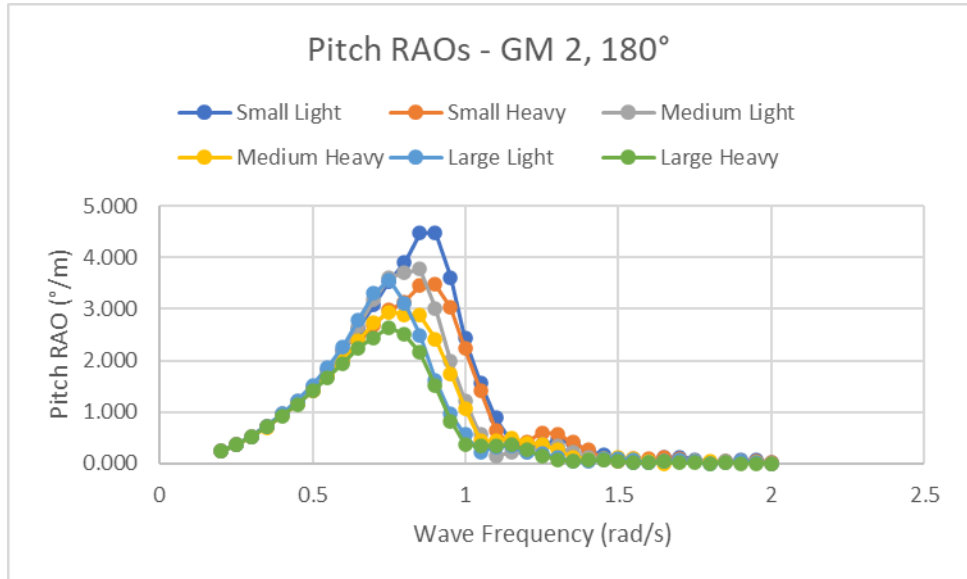
Figure 3-18: Pitch RAOs by OSV, Following Seas, GM = 2.0 m
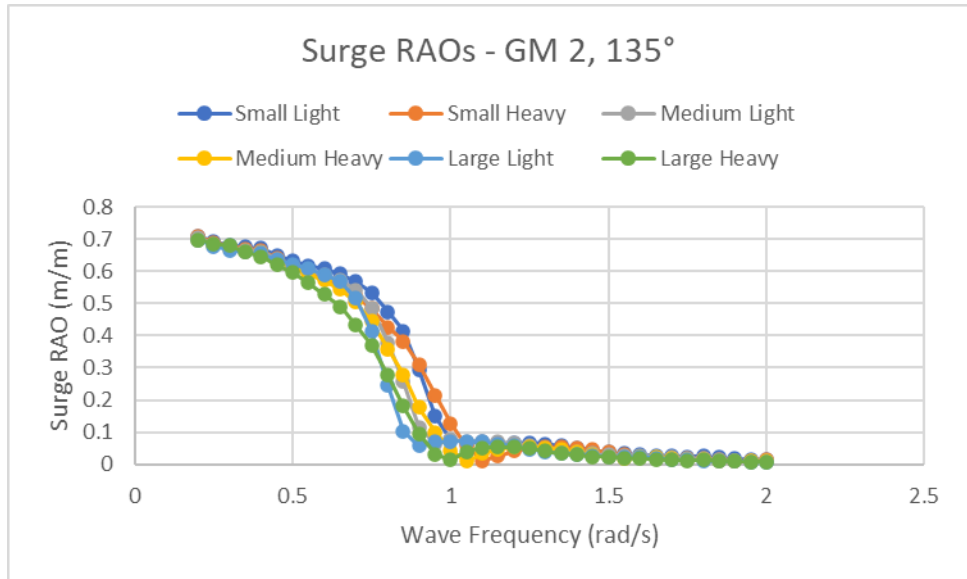
Figure 3-19: Surge RAOs by OSV, Stern Quartering, GM = 2.0 m
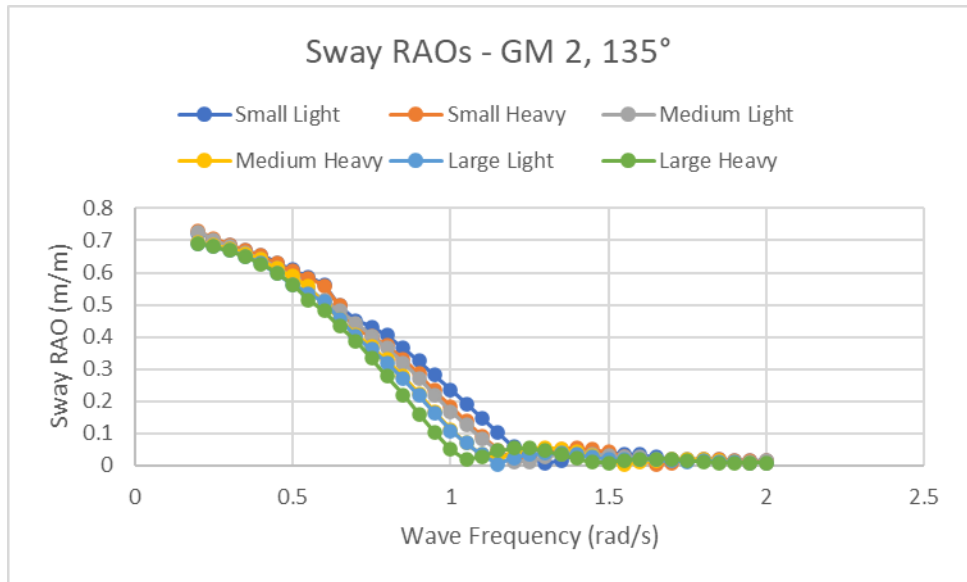
Figure 3-20: Sway RAOs by OSV, Stern Quartering, GM = 2.0 m
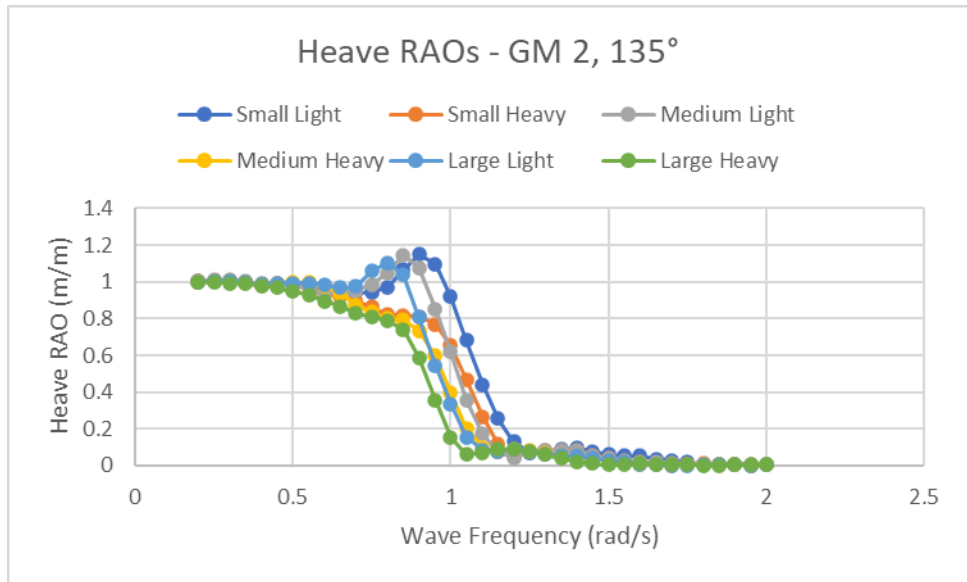
Figure 3-21: Heave RAOs by OSV, Stern Quartering, GM = 2.0 m
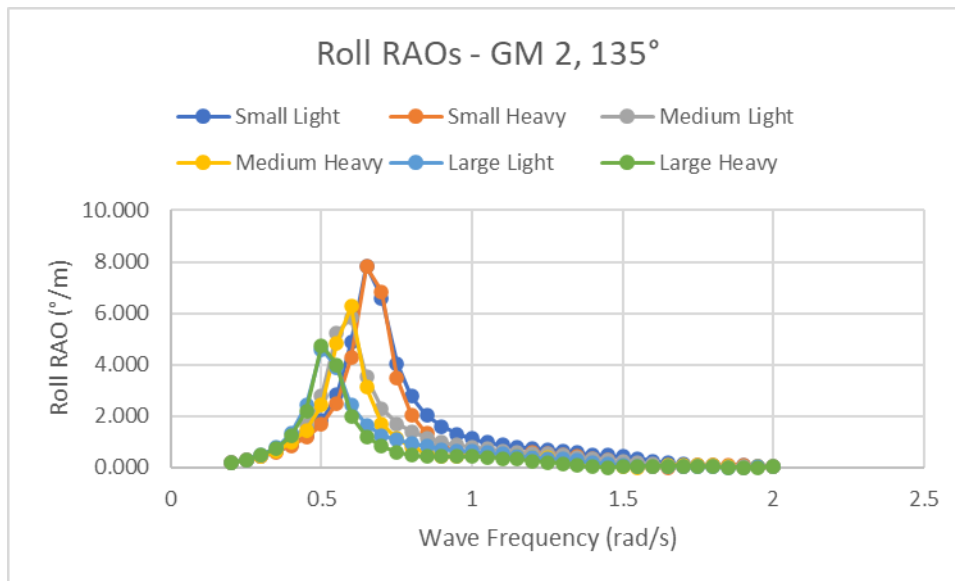
Figure 3-22: Roll RAOs by OSV, Stern Quartering, GM = 2.0 m
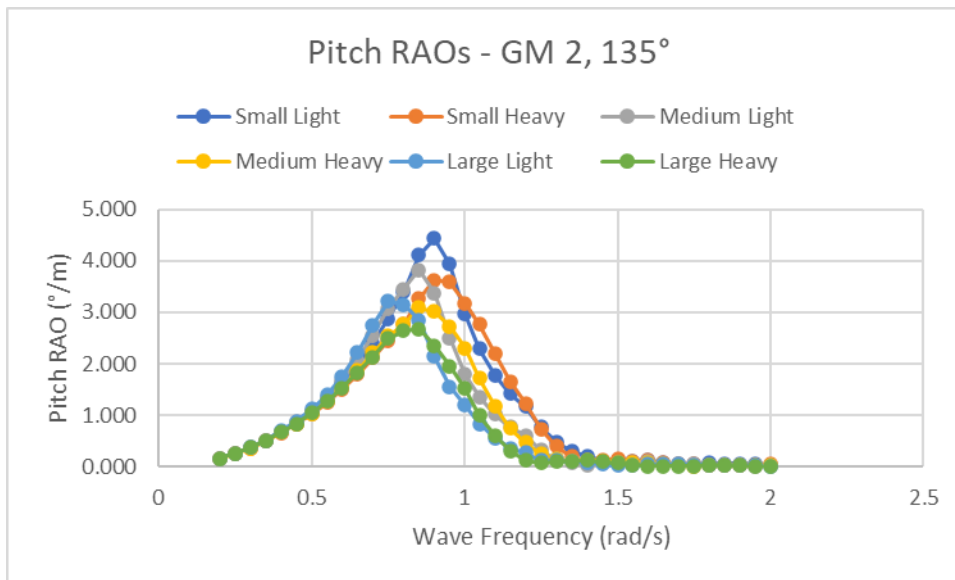
Figure 3-23: Pitch RAOs by OSV, Stern Quartering, GM = 2.0 m
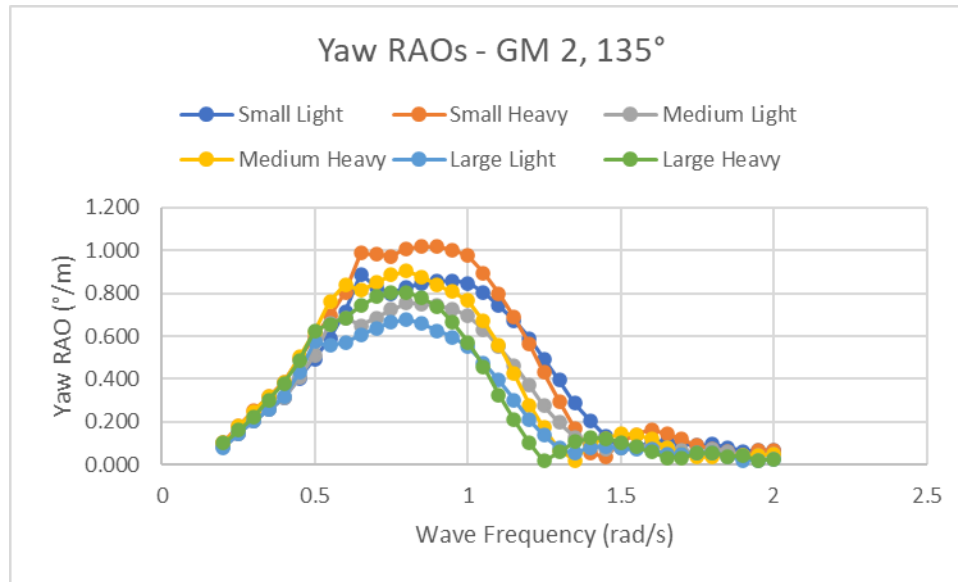
Figure 3-24: Yaw RAOs by OSV, Stern Quartering, GM = 2.0 m

As shown in above, the results for aft-incoming waves are reasonably similar to the corresponding seastate for forward-incoming waves. This validates the decision to consider 3 seastates in detail. However, this is an opportunity for further work to investigate the efficacy and feasibility of weathervaning with the stern towards the incoming wave direction.

3.2.5 Frequency Domain Results – GM Comparison

All results presented in Sections 3.2.1 through 3.2.4 above have a consistent transverse GM of 2.0 m. Figure 3-25 through Figure 3-36 below present a comparison of OSV response against varying GM, across all 6 DOF, for 2 OSVs *(Large-Light & Large-Heavy)*.
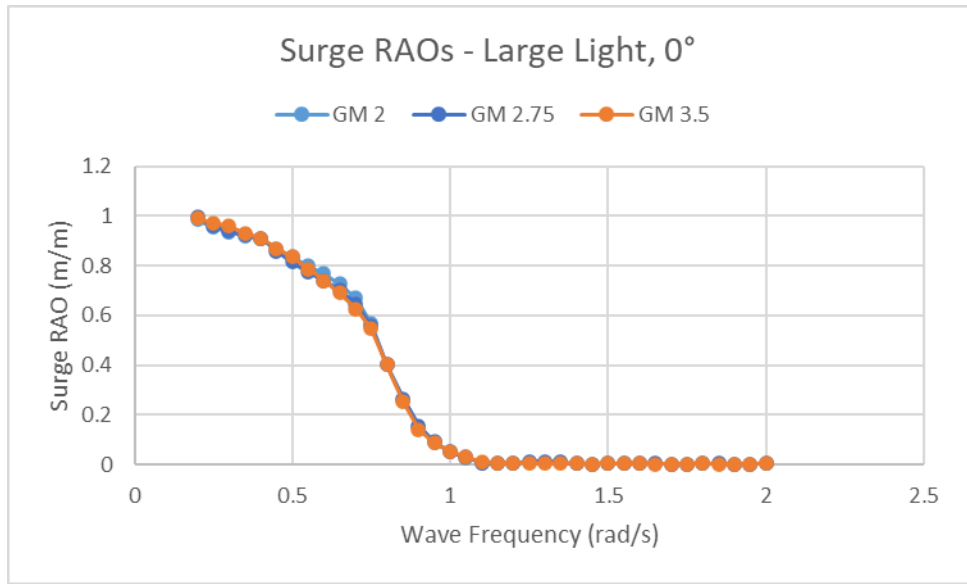
Figure 3-25: Surge RAOs by GM, Head Seas, Large-Light
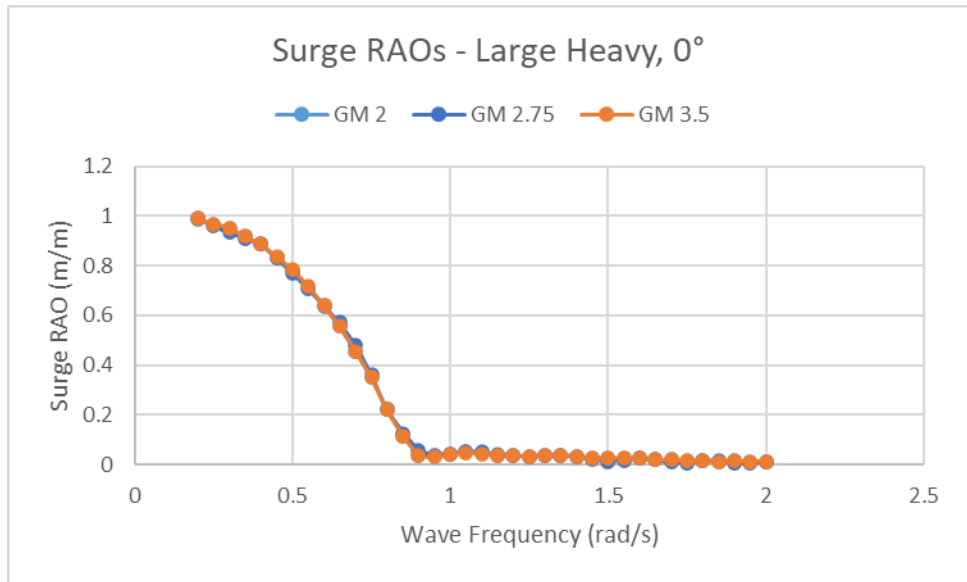
Figure 3-26: Surge RAOs by GM, Head Seas, Large-Heavy
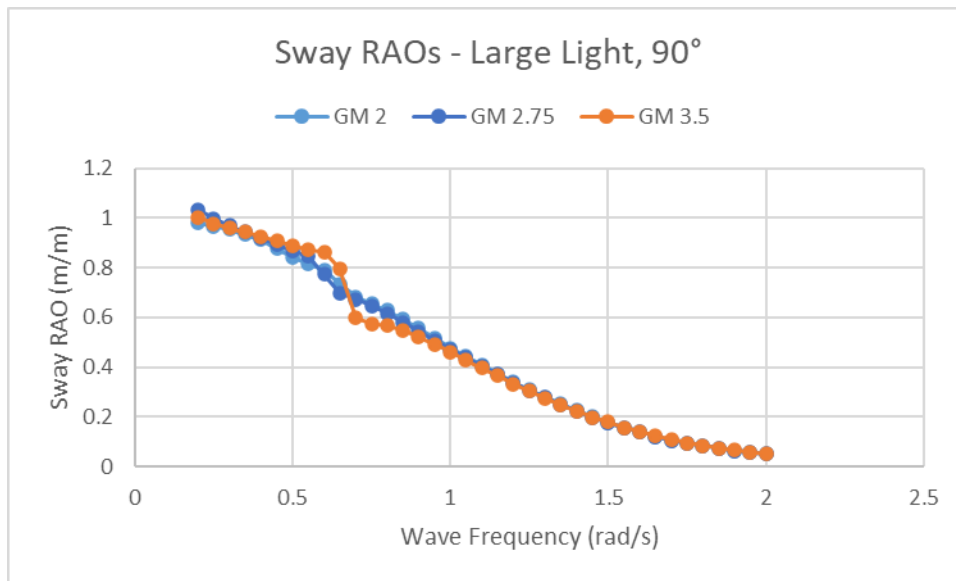
Figure 3-27: Sway RAOs by GM, Beam Seas, Large-Light
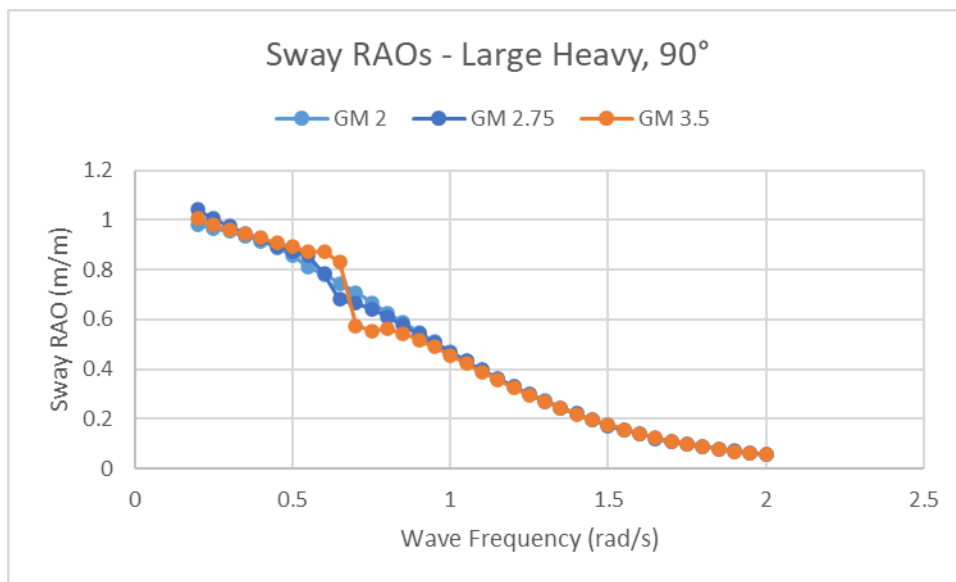
Figure 3-28: Sway RAOs by GM, Beam Seas, Large-Heavy
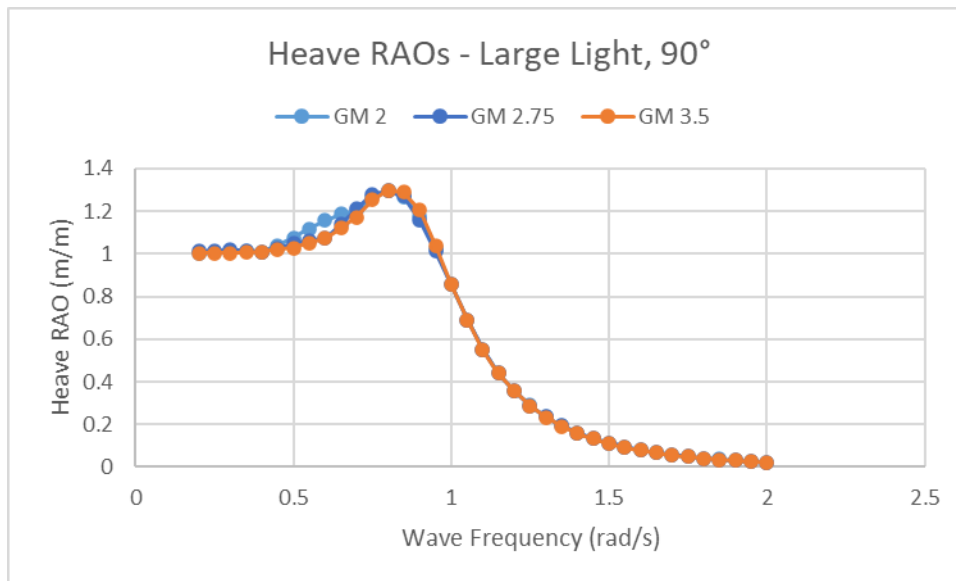
Figure 3-29: Heave RAOs by GM, Beam Seas, Large-Light
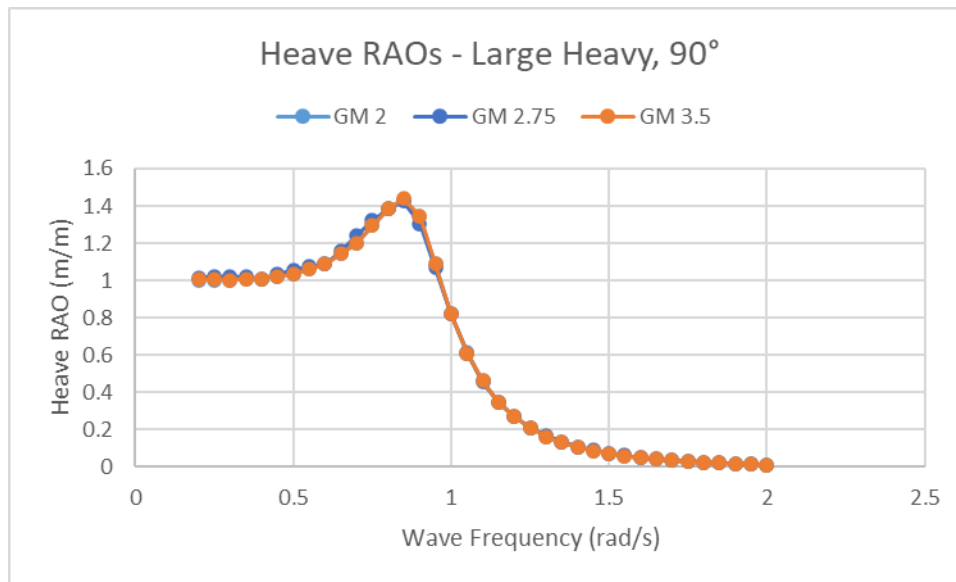
Figure 3-30: Heave RAOs by GM, Beam Seas, Large-Heavy
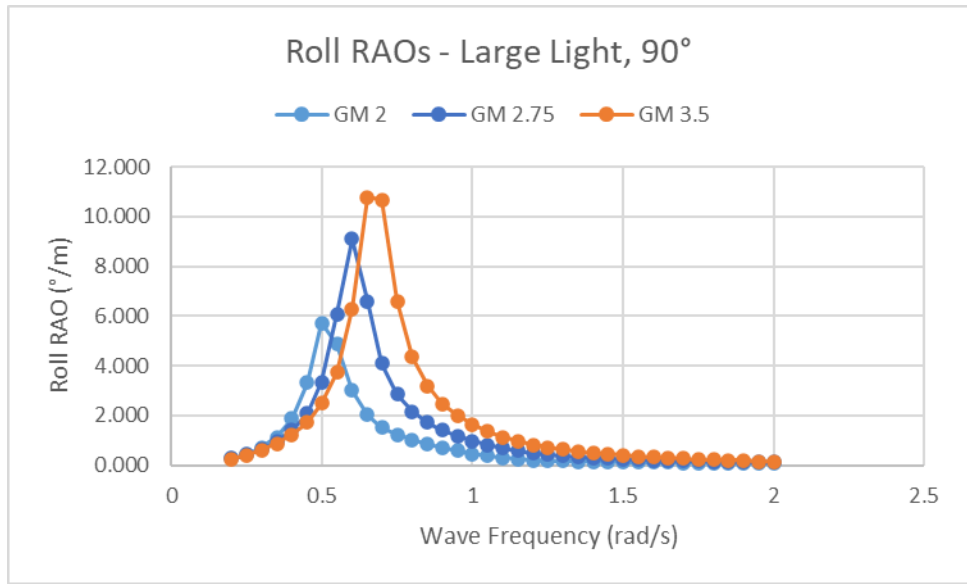
Figure 3-31: Roll RAOs by GM, Beam Seas, Large-Light
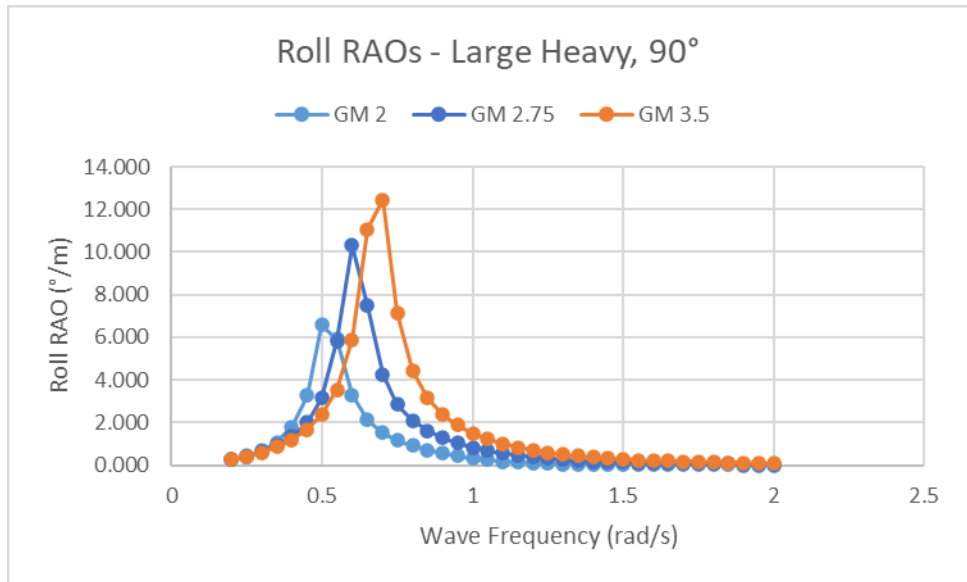
Figure 3-32: Roll RAOs by GM, Beam Seas, Large-Heavy
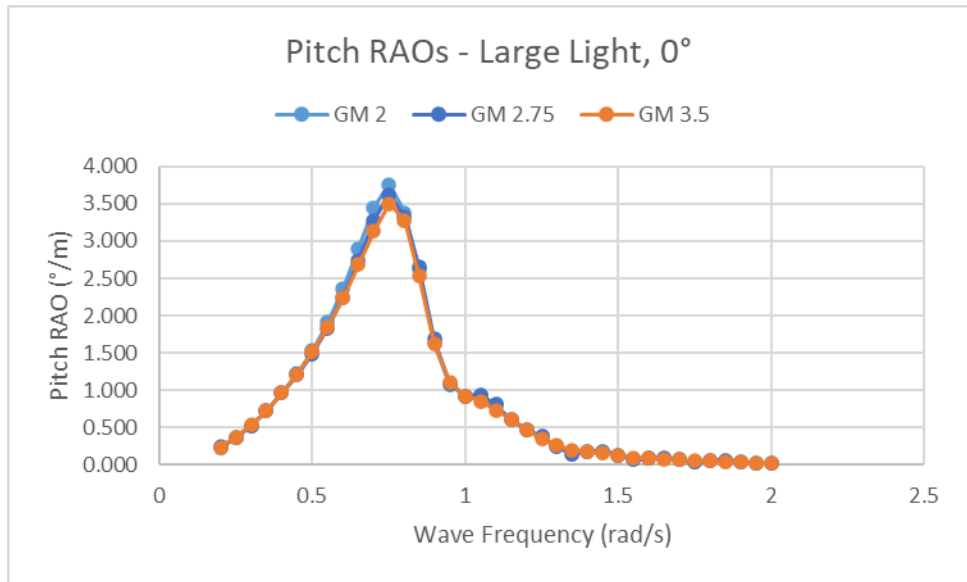
Figure 3-33: Pitch RAOs by GM, Head Seas, Large-Light
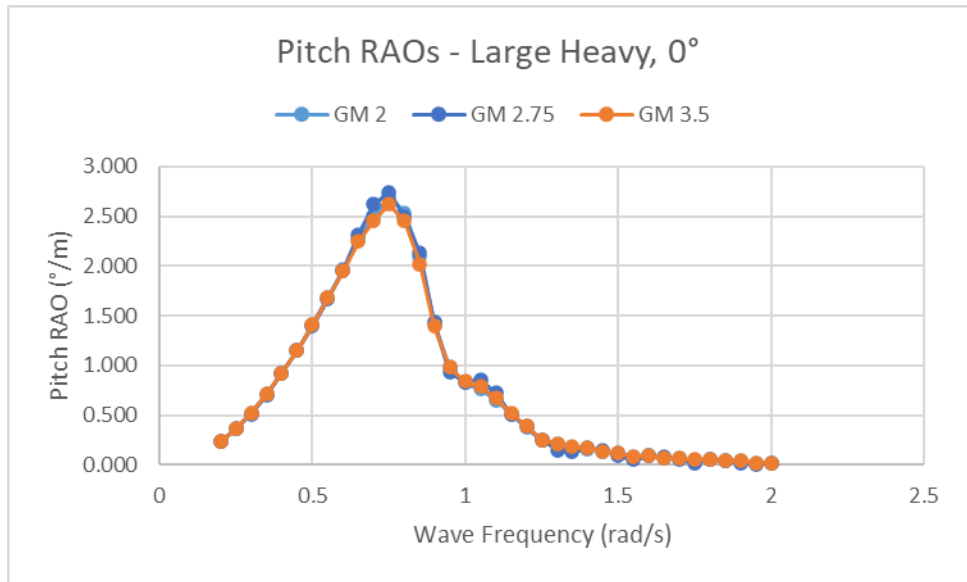
Figure 3-34: Pitch RAOs by GM, Head Seas, Large-Heavy
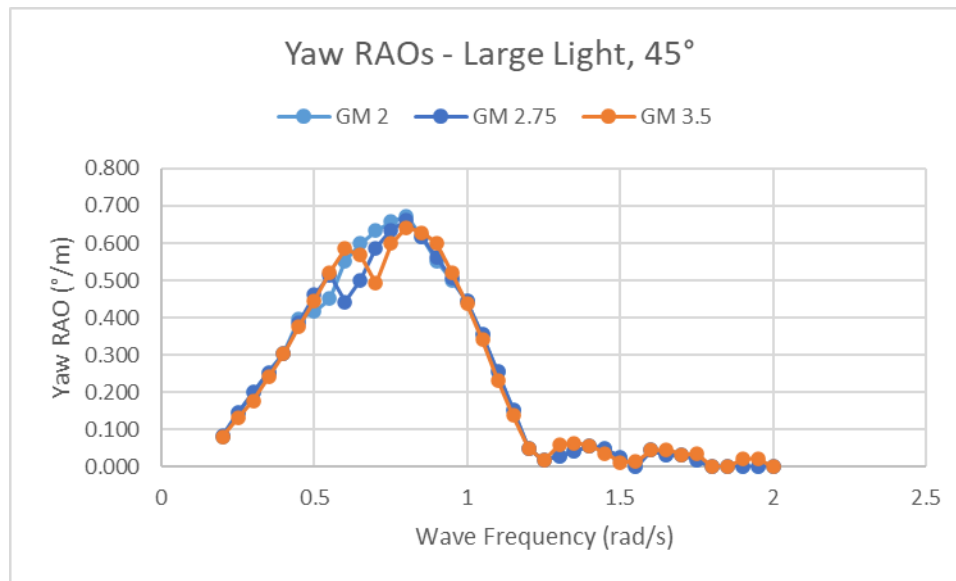
Figure 3-35: Yaw RAOs by GM, Bow Quartering, Large-Light
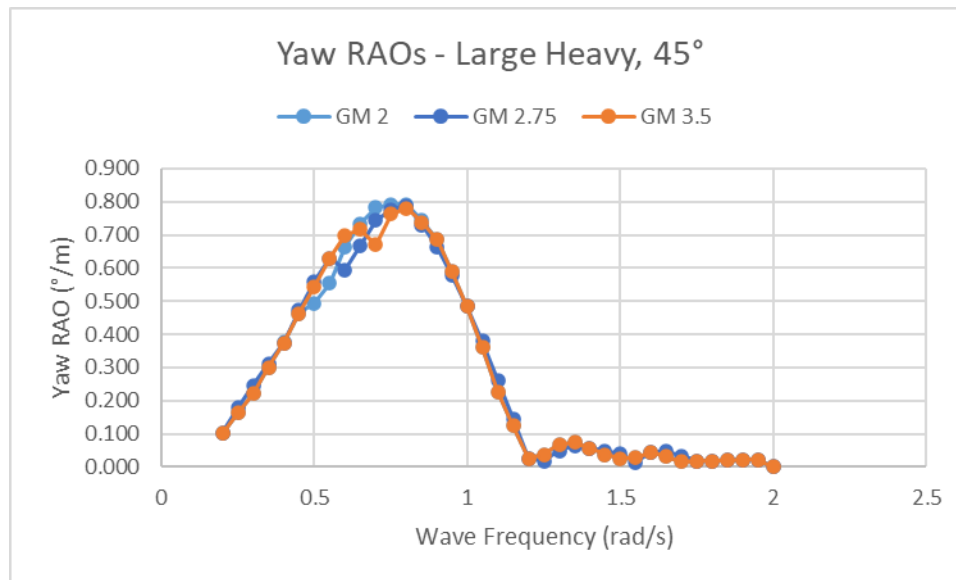
Figure 3-36: Yaw RAOs by GM, Bow Quartering, Large-Heavy

It is evident from the figures presented above that varying GM has a much larger effect on the pitch and roll motions than any of the other degrees of freedom. In particular, the

translational degrees of freedom (surge, sway, and heave), are practically unaffected by a change in GM. This is as expected, since the metacentric height should in theory only affect the righting moments, and should not have any effect on the horizontal motions.

3.3   Time Domain Results

Simply using the current operating limits for crew transfer, ($H_s < 4.0$ m/s), the following percentages of operable time for the winter and summer season are obtained:

- % Operable (Summer) = 93.15 %
- % Operable (Winter) = 36.65 %

This shows that with the current limits, it is already possible to complete crew and cargo transfer 93.15% of the time during the summer season, compared to 36.65% in the winter season. This illustrates the importance of having more rigorously defined limits for the winter season, in order to increase this operational percentage of time to a practical level.

3.3.1   Operability Contours

Through the use of the methods described in section 2.2.1 above, peak period-specific operability limits were determined for each heading. Every single one of the different ships and loading conditions were within the operability limits of the FROG-6 capsule at 6.0 m H_s in the head seas condition. This indicates the possibility that if the OSV is capable of effectively weathervaning (changing heading to the most favourable – into the waves), then the wave height limit for crew and cargo transfer could be raised as high as a

flat 6.0 m. However, it should be noted that in the real environment, wave spectra are not unidirectional, and weathervaning may not always be possible due to operation-specific reasons, so the other headings should be considered more carefully. The limiting wave heights for each peak energy period in bow quartering and beam seas are therefore shown in Table 3-2 and Table 3-3 below, respectively:

Table 3-2: Operability Limits for Bow Quartering Seas

OSV Properties			Limiting Significant Wave Heights (m) - Bow Quartering				
Length (m)	Cb	GMt (m)	Tp = 6.0 s	Tp = 7.5 s	Tp = 11.5 s	Tp = 15.5 s	Tp = 18.0 s
70.0	0.65	2.00	5.00	6.00	5.61	6.00	6.00
70.0	0.79	2.00	5.00	6.00	6.00	6.00	6.00
80.0	0.65	2.00	5.00	6.00	5.88	6.00	6.00
80.0	0.79	2.00	5.00	6.00	6.00	6.00	6.00
90.0	0.65	2.00	5.00	6.00	5.94	6.00	6.00
90.0	0.79	2.00	5.00	6.00	6.00	6.00	6.00
70.0	0.65	2.75	5.00	5.67	5.60	6.00	6.00
70.0	0.79	2.75	5.00	6.00	6.00	6.00	6.00
80.0	0.65	2.75	5.00	6.00	6.00	6.00	6.00
80.0	0.79	2.75	5.00	6.00	6.00	6.00	6.00
90.0	0.65	2.75	5.00	6.00	6.00	6.00	6.00
90.0	0.79	2.75	5.00	6.00	6.00	6.00	6.00

Table 3-3: Operability Limits for Beam Seas

OSV Properties			Limiting Significant Wave Heights (m) - Bow Quartering				
Length (m)	Cb	GMt (m)	Tp = 6.0 s	Tp = 7.5 s	Tp = 11.5 s	Tp = 15.5 s	Tp = 18.0 s
70.0	0.65	2.00	4.20	4.08	4.59	5.57	6.00
70.0	0.79	2.00	4.27	4.09	4.61	5.59	6.00
80.0	0.65	2.00	4.92	4.65	4.70	5.83	6.00
80.0	0.79	2.00	5.00	4.67	4.70	5.90	6.00
90.0	0.65	2.00	5.00	5.24	5.15	6.00	6.00
90.0	0.79	2.00	5.00	5.12	4.79	5.93	6.00
70.0	0.65	2.75	3.90	3.74	4.39	5.59	6.00
70.0	0.79	2.75	3.93	3.57	4.33	5.56	6.00
80.0	0.65	2.75	4.61	4.36	4.84	5.81	6.00
80.0	0.79	2.75	4.65	4.33	4.88	5.83	6.00
90.0	0.65	2.75	5.00	4.93	4.94	6.00	6.00
90.0	0.79	2.75	5.00	4.91	4.97	6.00	6.00

The above period-specific operability limits and linear interpolation were used to create new operability contours, which are presented in Figure 3-37 through Figure 3-43 below. Note that the winter operability contours are shown below for illustration purposes. The summer operability contours have the exact same shape, but with different probabilities of occurrence for each wave height/period combination; see Appendix B for the wave height/period probability distributions for both winter and summer months. As such, they are not presented.

In the contours below:

- The green region identifies seastates where all 3 OSV lengths are in the operable region.

- The blue region identifies seastates where the 80 m and 90 m long OSVs are in the operable region.

- The orange region identifies seastates where only the 90 m long OSV is in the operable region.

- The red region identifies seastates where none of the considered OSV lengths are in the operable region.

Figure 3-37

Cell: 337 (48.25°N, 46.5°W)

Significant Wave Height and Period - Joint Probability Distribution for Winter Months

Significant Wave Height (m)

Wave Period (s)	0-1	1-2	2-3	3-4	4-5	5-6	6-7	7-8	8-9	9-10	10-11	11-12	12-13	13-14	14-15	15-16	16-17
0-1	0	0	0	0	0	0	0	0	0	0	0	0	0	0	0	0	0
1-2	0	0	0	0	0	0	0	0	0	0	0	0	0	0	0	0	0
2-3	0	0	0	0	0	0	0	0	0	0	0	0	0	0	0	0	0
3-4	0	0	0	0	0	0	0	0	0	0	0	0	0	0	0	0	0
4-5	0.005	0.0085	0	0	0	0	0	0	0	0	0	0	0	0	0	0	0
5-6	0	0.01175	0.03125	0.001	0	0	0	0	0	0	0	0	0	0	0	0	0
6-7	0	0.0185	0.45425	0.12975	0.001	0	0	0	0	0	0	0	0	0	0	0	0
7-8	0	0.08275	1.146	1.98925	0.286	0.0035	0	0	0	0	0	0	0	0	0	0	0
8-9	0	0.18275	1.615	3.15875	3.0675	0.242	0.002	0	0	0	0	0	0	0	0	0	0
9-10	0	0.129	2.51125	3.79725	5.38025	2.67625	0.18325	0.0005	0	0	0	0	0	0	0	0	0
10-11	0	0.1165	2.48575	5.481	4.69975	5.21725	1.92875	0.14375	0.00675	0	0	0	0	0	0	0	0
11-12	0	0.02425	1.29725	5.7355	5.09125	3.546	3.59275	1.48975	0.21625	0.0075	0	0	0	0	0	0	0
12-13	0	0.045	0.844	2.59625	3.0375	1.95	1.62475	1.9135	1.13175	0.529	0.056	0.0005	0	0	0	0	0
13-14	0	0.0105	0.3005	1.6075	2.3585	1.74375	1.16225	0.725	0.68925	0.877	0.718	0.189	0.009	0	0	0	0
14-15	0	0.0035	0.06825	0.6625	1.6475	1.40425	0.749	0.396	0.2095	0.23375	0.312	0.384	0.215	0.023	0	0	0
15-16	0	0	0.001	0.03625	0.10325	0.243	0.177	0.07425	0.0415	0.013	0.019	0.03075	0.107	0.096	0.009	0	0
16-17	0	0	0.0165	0.04325	0.115	0.08175	0.02025	0.0115	0.0045	0	0.0005	0.00475	0.001	0.03025	0.0235	0.00925	0
17-18	0	0	0	0.00225	0.02575	0.024	0.00475	0.0025	0	0	0	0	0	0	0.0005	0.00375	0
18-19	0	0	0	0	0	0	0	0	0	0	0	0	0	0	0	0	0
19-20	0	0	0	0	0	0	0	0	0	0	0	0	0	0	0	0	0

51.95%   6.04%   9.63%   32.38%

Figure 3-37: Operability Contours - Cb = 0.65, Beam Seas, GM = 2.0 m

---

Figure 3-38

Cell: 337 (48.25°N, 46.5°W)

Significant Wave Height and Period - Joint Probability Distribution for Winter Months

Significant Wave Height (m)

Wave Period (s)	0-1	1-2	2-3	3-4	4-5	5-6	6-7	7-8	8-9	9-10	10-11	11-12	12-13	13-14	14-15	15-16	16-17
0-1	0	0	0	0	0	0	0	0	0	0	0	0	0	0	0	0	0
1-2	0	0	0	0	0	0	0	0	0	0	0	0	0	0	0	0	0
2-3	0	0	0	0	0	0	0	0	0	0	0	0	0	0	0	0	0
3-4	0	0	0	0	0	0	0	0	0	0	0	0	0	0	0	0	0
4-5	0.005	0.0085	0	0	0	0	0	0	0	0	0	0	0	0	0	0	0
5-6	0	0.01175	0.03125	0.001	0	0	0	0	0	0	0	0	0	0	0	0	0
6-7	0	0.0185	0.45425	0.12975	0.001	0	0	0	0	0	0	0	0	0	0	0	0
7-8	0	0.08275	1.146	1.98925	0.286	0.0035	0	0	0	0	0	0	0	0	0	0	0
8-9	0	0.18275	1.615	3.15875	3.0675	0.242	0.002	0	0	0	0	0	0	0	0	0	0
9-10	0	0.129	2.51125	3.79725	5.38025	2.67625	0.18325	0.0005	0	0	0	0	0	0	0	0	0
10-11	0	0.1165	2.48575	5.481	4.69975	5.21725	1.92875	0.14375	0.00675	0	0	0	0	0	0	0	0
11-12	0	0.02425	1.29725	5.7355	5.09125	3.546	3.59275	1.48975	0.21625	0.0075	0	0	0	0	0	0	0
12-13	0	0.045	0.844	2.59625	3.0375	1.95	1.62475	1.9135	1.13175	0.529	0.056	0.0005	0	0	0	0	0
13-14	0	0.0105	0.3005	1.6075	2.3585	1.74375	1.16225	0.725	0.68925	0.877	0.718	0.189	0.009	0	0	0	0
14-15	0	0.0035	0.06825	0.6625	1.6475	1.40425	0.749	0.396	0.2095	0.23375	0.312	0.384	0.215	0.023	0	0	0
15-16	0	0	0.001	0.03625	0.10325	0.243	0.177	0.07425	0.0415	0.013	0.019	0.03075	0.107	0.096	0.009	0	0
16-17	0	0	0.0165	0.04325	0.115	0.08175	0.02025	0.0115	0.0045	0	0.0005	0.00475	0.001	0.03025	0.0235	0.00925	0
17-18	0	0	0	0.00225	0.02575	0.024	0.00475	0.0025	0	0	0	0	0	0	0.0005	0.00375	0
18-19	0	0	0	0	0	0	0	0	0	0	0	0	0	0	0	0	0
19-20	0	0	0	0	0	0	0	0	0	0	0	0	0	0	0	0	0

52.43%   5.87%   4.22%   37.48%

Figure 3-38: Operability Contours - Cb = 0.79, Beam Seas, GM = 2.0 m

---

Figure 3-39

Cell: 337 (48.25°N, 46.5°W)

Significant Wave Height and Period - Joint Probability Distribution for Winter Months

Significant Wave Height (m)

Wave Period (s)	0-1	1-2	2-3	3-4	4-5	5-6	6-7	7-8	8-9	9-10	10-11	11-12	12-13	13-14	14-15	15-16	16-17
0-1	0	0	0	0	0	0	0	0	0	0	0	0	0	0	0	0	0
1-2	0	0	0	0	0	0	0	0	0	0	0	0	0	0	0	0	0
2-3	0	0	0	0	0	0	0	0	0	0	0	0	0	0	0	0	0
3-4	0	0	0	0	0	0	0	0	0	0	0	0	0	0	0	0	0
4-5	0.005	0.0085	0	0	0	0	0	0	0	0	0	0	0	0	0	0	0
5-6	0	0.01175	0.03125	0.001	0	0	0	0	0	0	0	0	0	0	0	0	0
6-7	0	0.0185	0.45425	0.12975	0.001	0	0	0	0	0	0	0	0	0	0	0	0
7-8	0	0.08275	1.146	1.98925	0.286	0.0035	0	0	0	0	0	0	0	0	0	0	0
8-9	0	0.18275	1.615	3.15875	3.0675	0.242	0.002	0	0	0	0	0	0	0	0	0	0
9-10	0	0.129	2.51125	3.79725	5.38025	2.67625	0.18325	0.0005	0	0	0	0	0	0	0	0	0
10-11	0	0.1165	2.48575	5.481	4.69975	5.21725	1.92875	0.14375	0.00675	0	0	0	0	0	0	0	0
11-12	0	0.02425	1.29725	5.7355	5.09425	3.546	3.59275	1.48975	0.21625	0.0075	0	0	0	0	0	0	0
12-13	0	0.045	0.844	2.59625	3.0375	1.95	1.62475	1.9135	1.13175	0.529	0.056	0.0005	0	0	0	0	0
13-14	0	0.0105	0.3005	1.6075	2.3585	1.74375	1.16225	0.725	0.68925	0.877	0.718	0.189	0.009	0	0	0	0
14-15	0	0.0035	0.06825	0.6625	1.6475	1.40425	0.749	0.396	0.2095	0.23375	0.312	0.384	0.215	0.023	0	0	0
15-16	0	0	0.001	0.03625	0.10325	0.243	0.177	0.07425	0.0415	0.013	0.019	0.03075	0.107	0.096	0.009	0	0
16-17	0	0	0.0165	0.04325	0.115	0.08175	0.02025	0.0115	0.0045	0	0.0005	0.00475	0.001	0.03025	0.0235	0.00925	0
17-18	0	0	0	0.00225	0.02575	0.024	0.00375	0.0025	0	0	0	0	0	0	0.0005	0.00375	0
18-19	0	0	0	0	0	0	0	0	0	0	0	0	0	0	0	0	0
19-20	0	0	0	0	0	0	0	0	0	0	0	0	0	0	0	0	0

46.19%   12.11%   5.59%   36.11%

Figure 3-39: Operability Contours - Cb = 0.65, Beam Seas, GM = 2.75 m

58

Figure 3-40

Cell: 337 (48.25°N, 46.5°W)

Significant Wave Height and Period - Joint Probability Distribution for Winter Months

Significant Wave Height (m)

Wave Period (s)	0-1	1-2	2-3	3-4	4-5	5-6	6-7	7-8	8-9	9-10	10-11	11-12	12-13	13-14	14-15	15-16	16-17
0-1	0	0	0	0	0	0	0	0	0	0	0	0	0	0	0	0	0
1-2	0	0	0	0	0	0	0	0	0	0	0	0	0	0	0	0	0
2-3	0	0	0	0	0	0	0	0	0	0	0	0	0	0	0	0	0
3-4	0	0	0	0	0	0	0	0	0	0	0	0	0	0	0	0	0
4-5	0.005	0.0085	0	0	0	0	0	0	0	0	0	0	0	0	0	0	0
5-6	0	0.01175	0.03125	0.001	0	0	0	0	0	0	0	0	0	0	0	0	0
6-7	0	0.0185	0.45425	0.12975	0.001	0	0	0	0	0	0	0	0	0	0	0	0
7-8	0	0.08275	1.146	1.98925	0.286	0.0035	0	0	0	0	0	0	0	0	0	0	0
8-9	0	0.18275	1.615	3.15875	3.0675	0.242	0.002	0	0	0	0	0	0	0	0	0	0
9-10	0	0.129	2.51125	3.79725	5.38025	2.67625	0.18325	0.0005	0	0	0	0	0	0	0	0	0
10-11	0	0.1165	2.48575	5.481	4.69475	5.21725	1.92875	0.14375	0.00675	0	0	0	0	0	0	0	0
11-12	0	0.02425	1.29725	5.7355	5.09425	3.546	3.59275	1.48975	0.21625	0.0075	0	0	0	0	0	0	0
12-13	0	0.045	0.844	2.59625	3.03775	1.95	1.62475	1.9135	1.13175	0.529	0.056	0.0005	0	0	0	0	0
13-14	0	0.0105	0.3005	1.6075	2.3585	1.74375	1.16225	0.725	0.68925	0.877	0.718	0.189	0.009	0	0	0	0
14-15	0	0.0035	0.06825	0.6625	1.6475	1.40425	0.749	0.396	0.2095	0.23375	0.312	0.384	0.215	0.023	0	0	0
15-16	0	0	0.001	0.03625	0.10325	0.245	0.177	0.07425	0.0415	0.013	0.019	0.03075	0.107	0.096	0.009	0	0
16-17	0	0	0.0165	0.04325	0.115	0.08175	0.02025	0.0115	0.0045	0	0.0005	0.00475	0.001	0.03025	0.0235	0.00925	0
17-18	0	0	0	0.00225	0.02575	0.024	0.00475	0.0025	0	0	0	0	0	0	0.0005	0.00375	0
18-19	0	0	0	0	0	0	0	0	0	0	0	0	0	0	0	0	0
19-20	0	0	0	0	0	0	0	0	0	0	0	0	0	0	0	0	0

43.81%   14.88%   5.61%   35.71%

Figure 3-40: Operability Contours - Cb = 0.79, Beam Seas, GM = 2.75 m

Figure 3-41

Cell: 337 (48.25°N, 46.5°W)

Significant Wave Height and Period - Joint Probability Distribution for Winter Months

Significant Wave Height (m)

Wave Period (s)	0-1	1-2	2-3	3-4	4-5	5-6	6-7	7-8	8-9	9-10	10-11	11-12	12-13	13-14	14-15	15-16	16-17
0-1	0	0	0	0	0	0	0	0	0	0	0	0	0	0	0	0	0
1-2	0	0	0	0	0	0	0	0	0	0	0	0	0	0	0	0	0
2-3	0	0	0	0	0	0	0	0	0	0	0	0	0	0	0	0	0
3-4	0	0	0	0	0	0	0	0	0	0	0	0	0	0	0	0	0
4-5	0.005	0.0085	0	0	0	0	0	0	0	0	0	0	0	0	0	0	0
5-6	0	0.01175	0.03125	0.001	0	0	0	0	0	0	0	0	0	0	0	0	0
6-7	0	0.0185	0.45425	0.12975	0.001	0	0	0	0	0	0	0	0	0	0	0	0
7-8	0	0.08275	1.146	1.98925	0.286	0.0035	0	0	0	0	0	0	0	0	0	0	0
8-9	0	0.18275	1.615	3.15875	3.0675	0.242	0.002	0	0	0	0	0	0	0	0	0	0
9-10	0	0.129	2.51125	3.79725	5.38025	2.67625	0.18325	0.0005	0	0	0	0	0	0	0	0	0
10-11	0	0.1165	2.48575	5.481	4.69475	5.21725	1.92875	0.14375	0.00675	0	0	0	0	0	0	0	0
11-12	0	0.02425	1.29725	5.7355	5.09425	3.546	3.59275	1.48975	0.21625	0.0075	0	0	0	0	0	0	0
12-13	0	0.045	0.844	2.59625	3.03775	1.95	1.62475	1.9135	1.13175	0.529	0.056	0.0005	0	0	0	0	0
13-14	0	0.0105	0.3005	1.6075	2.3585	1.74375	1.16225	0.725	0.68925	0.877	0.718	0.189	0.009	0	0	0	0
14-15	0	0.0035	0.06825	0.6625	1.6475	1.40425	0.749	0.396	0.2095	0.23375	0.312	0.384	0.215	0.023	0	0	0
15-16	0	0	0.001	0.03625	0.10325	0.245	0.177	0.07425	0.0415	0.013	0.019	0.03075	0.107	0.096	0.009	0	0
16-17	0	0	0.0165	0.04325	0.115	0.08175	0.02025	0.0115	0.0045	0	0.0005	0.00475	0.001	0.03025	0.0235	0.00925	0
17-18	0	0	0	0.00225	0.02575	0.024	0.00475	0.0025	0	0	0	0	0	0	0.0005	0.00375	0
18-19	0	0	0	0	0	0	0	0	0	0	0	0	0	0	0	0	0
19-20	0	0	0	0	0	0	0	0	0	0	0	0	0	0	0	0	0

75.06%   3.12%   0.70%   21.12%

Figure 3-41: Operability Contours - Cb = 0.65, Bow Quartering, GM = 2.0 m

Figure 3-42

Cell: 337 (48.25°N, 46.5°W)

Significant Wave Height and Period - Joint Probability Distribution for Winter Months

Significant Wave Height (m)

Wave Period (s)	0-1	1-2	2-3	3-4	4-5	5-6	6-7	7-8	8-9	9-10	10-11	11-12	12-13	13-14	14-15	15-16	16-17
0-1	0	0	0	0	0	0	0	0	0	0	0	0	0	0	0	0	0
1-2	0	0	0	0	0	0	0	0	0	0	0	0	0	0	0	0	0
2-3	0	0	0	0	0	0	0	0	0	0	0	0	0	0	0	0	0
3-4	0	0	0	0	0	0	0	0	0	0	0	0	0	0	0	0	0
4-5	0.005	0.0085	0	0	0	0	0	0	0	0	0	0	0	0	0	0	0
5-6	0	0.01175	0.03125	0.001	0	0	0	0	0	0	0	0	0	0	0	0	0
6-7	0	0.0185	0.45425	0.12975	0.001	0	0	0	0	0	0	0	0	0	0	0	0
7-8	0	0.08275	1.146	1.98925	0.286	0.0035	0	0	0	0	0	0	0	0	0	0	0
8-9	0	0.18275	1.615	3.15875	3.0675	0.242	0.002	0	0	0	0	0	0	0	0	0	0
9-10	0	0.129	2.51125	3.79725	5.38025	2.67625	0.18325	0.0005	0	0	0	0	0	0	0	0	0
10-11	0	0.1165	2.48575	5.481	4.69475	5.21725	1.92875	0.14375	0.00675	0	0	0	0	0	0	0	0
11-12	0	0.02425	1.29725	5.7355	5.09425	3.546	3.59275	1.48975	0.21625	0.0075	0	0	0	0	0	0	0
12-13	0	0.045	0.844	2.59625	3.03775	1.95	1.62475	1.9135	1.13175	0.529	0.056	0.0005	0	0	0	0	0
13-14	0	0.0105	0.3005	1.6075	2.3585	1.74375	1.16225	0.725	0.68925	0.877	0.718	0.189	0.009	0	0	0	0
14-15	0	0.0035	0.06825	0.6625	1.6475	1.40425	0.749	0.396	0.2095	0.23375	0.312	0.384	0.215	0.023	0	0	0
15-16	0	0	0.001	0.03625	0.10325	0.245	0.177	0.07425	0.0415	0.013	0.019	0.03075	0.107	0.096	0.009	0	0
16-17	0	0	0.0165	0.04325	0.115	0.08175	0.02025	0.0115	0.0045	0	0.0005	0.00475	0.001	0.03025	0.0235	0.00925	0
17-18	0	0	0	0.00225	0.02575	0.024	0.00475	0.0025	0	0	0	0	0	0	0.0005	0.00375	0
18-19	0	0	0	0	0	0	0	0	0	0	0	0	0	0	0	0	0
19-20	0	0	0	0	0	0	0	0	0	0	0	0	0	0	0	0	0

74.01%   5.59%   20.41%

Figure 3-42: Operability Contours - Cb = 0.65, Bow Quartering, GM = 2.75 m

The operability contours presented above provide a visual representation of the benefit gained through switching to a larger OSV. It is evident that switching to a larger OSV in general results in an increase in percentage operability, especially so for the beam seas cases.

There are several loading conditions where changing the OSV length did not have any impact on the operability contours. I.e., none of the considered vessels exceeded the deck velocity limits, for any peak period, up to a wave height of 6.0 m. This is the case for all the head seas simulations, and for all the bow quartering simulations with the "heavy" OSVs (Cb = 0.79). The general operability contour for this case is shown in Figure 3-43 below.

Cell: 337 (48.25°N, 46.5°W)	Significant Wave Height and Period - Joint Probability Distribution for Winter Months																
	Significant Wave Height (m)																
Wave Period (s)	0-1	1-2	2-3	3-4	4-5	5-6	6-7	7-8	8-9	9-10	10-11	11-12	12-13	13-14	14-15	15-16	16-17
0-1	0	0	0	0	0	0	0	0	0	0	0	0	0	0	0	0	0
1-2	0	0	0	0	0	0	0	0	0	0	0	0	0	0	0	0	0
2-3	0	0	0	0	0	0	0	0	0	0	0	0	0	0	0	0	0
3-4	0	0	0	0	0	0	0	0	0	0	0	0	0	0	0	0	0
4-5	0.005	0.0085	0	0	0	0	0	0	0	0	0	0	0	0	0	0	0
5-6	0	0.01175	0.03125	0.001	0	0	0	0	0	0	0	0	0	0	0	0	0
6-7	0	0.0185	0.45425	0.12975	0.001	0	0	0	0	0	0	0	0	0	0	0	0
7-8	0	0.08275	1.146	1.98925	0.286	0.0035	0	0	0	0	0	0	0	0	0	0	0
8-9	0	0.18275	1.615	3.15875	3.0675	0.242	0.002	0	0	0	0	0	0	0	0	0	0
9-10	0	0.129	2.51125	3.79725	5.38025	2.67625	0.18325	0.0005	0	0	0	0	0	0	0	0	0
10-11	0	0.1165	2.48575	5.481	4.69475	5.21725	1.92875	0.14375	0.00675	0	0	0	0	0	0	0	0
11-12	0	0.02425	1.29725	5.7355	5.09425	3.546	3.59275	1.48975	0.21625	0.0075	0	0	0	0	0	0	0
12-13	0	0.045	0.844	2.59625	3.03775	1.95	1.62475	1.9135	1.13175	0.529	0.056	0.0005	0	0	0	0	0
13-14	0	0.0105	0.3005	1.6075	2.3585	1.74375	1.16225	0.725	0.68925	0.877	0.718	0.189	0.009	0	0	0	0
14-15	0	0.0035	0.06825	0.6625	1.6475	1.40425	0.749	0.396	0.2095	0.23375	0.312	0.384	0.215	0.023	0	0	0
15-16	0	0	0.001	0.03625	0.10325	0.245	0.177	0.07425	0.0415	0.013	0.019	0.03075	0.107	0.096	0.009	0	0
16-17	0	0	0.0165	0.04325	0.115	0.08175	0.02025	0.0115	0.0045	0	0.0005	0.00475	0.001	0.03025	0.0235	0.00925	0
17-18	0	0	0	0.00225	0.02575	0.024	0.00475	0.0025	0	0	0	0	0	0	0.0005	0.00375	0
18-19	0	0	0	0	0	0	0	0	0	0	0	0	0	0	0	0	0
19-20	0	0	0	0	0	0	0	0	0	0	0	0	0	0	0	0	0

79.59%   20.41%

Figure 3-43: Operability Contours - All Head Seas Cases, and Cb = 0.79 Bow Quartering

The operability percentages shown above are summarized below in Table 3-4 and Table 3-5. As noted above, the operability percentages for all ships in the head seas case were:

- % Operable (Summer) = 99.26 %

- % Operable (Winter) = 79.59 %

Table 3-4: Operability Percentages for Bow Quartering Seas

Length (m)	Cb	GMt (m)	Winter Operational Percentage (%)	Summer Operational Percentage (%)
70.0	0.65	2.00	75.06	98.83
70.0	0.79	2.00	79.59	99.26
80.0	0.65	2.00	78.18	99.13
80.0	0.79	2.00	79.59	99.26
90.0	0.65	2.00	78.88	99.20
90.0	0.79	2.00	79.59	99.26
70.0	0.65	2.75	74.01	98.72
70.0	0.79	2.75	79.59	99.26
80.0	0.65	2.75	79.59	99.26
80.0	0.79	2.75	79.59	99.26
90.0	0.65	2.75	79.59	99.26
90.0	0.79	2.75	79.59	99.26

Table 3-5: Operability Percentages for Beam Seas

Length (m)	Cb	GMt (m)	Winter Operational Percentage (%)	Summer Operational Percentage (%)
70.0	0.65	2.00	51.95	95.08
70.0	0.79	2.00	52.43	95.16
80.0	0.65	2.00	58.00	96.42
80.0	0.79	2.00	58.30	96.46
90.0	0.65	2.00	67.62	98.09
90.0	0.79	2.00	62.52	97.50
70.0	0.65	2.75	46.19	92.54
70.0	0.79	2.75	43.81	90.74
80.0	0.65	2.75	58.30	96.27
80.0	0.79	2.75	58.69	96.31
90.0	0.65	2.75	63.89	97.57
90.0	0.79	2.75	64.29	97.63

The operability percentages for the winter season have been plotted in Figure 3-44, Figure 3-45, Figure 3-46, and Figure 3-47 below. The red lines on these plots denote the operability percentage of 36.65 % that is obtained through the flat H_s limit of 4.0 m.

Note: The corresponding plots for the summer season have not been included since they display the exact same trends, just with less relative difference in % operability.
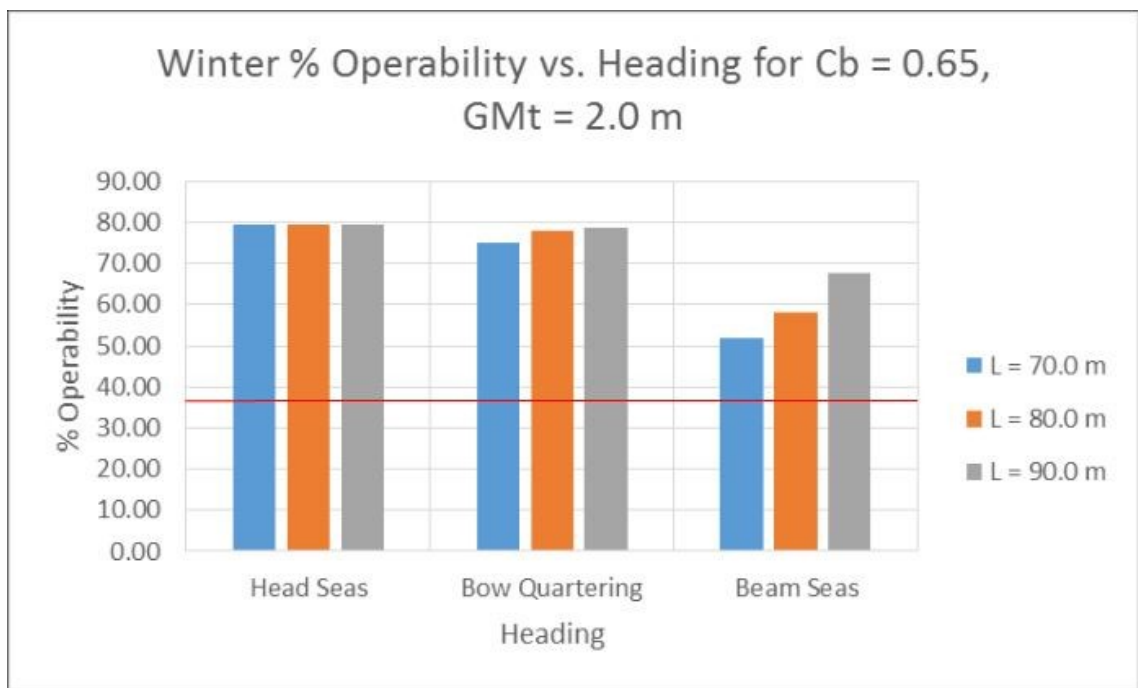
Figure 3-44: Winter % Operability vs. Heading for C_b = 0.65, GM_t = 2.0 m
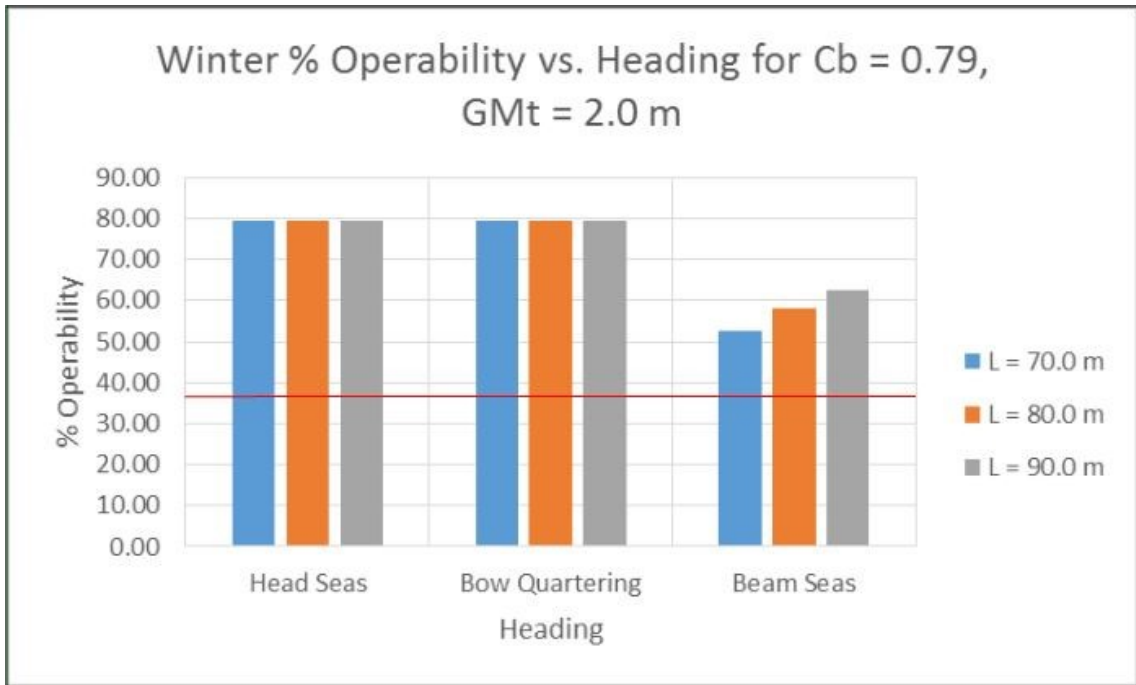
Figure 3-45: Winter % Operability vs. Heading for C_b = 0.79, GM_t = 2.0 m

From Figure 3-44 and Figure 3-45 above, it can easily be seen that an increase in ship size results in a corresponding increase in operability percentage.
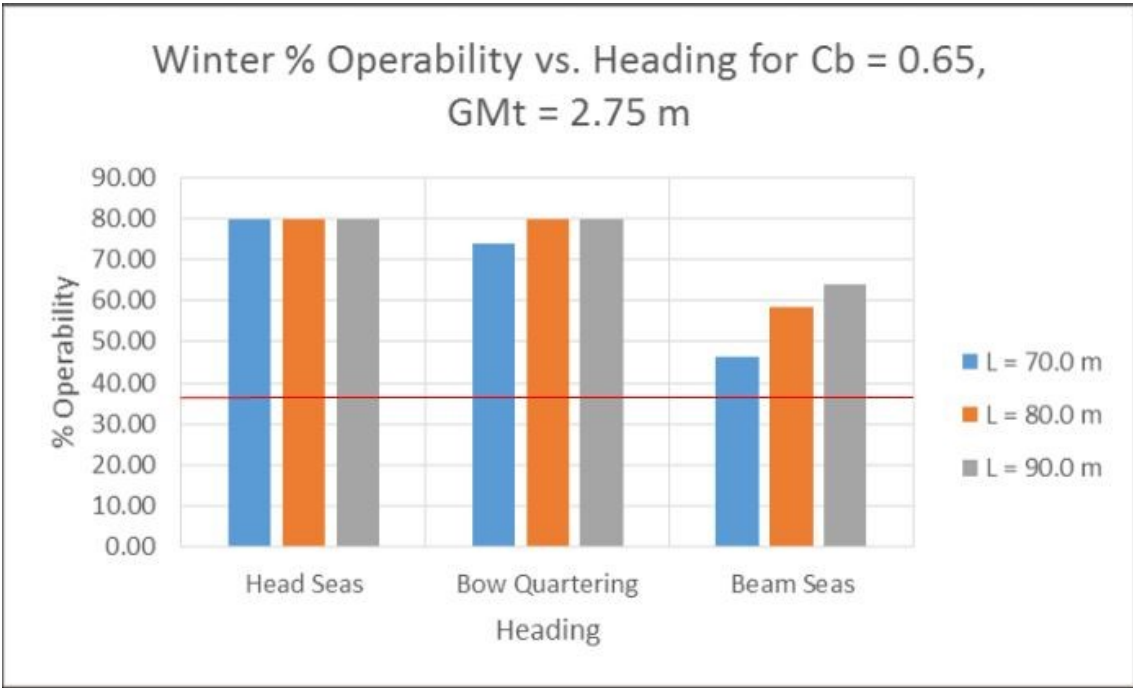
Figure 3-46: Winter % Operability vs. Heading for C_b = 0.65, GM_t = 2.75 m
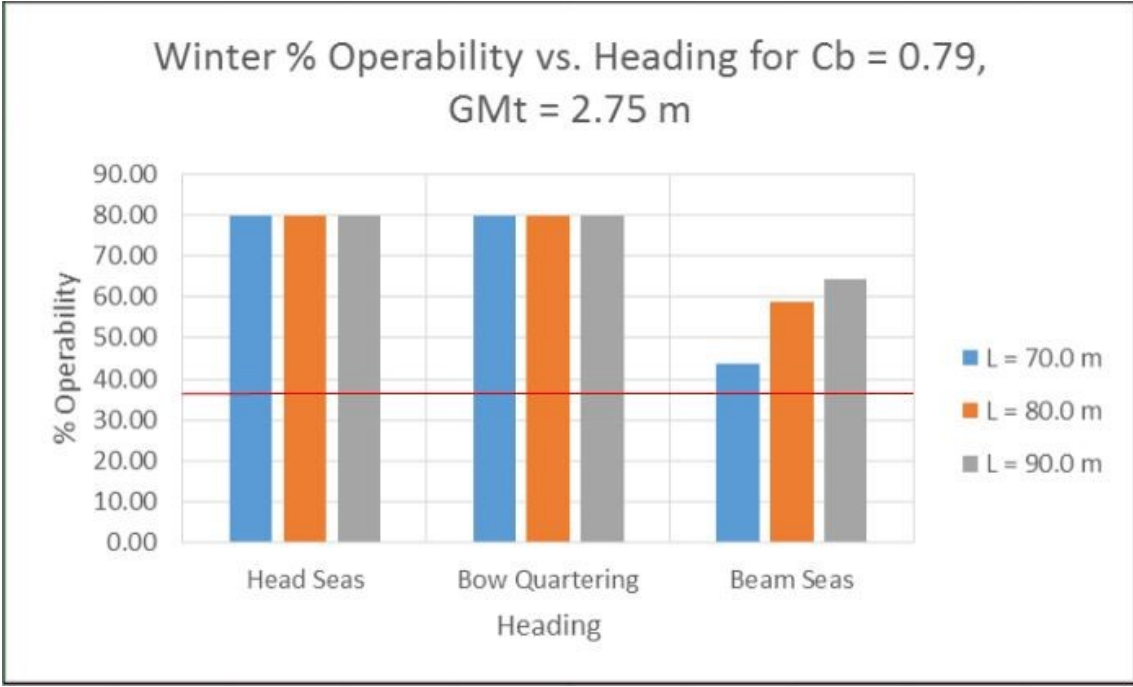
Figure 3-47: Winter % Operability vs. Heading for C_b = 0.79, GM_t = 2.75 m

Figure 3-46 and Figure 3-47 display the same trend as was seen for the case where GM_t = 2.0 m, that is, an increase in operability percentage with an increasing ship size.

Note: There are head seas and bow quartering cases above where the operability percentages remain constant with increasing ship length. However, in all cases the deck velocities did decrease in magnitude with an increasing ship length, it is just that the overall velocity magnitude was small enough that the artificially imposed limit of H_s = 6.0 m was reached before the FROG-6 capsule limits.

Assuming:

   I.   Waves are equally likely to occur from any direction.

  II.   The OSV will attempt to "weathervane" head into the waves, but will still experience waves coming into the beam and bow-quarter.

Then we can determine the total operational percentages by simply taking the mean of the operability percentages for each of the 3 directions considered. This result is shown in Table 3-6 below.

Table 3-6: Total Operational Percentages

Length (m)	Cb	GMt (m)	Winter Operational Percentage (%)	Summer Operational Percentage (%)
70.0	0.65	2.00	68.87	97.72
70.0	0.79	2.00	70.54	97.90
80.0	0.65	2.00	71.92	98.27
80.0	0.79	2.00	72.50	98.33
90.0	0.65	2.00	75.36	98.85
90.0	0.79	2.00	73.90	98.68
70.0	0.65	2.75	66.60	96.84
70.0	0.79	2.75	67.67	96.42
80.0	0.65	2.75	72.50	98.27
80.0	0.79	2.75	72.63	98.28
90.0	0.65	2.75	74.36	98.70
90.0	0.79	2.75	74.49	98.72

The above percentages show significant variation between ships and loading conditions, further highlighting the need for specific wave height limits for different scenarios, especially so in the winter months, where the percentages are relatively low. A comparison against the operational percentages that result from a flat limit of $H_s < 4.0$ m is shown in Table 3-7.

Table 3-7: Increase in Operational Percentages

Length (m)	Cb	GMt (m)	Winter % Increase (Flat Limit = 36.65%)	Summer % Increase (Flat Limit = 93.15%)
70.0	0.65	2.00	87.91	4.91
70.0	0.79	2.00	92.47	5.10
80.0	0.65	2.00	96.24	5.50
80.0	0.79	2.00	97.81	5.56
90.0	0.65	2.00	105.64	6.12
90.0	0.79	2.00	101.65	5.93
70.0	0.65	2.75	81.72	3.96
70.0	0.79	2.75	84.63	3.52
80.0	0.65	2.75	97.81	5.49
80.0	0.79	2.75	98.16	5.51
90.0	0.65	2.75	102.90	5.96
90.0	0.79	2.75	103.26	5.98

For the winter months, there is a significant increase in operational percentage for all of the OSV/loading condition combinations considered. Even for the worst case shown in Table 3-6 above (Small / Light, $GM_t = 2.75$ m), this represents an 81.7% increase over the percentage obtained from the flat 4.0 m H_s limit. In the summer months, the difference is less pronounced. This is not surprising considering that the operational percentage in the summer was very high, even with the flat limit of 4.0 m H_s. Even so, there is a percentage increase associated with each OSV/loading condition combination for the summer months as well. The worst-case (Small / Heavy, $GM_t = 2.75$ m) is a 3.52% increase. This reinforces the conclusion that OSV/loading condition-specific limits (considering typical modern OSV particulars) will result in a higher operational fraction and therefore efficiency of operations.

Figure 3-48 and Figure 3-49 below show the variation in winter operability percentages

between ships for the case where GM_t = 2.0 m and 2.75 m, respectively.
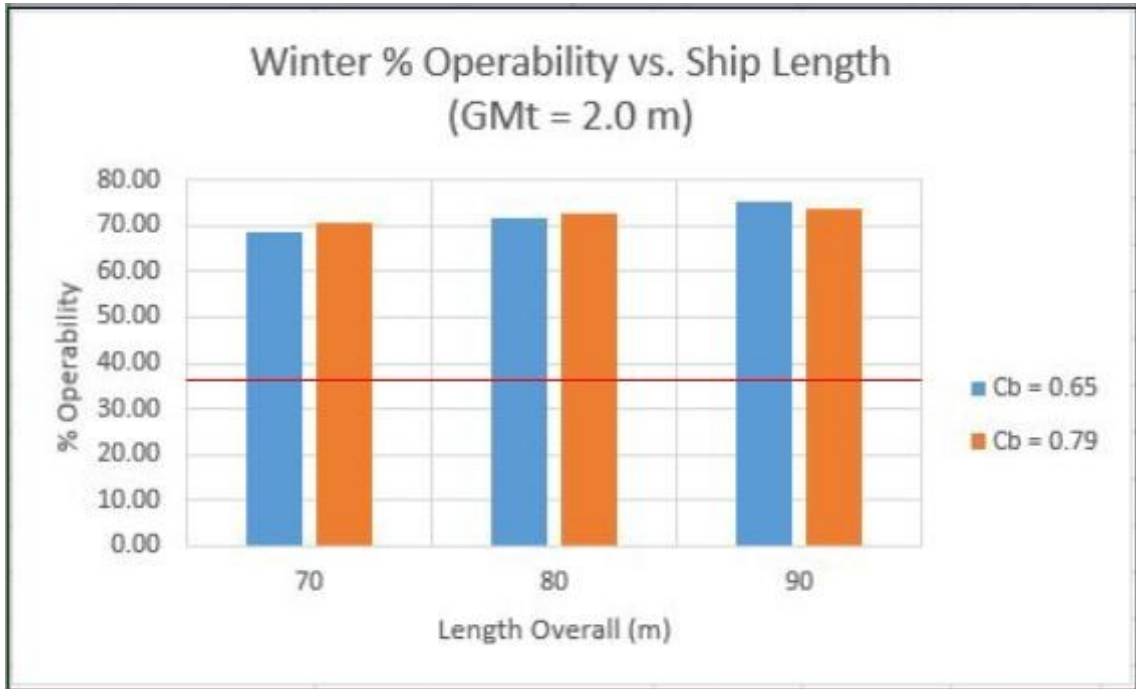
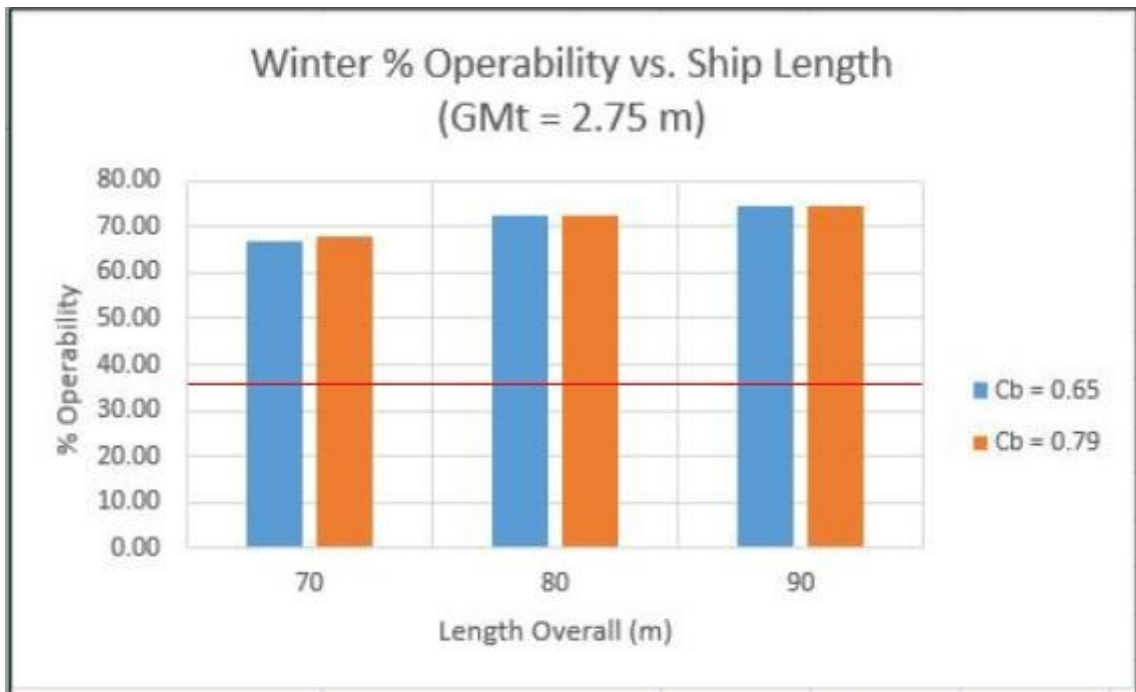**Figure 3-48: Winter % Operability vs. Ship Length for GM_t = 2.0 m**

Figure 3-49: Winter % Operability vs. Ship Length for $GM_t = 2.75$ m

Figure 3-48 and Figure 3-49 above clearly show an increasing trend in operability percentages from switching to a larger OSV. Switching from the "Small Light" OSV to the "Large Heavy" OSV results in a 7.3% increase in operability time over the winter season for the case where $GM_t = 2.0$ m, and 11.9% for the case where $GM_t = 2.75$ m. This increase in operable time would allow for a significantly more viable operation in the Flemish Pass region.

The results presented in this section show that the operability percentages vary with the value of the metacentric height. It is of critical importance to tune the GM for the specific OSV and operating environment. This includes ensuring that the natural rolling period is outside of the range of most commonly occurring wave periods in the operating region.

Differently sized and shaped ships will have different optimum GM_t such that the ship is safely stable and not overly stiff.

While exact operational limits obviously cannot be made from the output of one potential flow study, the large relative differences in operational fraction between different cases indicates that there is certainly a more efficient method than using a flat wave height limit. Also, while this study was completed with the offshore oil and gas industry in mind, the methods are equally applicable to any supply OSV to platform operation, for instance offshore wind or wave energy installations.

3.3.2   'Safe Time' Results

Table 3-8 below presents the lowest significant wave height that causes a deck velocity limit exceedance for a given OSV, peak period, GM, and heading.

Table 3-8: Lowest Failing Wave Heights

	GMt (m)	2.00					2.75				
	Tp (s)	6.00	7.50	11.50	15.50	18.00	6.00	7.50	11.50	15.50	18.00
Beam Seas: Limiting Hs (m) (For Each Ship)	Small / Light	5.0	5.0	5.0	6.0	> 6.0	4.0	4.0	5.0	6.0	> 6.0
	Small / Heavy	5.0	5.0	5.0	6.0	> 6.0	4.0	4.0	5.0	6.0	> 6.0
	Medium / Light	5.0	5.0	5.0	6.0	> 6.0	5.0	5.0	5.0	6.0	> 6.0
	Medium / Heavy	5.0	5.0	5.0	6.0	> 6.0	5.0	5.0	5.0	6.0	> 6.0
	Large / Light	> 6.0	6.0	6.0	> 6.0	> 6.0	> 6.0	5.0	5.0	> 6.0	> 6.0
	Large / Heavy	> 6.0	6.0	5.0	6.0	> 6.0	> 6.0	5.0	5.0	> 6.0	> 6.0
Bow Quartering: Limiting Hs (m) (For Each Ship)	Small / Light	> 6.0	> 6.0	6.0	> 6.0	> 6.0	> 6.0	6.0	6.0	> 6.0	> 6.0
	Small / Heavy	> 6.0	> 6.0	> 6.0	> 6.0	> 6.0	> 6.0	> 6.0	> 6.0	> 6.0	> 6.0
	Medium / Light	> 6.0	> 6.0	6.0	> 6.0	> 6.0	> 6.0	> 6.0	> 6.0	> 6.0	> 6.0
	Medium / Heavy	> 6.0	> 6.0	> 6.0	> 6.0	> 6.0	> 6.0	> 6.0	> 6.0	> 6.0	> 6.0
	Large / Light	> 6.0	> 6.0	6.0	> 6.0	> 6.0	> 6.0	> 6.0	> 6.0	> 6.0	> 6.0
	Large / Heavy	> 6.0	> 6.0	> 6.0	> 6.0	> 6.0	> 6.0	> 6.0	> 6.0	> 6.0	> 6.0

The average amount of "safe time" (i.e. time with deck velocities below the FROG-6 limits) across all of these lowest failing wave heights was 99.8 % of the 480 minute

simulation duration (479.11 min). This means that virtually all of the time in these "inoperable" sea states may actually be usable for cargo transfer.

To verify this hypothesis, 8 hour simulations were completed for a series of the lowest failing wave heights, as summarized in Table 2-3 above. An additional case is also considered for the most probable wave period with an $H_s = 8.0$ m, to see how the distributions of safe times look at a wave height much higher than the current operational limit of $H_s = 4.0$ m. The most probable period for this wave height in the Flemish Pass region is $T_p = 12.5$ s, occurring approximately 1.91 % of the time in the winter months [5]. OSVs typically attempt to weathervane into the heading of the waves during cargo transfer to reduce OSV motions, if possible for the given operation. Therefore, only the bow quartering and head seas responses were recorded for the 8.0 m H_s cases, as they are the most realistic when attempting cargo transfer in higher wave heights.

A key measure of the safe time considered below is the "total useable time", created by summing all of the safe times for a given condition that were greater than 10 minutes, a reasonable assumption for how long one lift will take. Summary results for each of the considered conditions are presented in Sections 3.3.2.1 through 3.3.2.11 below.

3.3.2.1 'Safe Time' Results – GM=2.0 m, Hs=5.0 m, Beam Seas

Individual summary results for each peak period are presented in Table 3-9 through Table 3-11.

Table 3-9: Safe Time Results, GM=2.0 m, Hs=5.0 m, Tp=6.0 s, Beam Seas

Ship	Number of Limit Exceedances	Mean Safe Time (min)	Total Safe Time (min)	Safe Time Standard Deviation (min)	Number of Useable Times	Mean Useable Time (min)	Total Useable Time (min)	Percentage of Useable Time
Small/Light	100	4.74	478.93	6.52	17	16.61	282.29	58.8%
Small/Heavy	102	4.65	478.94	6.50	17	16.72	284.20	59.2%
Medium/Light	16	28.23	479.89	23.18	12	38.62	463.41	96.5%
Medium/Heavy	12	36.92	479.91	40.29	9	52.52	472.72	98.5%
Large/Light	0	480.00	480.00	N/A	1	480.00	480.00	100.0%
Large/Heavy	0	480.00	480.00	N/A	1	480.00	480.00	100.0%

Distributions of both the "safe time" and "useable time" for the results shown in Table 3-9 are presented graphically through box and whisker plots in Figure 3-50 and Figure 3-51, respectively.
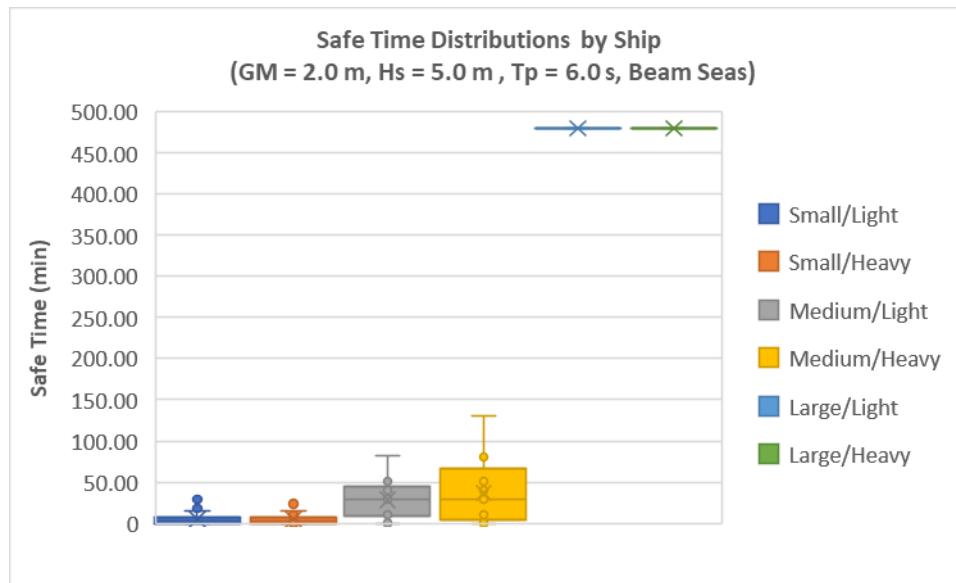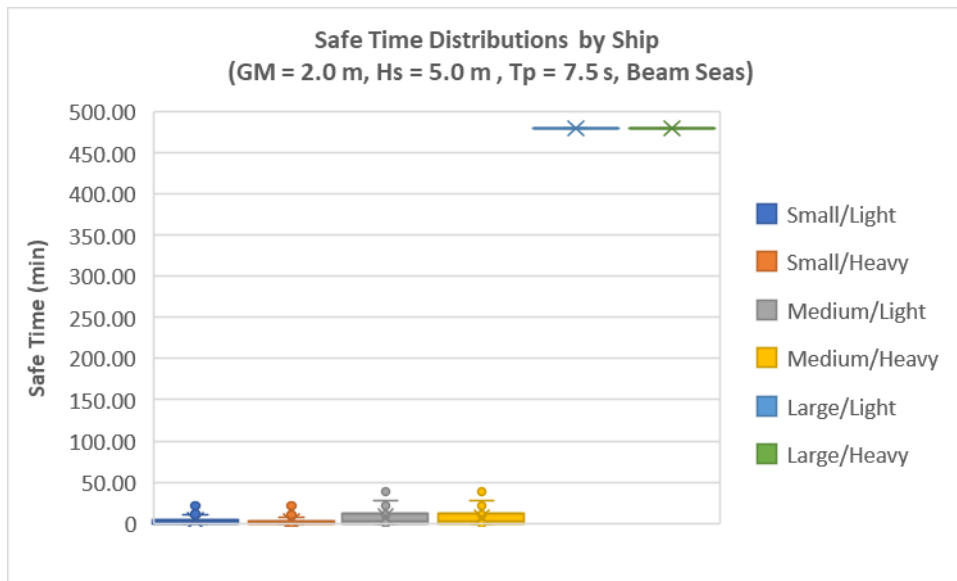

Figure 3-50: Safe Time Distributions, GM=2.0 m, Hs=5.0 m, Tp=6.0 s, Beam Seas
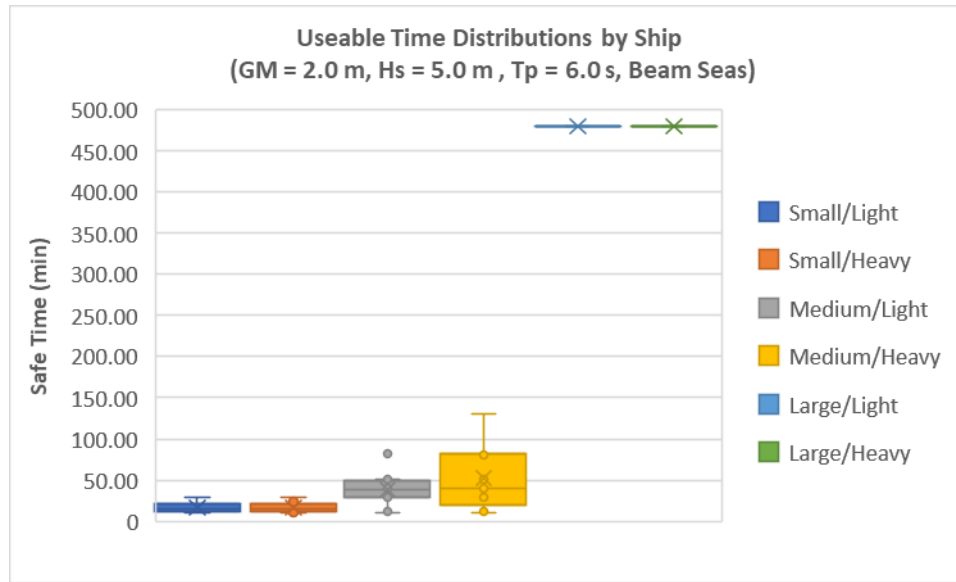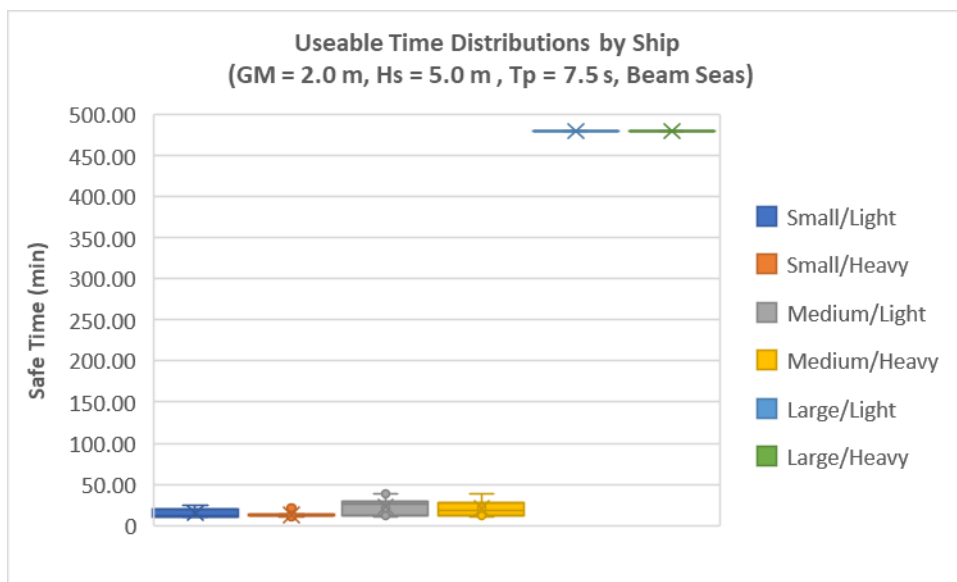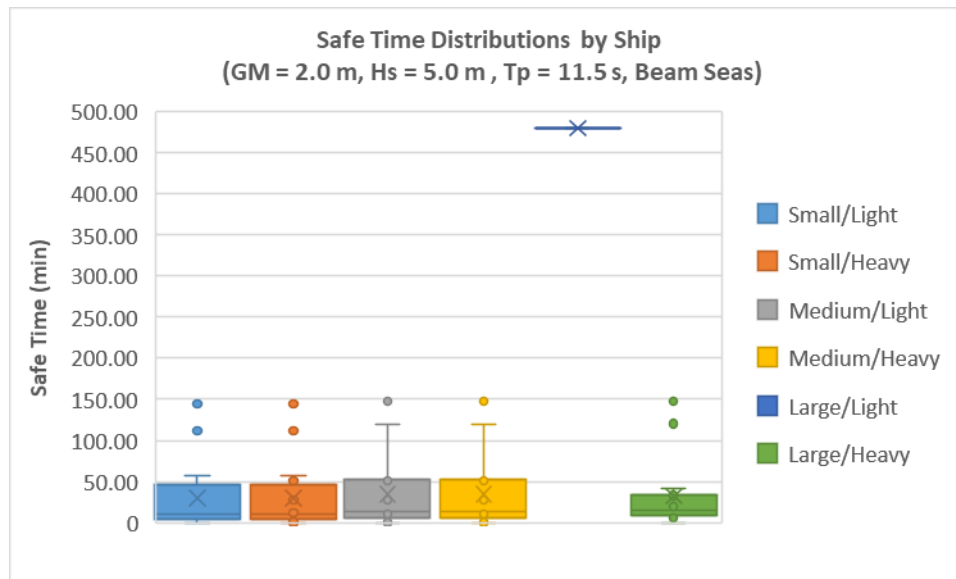
Figure 3-51: Useable Time Distributions, GM=2.0 m, Hs=5.0 m, Tp=6.0 s, Beam Seas

Table 3-10: Safe Time Results, GM=2.0 m, Hs=5.0 m, Tp=7.5 s, Beam Seas

Ship	Number of Limit Exceedances	Mean Safe Time (min)	Total Safe Time (min)	Safe Time Standard Deviation (min)	Number of Useable Times	Mean Useable Time (min)	Total Useable Time (min)	Percentage of Useable Time
Small/Light	157	3.02	477.83	3.95	8	14.83	118.66	24.7%
Small/Heavy	202	2.35	477.27	3.25	7	12.96	90.74	18.9%
Medium/Light	57	8.26	479.37	11.02	17	22.95	390.15	81.3%
Medium/Heavy	69	6.85	479.21	9.53	19	20.10	381.98	79.6%
Large/Light	0	480.00	480.00	N/A	1	480.00	480.00	100.0%
Large/Heavy	0	480.00	480.00	N/A	1	480.00	480.00	100.0%

Distributions of both the "safe time" and "useable time" for the results shown in Table

3-10 are presented graphically through box and whisker plots in Figure 3-52 and Figure

3-53, respectively.

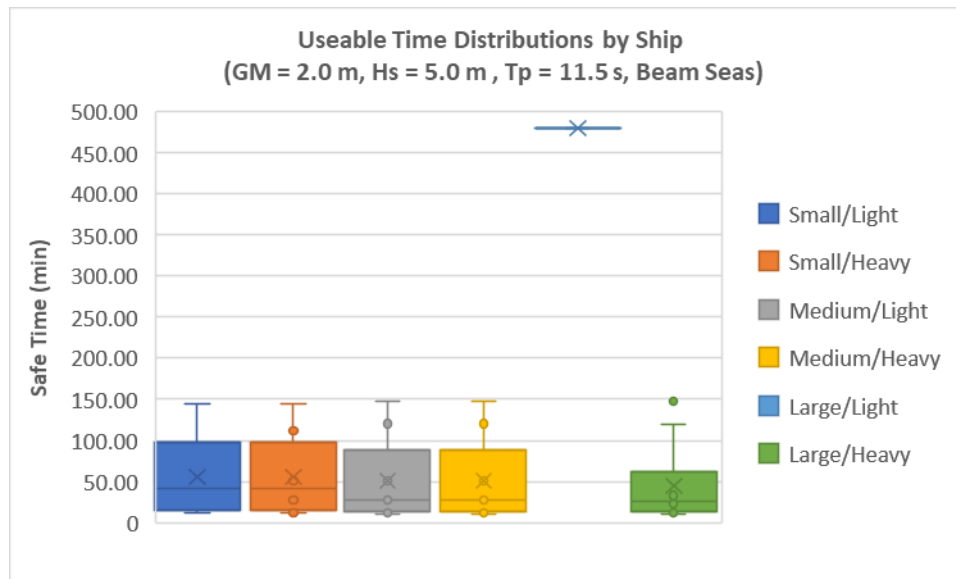**Figure 3-52: Safe Time Distributions, GM=2.0 m, Hs=5.0 m, Tp=7.5 s, Beam Seas**

Figure 3-53: Useable Time Distributions, GM=2.0 m, Hs=5.0 m, Tp=7.5 s, Beam Seas

74

Table 3-11: Safe Time Results, GM=2.0 m, Hs=5.0 m, Tp=11.5 s, Beam Seas

Ship	Number of Limit Exceedances	Mean Safe Time (min)	Total Safe Time (min)	Safe Time Standard Deviation (min)	Number of Useable Times	Mean Useable Time (min)	Total Useable Time (min)	Percentage of Useable Time
Small/Light	15	29.99	479.80	42.43	8	55.63	445.06	92.7%
Small/Heavy	15	29.99	479.80	42.43	8	55.63	445.06	92.7%
Medium/Light	13	34.27	479.84	45.88	9	51.06	459.50	95.7%
Medium/Heavy	13	34.27	479.84	45.88	9	51.06	459.50	95.7%
Large/Light	0	480.00	480.00	N/A	1	480.00	480.00	100.0%
Large/Heavy	14	31.99	479.82	43.22	10	45.04	450.41	93.8%

Distributions of both the "safe time" and "useable time" for the results shown in Table 3-11 are presented graphically through box and whisker plots in Figure 3-54 and Figure 3-55, respectively.

Figure 3-54: Safe Time Distributions, GM=2.0 m, Hs=5.0 m, Tp=11.5 s, Beam Seas

Figure 3-55: Useable Time Distributions, GM=2.0 m, Hs=5.0 m, Tp=11.5 s, Beam Seas

As shown by the results above, there is a significant difference between the total safe time (i.e. the total amount of time during the simulation where the deck velocity is below the prescribed limits), and the total useable time (i.e. the total safe time after filtering out safe times with a duration less than 10 minutes). For example, for the Small/Light vessel, GM = 2.0 m, H_s = 5.0 m, Tp = 6.0 s, Beam Seas, the total safe time is 478.93 minutes. At first glance, this implies that nearly the whole simulation duration is safe for crew and cargo transfer operations. However, the total useable time in this case is 282.29 minutes. There is significant useable time, but it is much less than the total safe time considering the duration of a crew transfer operation. This highlights the importance of the "useable time" as a measure of operability.

Combining the results from the 3 simulated peak periods above yields the following results for a combined 24 hour (1440 minute) simulation. Note that as these results are from 3 separate simulations, the maximum useable time is shown as 480 minutes, even if there are no limit exceedances at any point in the combined 1440 minutes of simulation time. This irregularity in result reporting has no effect on the percentage of useable time.

Table 3-12: Safe Time Results, GM=2.0 m, Hs=5.0 m, Tp=6.0,7.5,11.5 s, Beam Seas

Ship	Total Number of Limit Exceedances	Mean Safe Time (min)	Total Safe Time (min)	Safe Time Standard Deviation (min)	Number of Useable Times	Mean Useable Time (min)	Total Useable Time (min)	Percentage of Useable Time
Small/Light	272	5.22	1436.56	12.71	33	25.64	846	58.8%
Small/Heavy	319	4.46	1436.00	11.81	32	25.63	820	56.9%
Medium/Light	86	16.17	1439.10	24.67	38	34.55	1313	91.2%
Medium/Heavy	94	14.83	1438.96	26.85	37	35.52	1314	91.3%
Large/Light	0	480.00	1440.00	N/A	3	480.00	1440	100.0%
Large/Heavy	14	84.70	1439.82	154.18	12	117.53	1410	97.9%
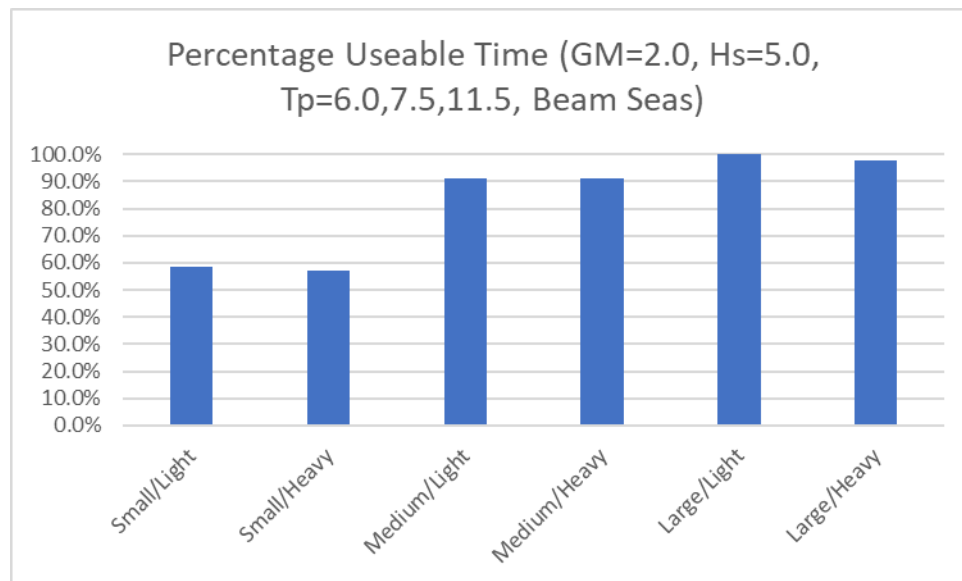
Figure 3-56: Percentage Useable Time, GM=2.0 m, Hs=5.0 m, Tp=6.0,7.5,11.5 s, Beam Seas

Distributions of both the "safe time" and "useable time" for the results shown in Table 3-12 are presented graphically through box and whisker plots in Figure 3-57 and Figure 3-58, respectively.
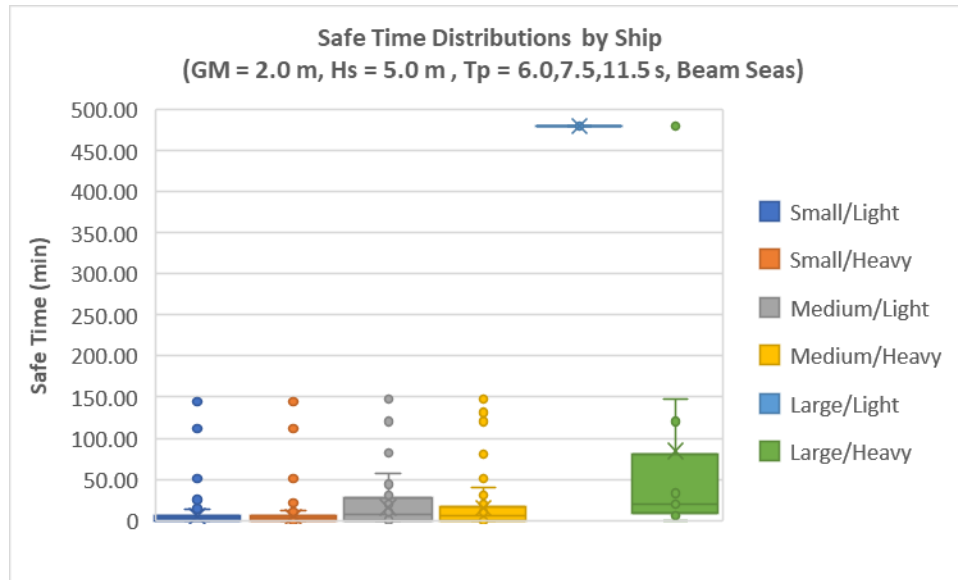
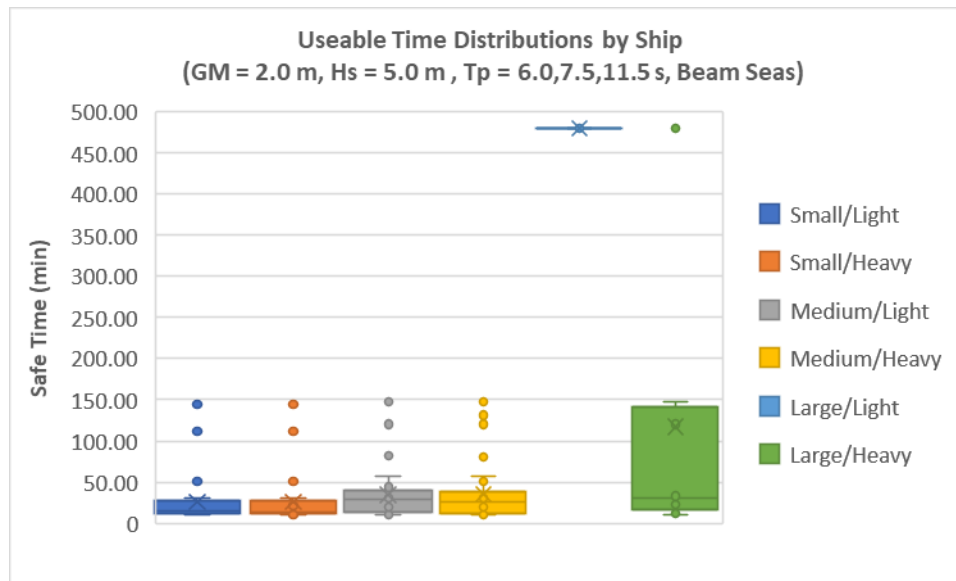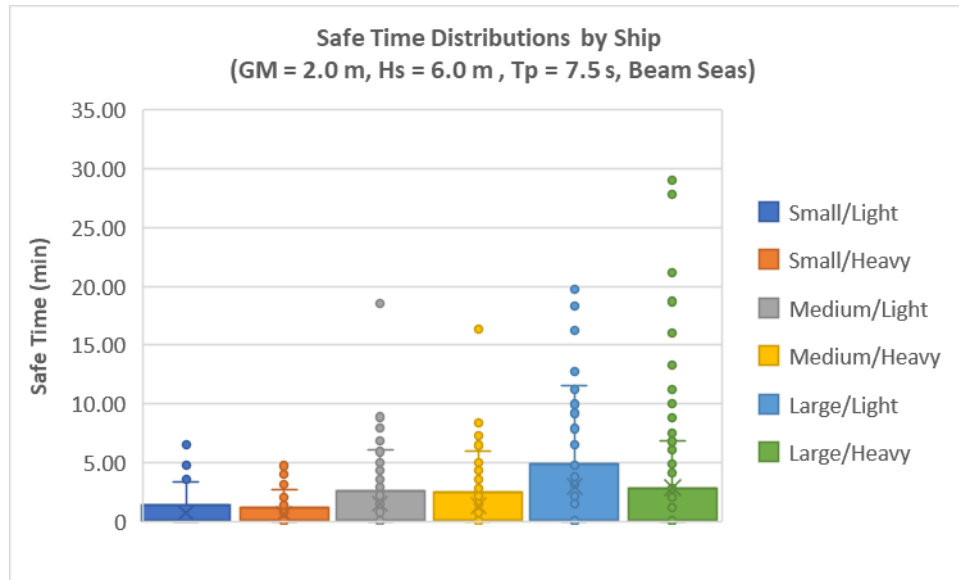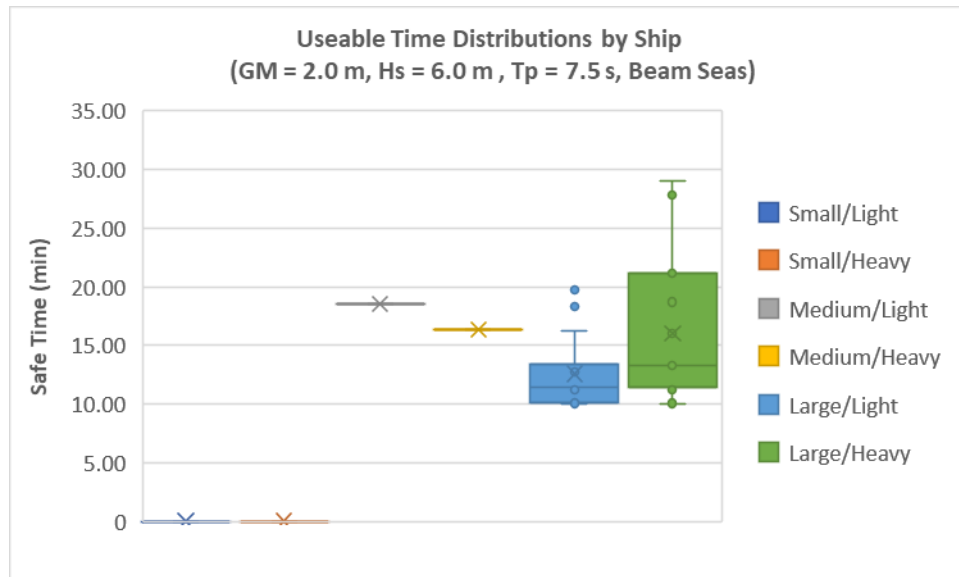**Figure 3-57: Safe Time Distributions, GM=2.0 m, Hs=5.0 m, Tp=6.0,7.5,11.5 s, Beam Seas**

Figure 3-58: Useable Time Distributions, GM=2.0 m, Hs=5.0 m, Tp=6.0,7.5,11.5 s, Beam Seas

3.3.2.2 'Safe Time' Results – GM=2.0 m, Hs=6.0 m, Beam Seas

Individual summary results for each peak period are presented in Table 3-13 through Table 3-15.

Table 3-13: Safe Time Results, GM=2.0 m, Hs=6.0 m, Tp=7.5 s, Beam Seas

Ship	Number of Limit Exceedances	Mean Safe Time (min)	Total Safe Time (min)	Safe Time Standard Deviation (min)	Number of Useable Times	Mean Useable Time (min)	Total Useable Time (min)	Percentage of Useable Time
Small/Light	667	0.70	469.14	0.98	0	0.00	0.00	0.0%
Small/Heavy	755	0.62	467.13	0.88	0	0.00	0.00	0.0%
Medium/Light	322	1.47	475.09	2.21	1	18.55	18.55	3.9%
Medium/Heavy	363	1.30	474.26	2.00	1	16.33	16.33	3.4%
Large/Light	160	2.97	477.98	4.14	16	12.57	201.12	41.9%
Large/Heavy	166	2.86	477.58	5.10	15	16.03	240.51	50.1%

Distributions of both the "safe time" and "useable time" for the results shown in Table 3-13 are presented graphically through box and whisker plots in Figure 3-59 and Figure 3-60, respectively.
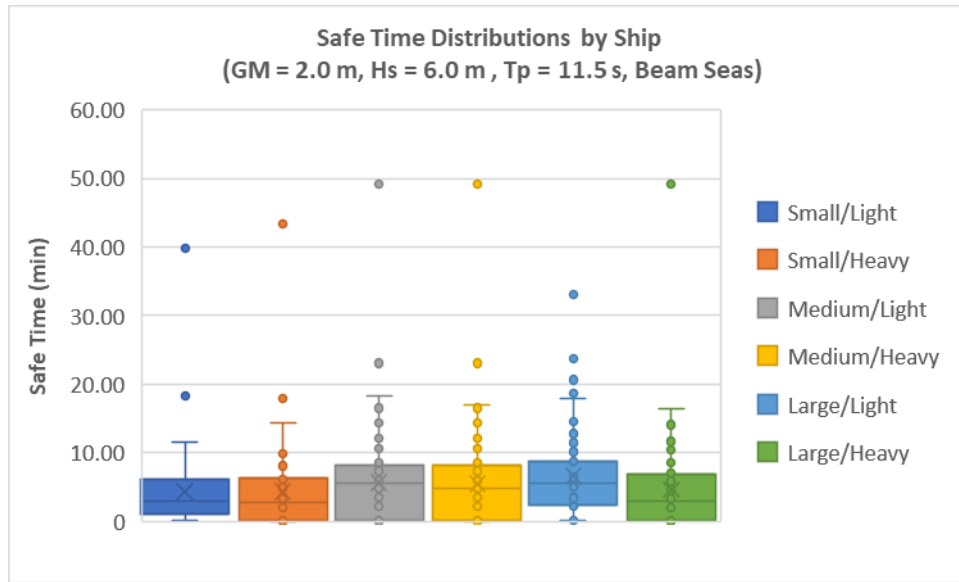
Figure 3-59: Safe Time Distributions, GM=2.0 m, Hs=6.0 m, Tp=7.5 s, Beam Seas

Figure 3-60: Useable Time Distributions, GM=2.0 m, Hs=6.0 m, Tp=7.5 s, Beam Seas

The comparison of Figure 3-59 and Figure 3-60 above further highlights the need to

analyze the distribution of safe times rather than just the total safe time within the

simulation duration. For the small OSVs, there is nearly 470 minutes of the 480 minute simulation where the deck velocities are below the limits. But, there are so many brief limit exceedances that there is not a single useable window of 10 minutes or greater. Both of the medium vessels show a similar result, but in that case there is one useable time window for each of them.

Table 3-14: Safe Time Results, GM=2.0 m, Hs=6.0 m, Tp=11.5 s, Beam Seas

Ship	Number of Limit Exceedances	Mean Safe Time (min)	Total Safe Time (min)	Safe Time Standard Deviation (min)	Number of Useable Times	Mean Useable Time (min)	Total Useable Time (min)	Percentage of Useable Time
Small/Light	109	4.35	478.01	4.84	6	16.95	101.70	21.2%
Small/Heavy	109	4.35	478.02	5.37	8	17.07	136.54	28.4%
Medium/Light	84	5.63	478.44	6.85	12	17.62	211.43	44.0%
Medium/Heavy	87	5.44	478.46	6.65	11	17.47	192.14	40.0%
Large/Light	72	6.56	478.79	6.49	15	16.88	253.26	52.8%
Large/Heavy	102	4.64	478.15	5.87	10	15.87	158.67	33.1%

Distributions of both the "safe time" and "useable time" for the results shown in Table 3-14 are presented graphically through box and whisker plots in Figure 3-61 and Figure 3-62, respectively.

81

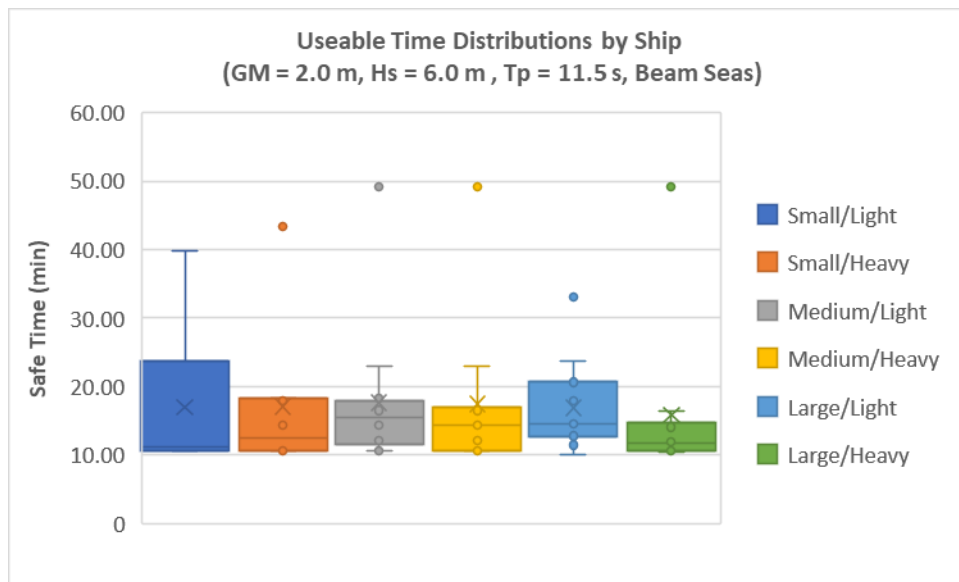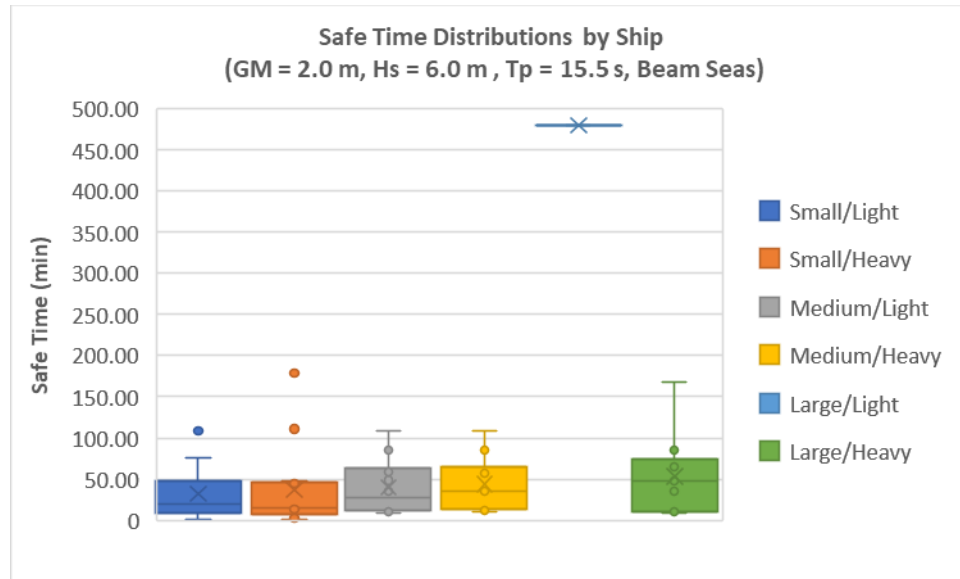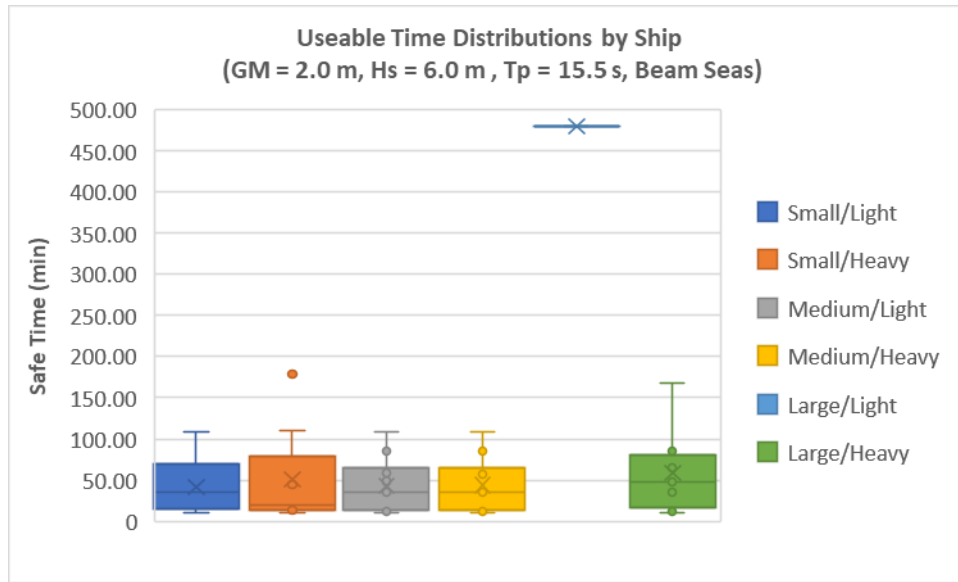**Figure 3-61: Safe Time Distributions, GM=2.0 m, Hs=6.0 m, Tp=11.5 s, Beam Seas**

Figure 3-62: Useable Time Distributions, GM=2.0 m, Hs=6.0 m, Tp=11.5 s, Beam

Seas

Table 3-15: Safe Time Results, GM=2.0 m, Hs=6.0 m, Tp=15.5 s, Beam Seas

Ship	Number of Limit Exceedances	Mean Safe Time (min)	Total Safe Time (min)	Safe Time Standard Deviation (min)	Number of Useable Times	Mean Useable Time (min)	Total Useable Time (min)	Percentage of Useable Time
Small/Light	14	31.99	479.78	31.79	11	41.87	460.60	96.0%
Small/Heavy	12	36.91	479.81	51.85	9	51.18	460.62	96.0%
Medium/Light	11	39.99	479.86	33.43	11	42.79	470.73	98.1%
Medium/Heavy	10	43.62	479.87	33.81	11	43.62	479.87	100.0%
Large/Light	0	480.00	480.00	N/A	1	480.00	480.00	100.0%
Large/Heavy	8	53.32	479.89	50.27	8	58.85	470.76	98.1%

Distributions of both the "safe time" and "useable time" for the results shown in Table 3-15 are presented graphically through box and whisker plots in Figure 3-63 and Figure 3-64, respectively.
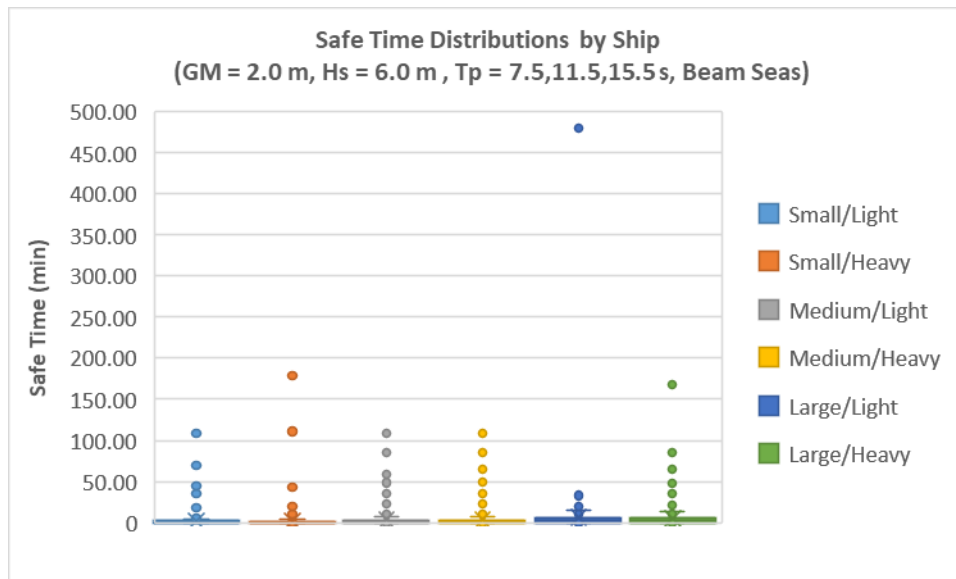

Figure 3-63: Safe Time Distributions, GM=2.0 m, Hs=6.0 m, Tp=15.5 s, Beam Seas

Figure 3-64: Useable Time Distributions, GM=2.0 m, Hs=6.0 m, Tp=15.5 s, Beam Seas

Combining the results from the 3 simulated peak periods above yields the following results for a combined 24 hour (1440 minute) simulation.

Table 3-16: Safe Time Results, GM=2.0 m, Hs=6.0 m, Tp=7.5,11.5,15.5 s, Beam Seas

Ship	Total Number of Limit Exceedances	Mean Safe Time (min)	Total Safe Time (min)	Safe Time Standard Deviation (min)	Number of Useable Times	Mean Useable Time (min)	Total Useable Time (min)	Percentage of Useable Time
Small/Light	790	1.80	1426.93	6.41	17	33.08	562	39.0%
Small/Heavy	876	1.62	1424.95	7.82	17	35.13	597	41.5%
Medium/Light	417	3.41	1433.39	9.21	24	29.20	701	48.7%
Medium/Heavy	460	3.09	1432.60	8.88	23	29.93	688	47.8%
Large/Light	232	6.11	1436.77	31.48	32	29.20	934	64.9%
Large/Heavy	276	5.15	1435.62	13.39	33	26.36	870	60.4%
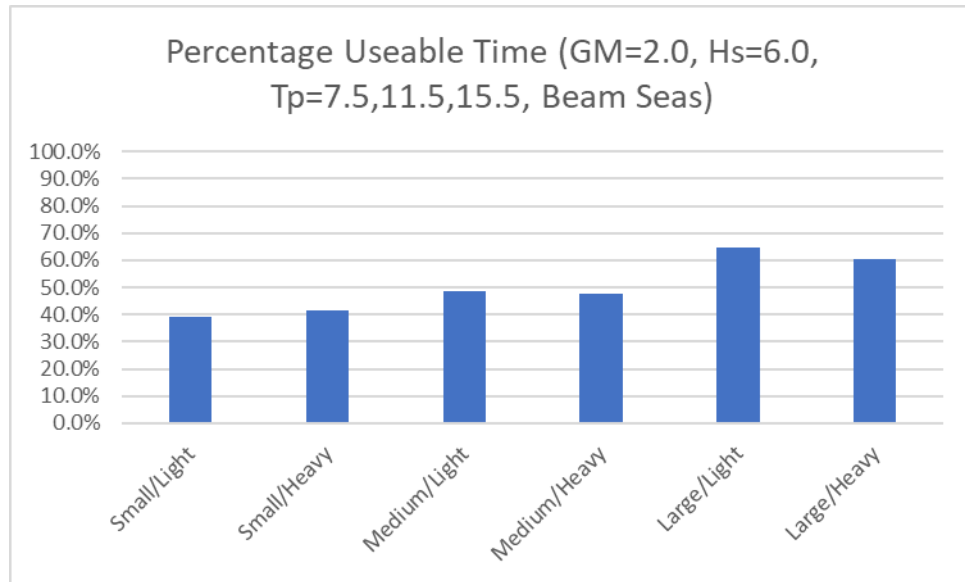
Figure 3-65: Percentage Useable Time, GM=2.0 m, Hs=6.0 m, Tp=7.5,11.5,15.5 s, Beam Seas

Distributions of both the "safe time" and "useable time" for the results shown in Table 3-16 are presented graphically through box and whisker plots in Figure 3-66 and Figure 3-67, respectively.

Figure 3-66: Safe Time Distributions, GM=2.0 m, Hs=6.0 m, Tp=7.5,11.5,15.5 s,
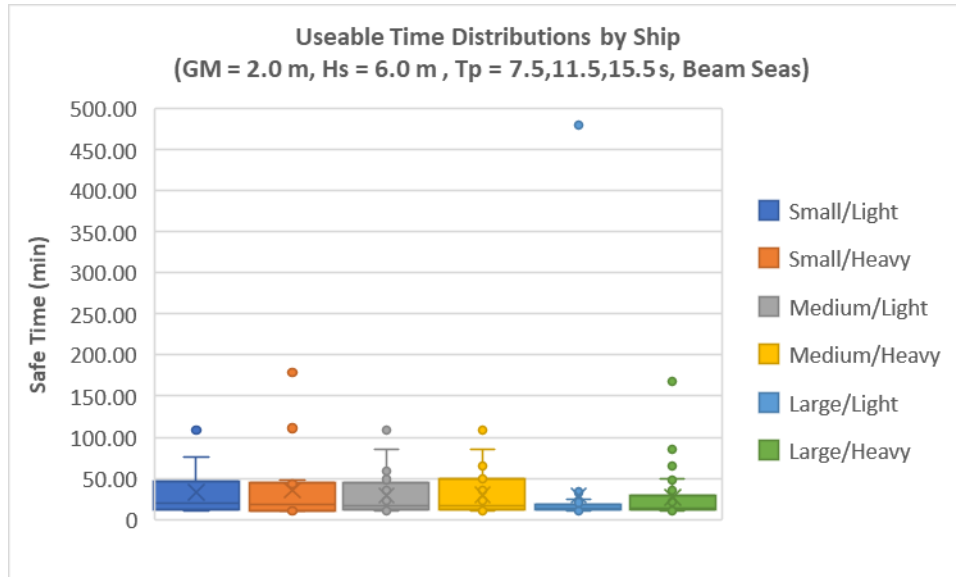
Beam Seas

Figure 3-67: Useable Time Distributions, GM=2.0 m, Hs=6.0 m, Tp=7.5,11.5,15.5 s,

Beam Seas

3.3.2.3 'Safe Time' Results – GM=2.0 m, Hs=6.0 m, Bow Quartering

Table 3-17: Safe Time Results, GM=2.0 m, Hs=6.0 m, Tp=11.5 s, Bow Quartering

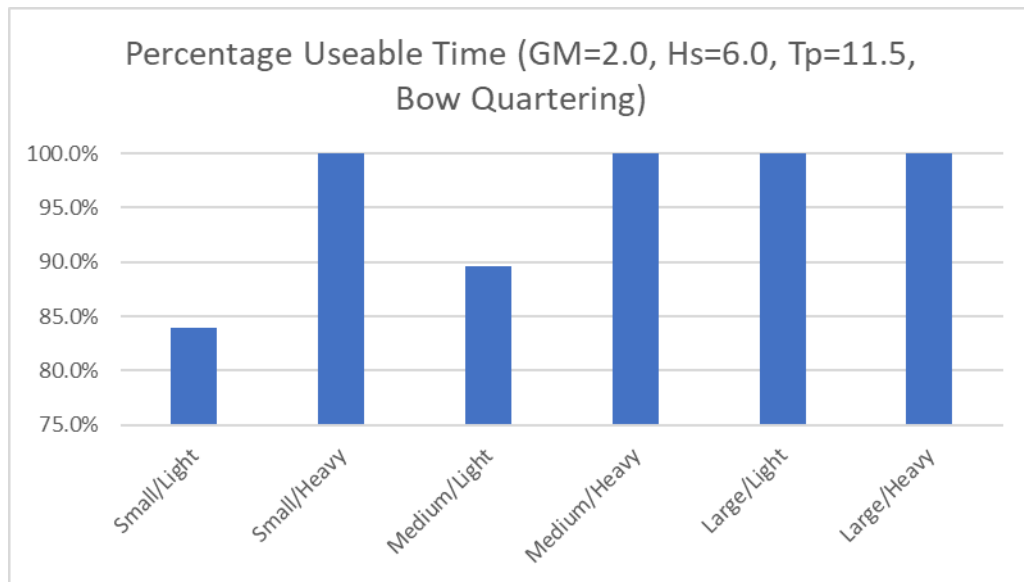| Ship	Number of Limit Exceedances	Mean Safe Time (min)	Total Safe Time (min)	Safe Time Standard Deviation (min)	Number of Useable Times	Mean Useable Time (min)	Total Useable Time (min)	Percentage of Useable Time
Small/Light	31	14.98	479.52	24.39	14	28.80	403.24	84.0%
Small/Heavy	0	480.00	480.00	N/A	1	480.00	480.00	100.0%
Medium/Light	20	22.84	479.74	32.12	12	35.85	430.15	89.6%
Medium/Heavy	0	480.00	480.00	N/A	1	480.00	480.00	100.0%
Large/Light	7	59.99	479.91	60.04	7	68.55	479.84	100.0%
Large/Heavy	0	480.00	480.00	N/A	1	480.00	480.00	100.0%

Figure 3-68: Percentage Useable Time, GM=2.0 m, Hs=6.0 m, Tp=11.5 s, Bow Quartering

Distributions of both the "safe time" and "useable time" for the results shown in Table 3-17 are presented graphically through box and whisker plots in Figure 3-69 and Figure 3-70, respectively.
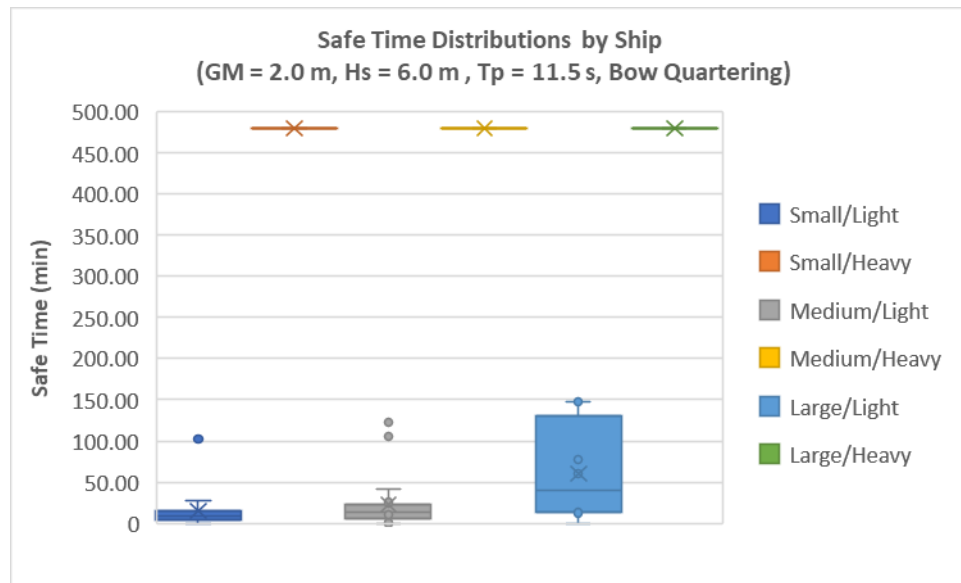

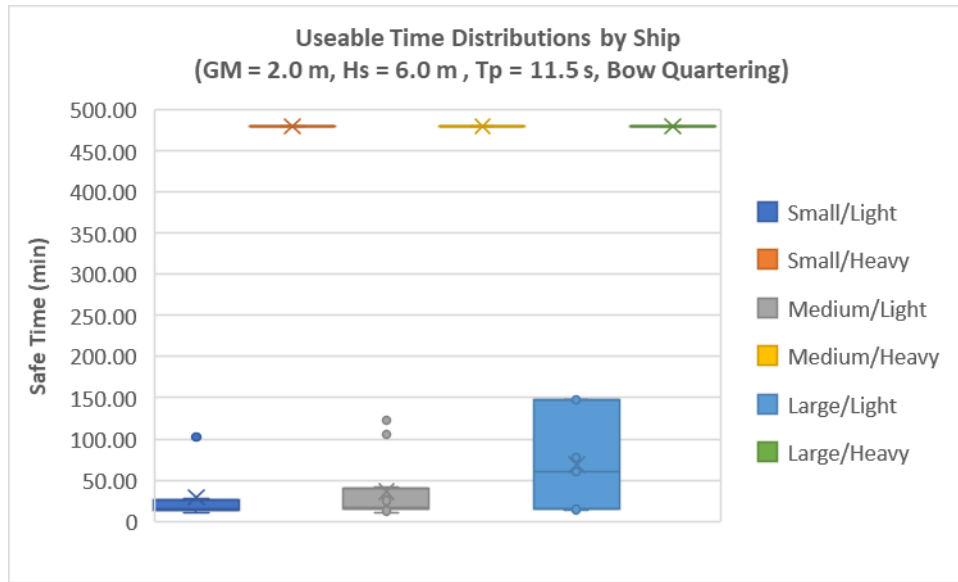**Figure 3-69: Safe Time Distributions, GM=2.0 m, Hs=6.0 m, Tp=11.5 s, Bow Quartering**

Figure 3-70: Useable Time Distributions, GM=2.0 m, Hs=6.0 m, Tp=11.5 s, Bow Quartering

3.3.2.4 'Safe Time' Results – GM=2.0 m, Hs=8.0 m, Head Seas

Table 3-18: Safe Time Results, GM=2.0 m, Hs=8.0 m, Tp=12.5 s, Head Seas

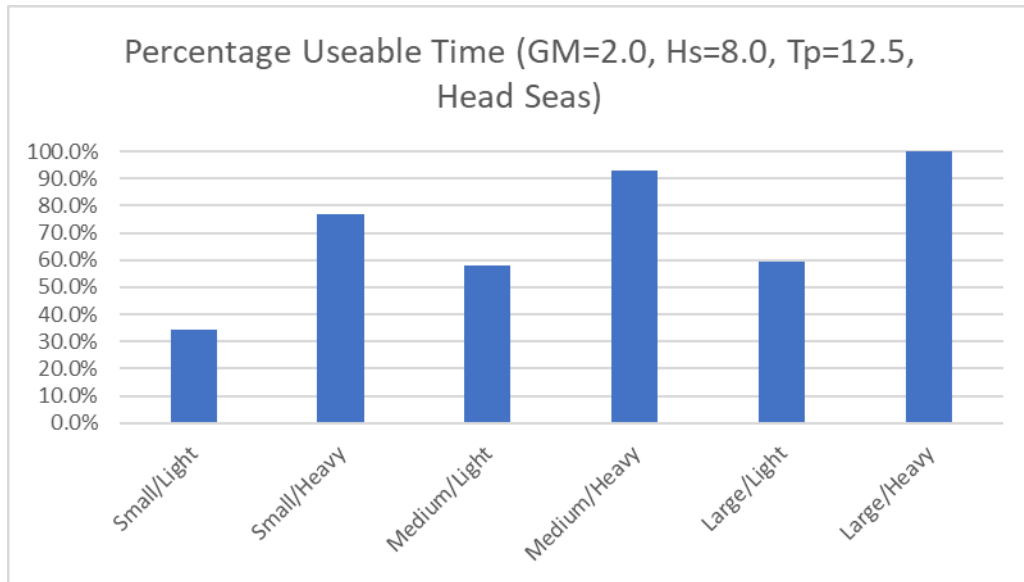| Ship	Number of Limit Exceedances	Mean Safe Time (min)	Total Safe Time (min)	Safe Time Standard Deviation (min)	Number of Useable Times	Mean Useable Time (min)	Total Useable Time (min)	Percentage of Useable Time
Small/Light	130	3.64	477.24	4.24	13	12.71	165.26	34.4%
Small/Heavy	53	8.87	479.01	9.77	20	18.46	369.10	76.9%
Medium/Light	76	6.21	478.52	6.30	19	14.62	277.76	57.9%
Medium/Heavy	26	17.76	479.56	17.33	17	26.29	446.95	93.1%
Large/Light	66	7.14	478.59	9.70	14	20.30	284.22	59.2%
Large/Heavy	3	119.99	479.96	90.25	3	159.96	479.89	100.0%

Figure 3-71: Percentage Useable Time, GM=2.0 m, Hs=8.0 m, Tp=12.5 s, Head Seas

Distributions of both the "safe time" and "useable time" for the results shown in Table 3-18 are presented graphically through box and whisker plots in Figure 3-72 and Figure 3-73, respectively.
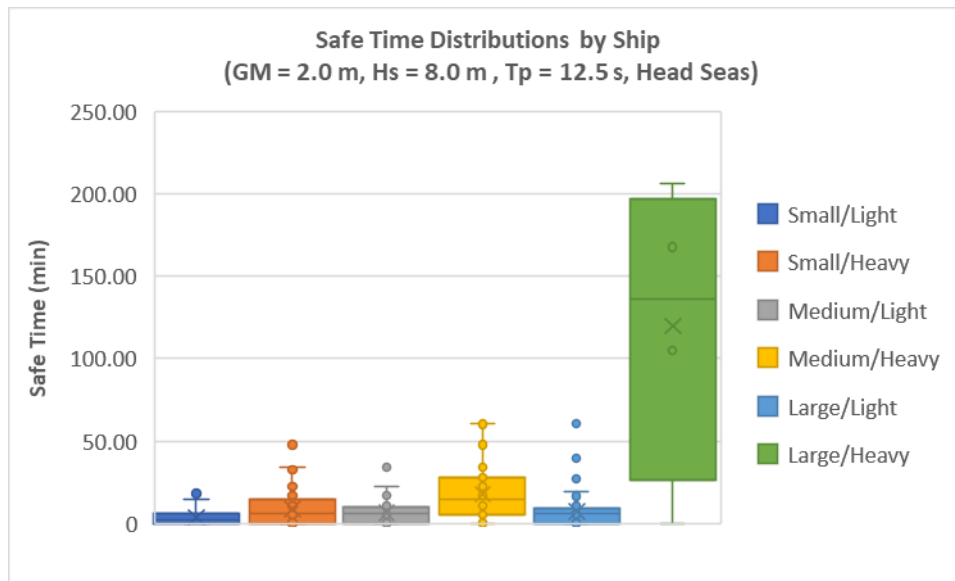
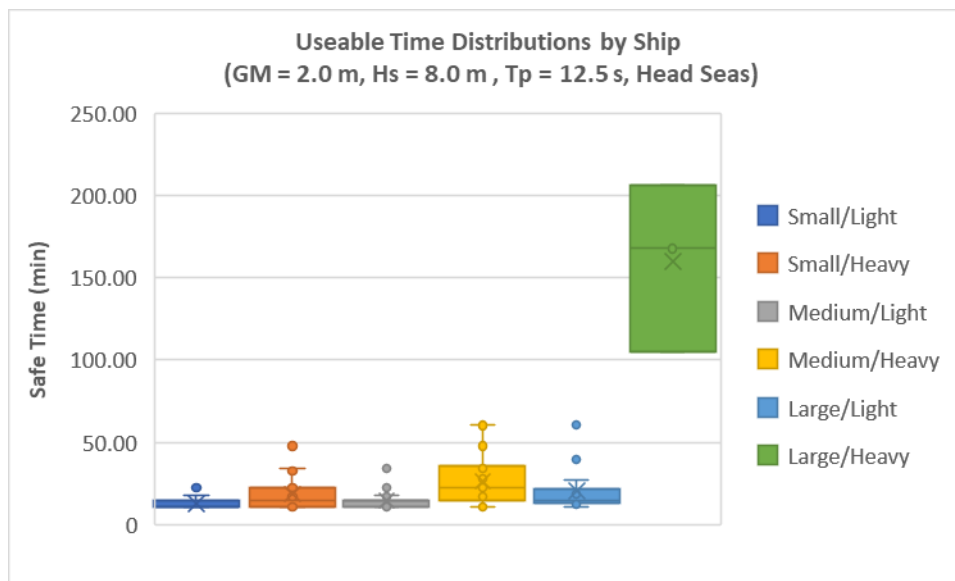**Figure 3-72: Safe Time Distributions, GM=2.0 m, Hs=8.0 m, Tp=12.5 s, Head Seas**

Figure 3-73: Useable Time Distributions, GM=2.0 m, Hs=8.0 m, Tp=12.5 s, Head

Seas

3.3.2.5 'Safe Time' Results – GM=2.0 m, Hs=8.0 m, Bow Quartering

Table 3-19: Safe Time Results, GM=2.0 m, Hs=8.0 m, Tp=12.5 s, Bow Quartering

| Ship	Number of Limit Exceedances	Mean Safe Time (min)	Total Safe Time (min)	Safe Time Standard Deviation (min)	Number of Useable Times	Mean Useable Time (min)	Total Useable Time (min)	Percentage of Useable Time
Small/Light	249	1.90	474.10	2.28	3	13.04	39.12	8.1%
Small/Heavy	183	2.59	476.04	3.19	10	12.19	121.94	25.4%
Medium/Light	183	2.59	475.81	3.18	10	11.81	118.06	24.6%
Medium/Heavy	131	3.61	477.17	3.95	12	12.27	147.22	30.7%
Large/Light	157	3.01	476.10	4.00	8	15.19	121.55	25.3%
Large/Heavy	98	4.83	477.93	4.85	19	12.44	236.38	49.2%
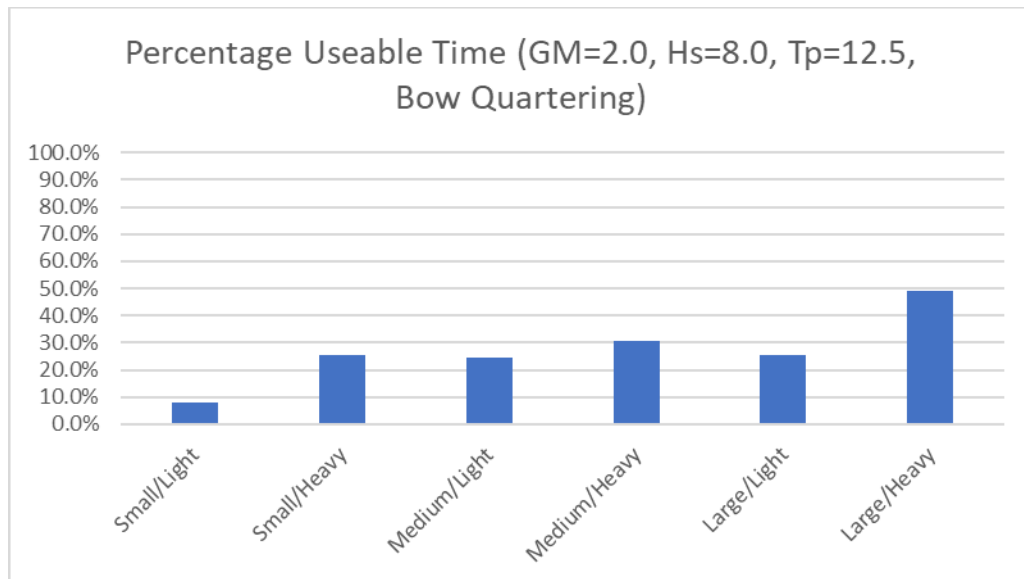
Figure 3-74: Percentage Useable Time, GM=2.0 m, Hs=8.0 m, Tp=12.5 s, Bow Quartering

Distributions of both the "safe time" and "useable time" for the results shown in Table 3-19 are presented graphically through box and whisker plots in Figure 3-75 and Figure 3-76, respectively.
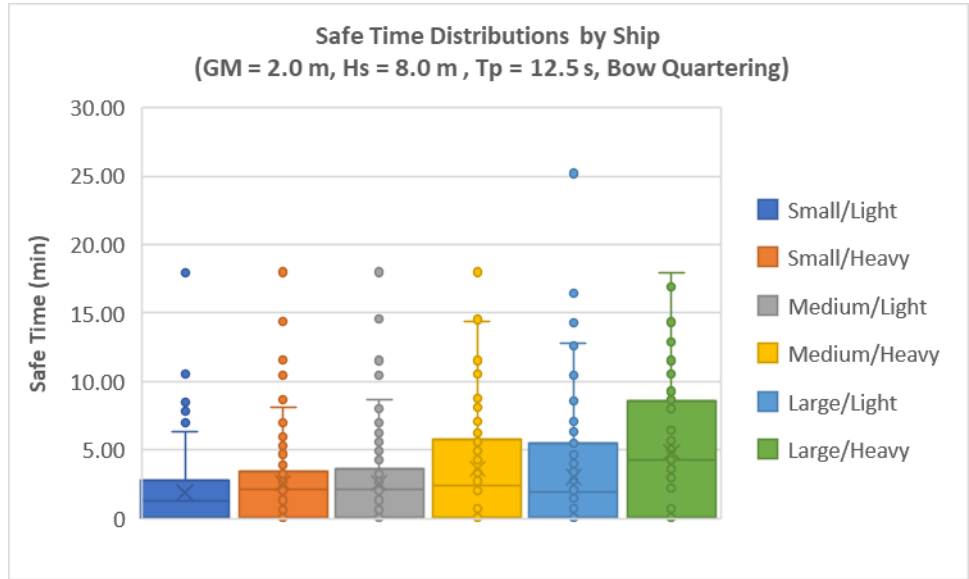
92

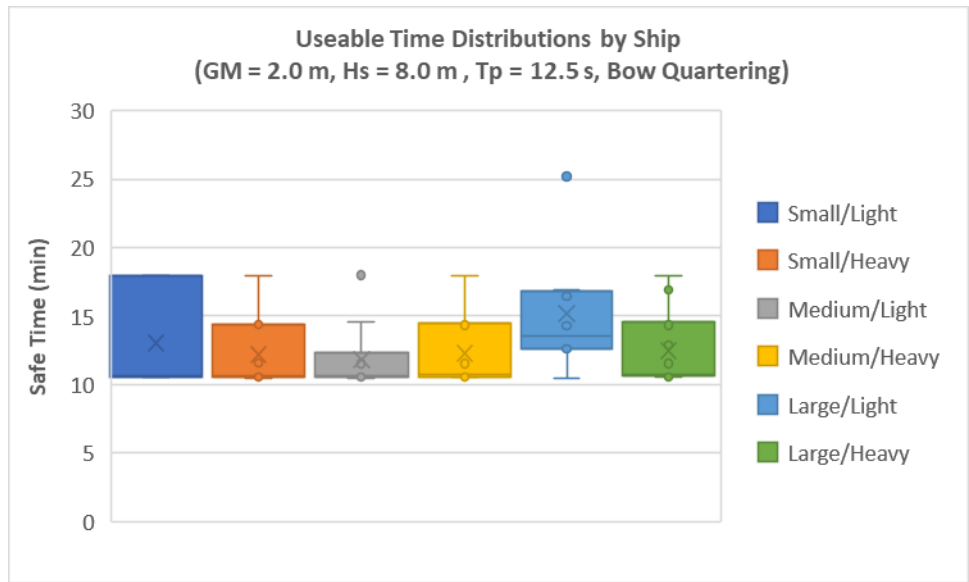**Figure 3-75: Safe Time Distributions, GM=2.0 m, Hs=8.0 m, Tp=12.5 s, Bow Quartering**

Figure 3-76: Useable Time Distributions, GM=2.0 m, Hs=8.0 m, Tp=12.5 s, Bow Quartering

3.3.2.6 'Safe Time' Results – GM=2.75 m, Hs=4.0 m, Beam Seas

Individual summary results for each peak period are presented in Table 3-20 through

Table 3-21.

Table 3-20: Safe Time Results, GM=2.75 m, Hs=4.0 m, Tp=6.0 s, Beam Seas

Ship	Number of Limit Exceedances	Mean Safe Time (min)	Total Safe Time (min)	Safe Time Standard Deviation (min)	Number of Useable Times	Mean Useable Time (min)	Total Useable Time (min)	Percentage of Useable Time
Small/Light	19	23.99	479.87	23.73	12	37.05	444.66	92.6%
Small/Heavy	25	18.45	479.80	17.28	15	28.87	433.01	90.2%
Medium/Light	0	480.00	480.00	N/A	1	480.00	480.00	100.0%
Medium/Heavy	0	480.00	480.00	N/A	1	480.00	480.00	100.0%
Large/Light	0	480.00	480.00	N/A	1	480.00	480.00	100.0%
Large/Heavy	0	480.00	480.00	N/A	1	480.00	480.00	100.0%

Distributions of both the "safe time" and "useable time" for the results shown in Table

3-20 are presented graphically through box and whisker plots in Figure 3-77 and Figure
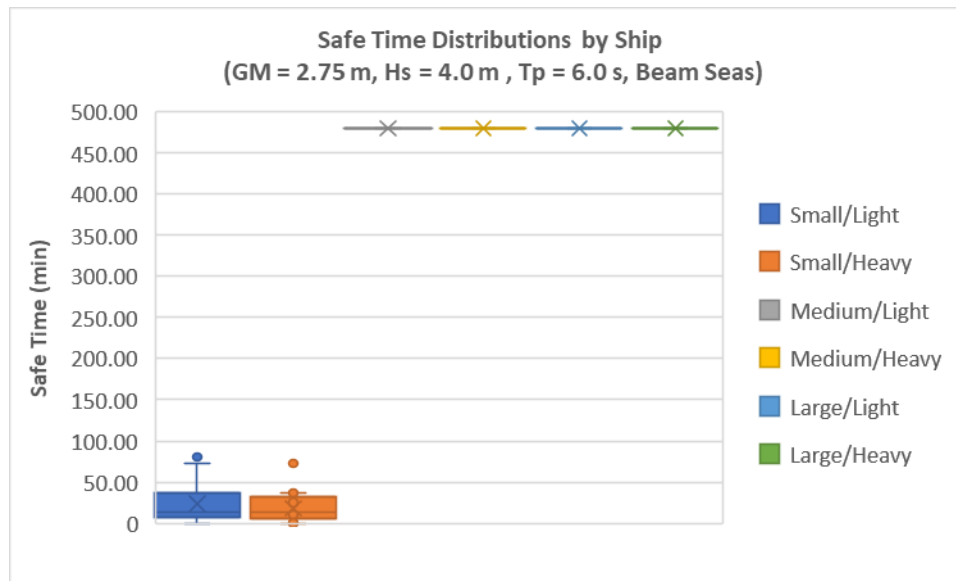
3-78, respectively.

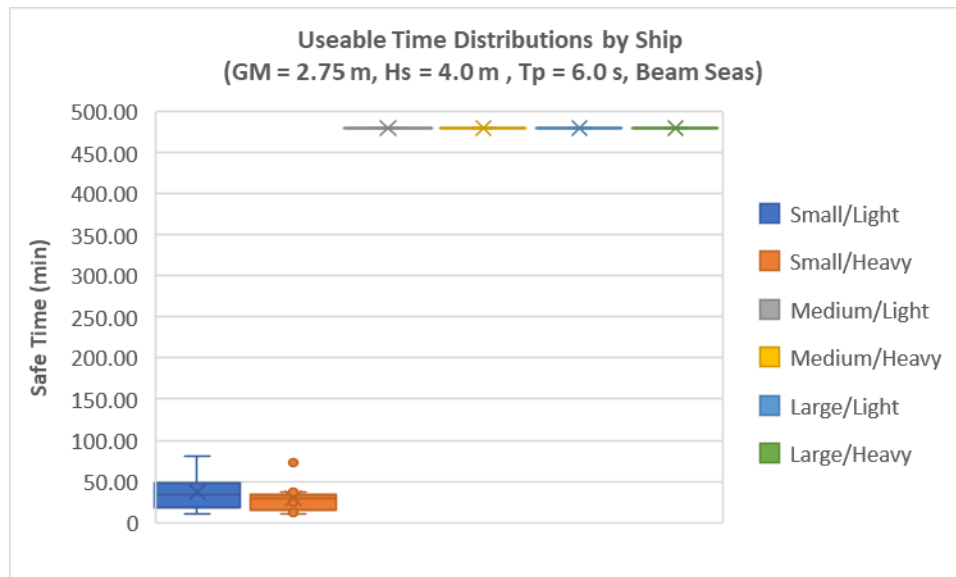**Figure 3-77: Safe Time Distributions, GM=2.75 m, Hs=4.0 m, Tp=6.0 s, Beam Seas**

Figure 3-78: Useable Time Distributions, GM=2.75 m, Hs=4.0 m, Tp=6.0 s, Beam

Seas

Table 3-21: Safe Time Results, GM=2.75 m, Hs=4.0 m, Tp=7.5 s, Beam Seas

Ship	Number of Limit Exceedances	Mean Safe Time (min)	Total Safe Time (min)	Safe Time Standard Deviation (min)	Number of Useable Times	Mean Useable Time (min)	Total Useable Time (min)	Percentage of Useable Time
Small/Light	40	11.70	479.65	11.42	18	22.71	408.72	85.1%
Small/Heavy	77	6.14	479.19	8.01	18	18.66	335.85	70.0%
Medium/Light	0	480.00	480.00	N/A	1	480.00	480.00	100.0%
Medium/Heavy	0	480.00	480.00	N/A	1	480.00	480.00	100.0%
Large/Light	0	480.00	480.00	N/A	1	480.00	480.00	100.0%
Large/Heavy	0	480.00	480.00	N/A	1	480.00	480.00	100.0%

Distributions of both the "safe time" and "useable time" for the results shown in Table 3-21 are presented graphically through box and whisker plots in Figure 3-79 and Figure 3-80, respectively.
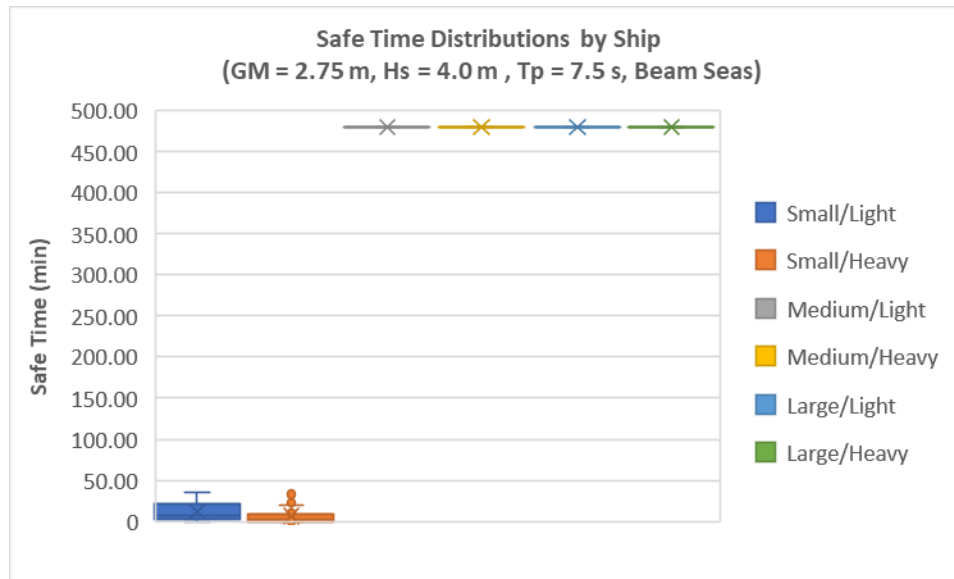

Figure 3-79: Safe Time Distributions, GM=2.75 m, Hs=4.0 m, Tp=7.5 s, Beam Seas
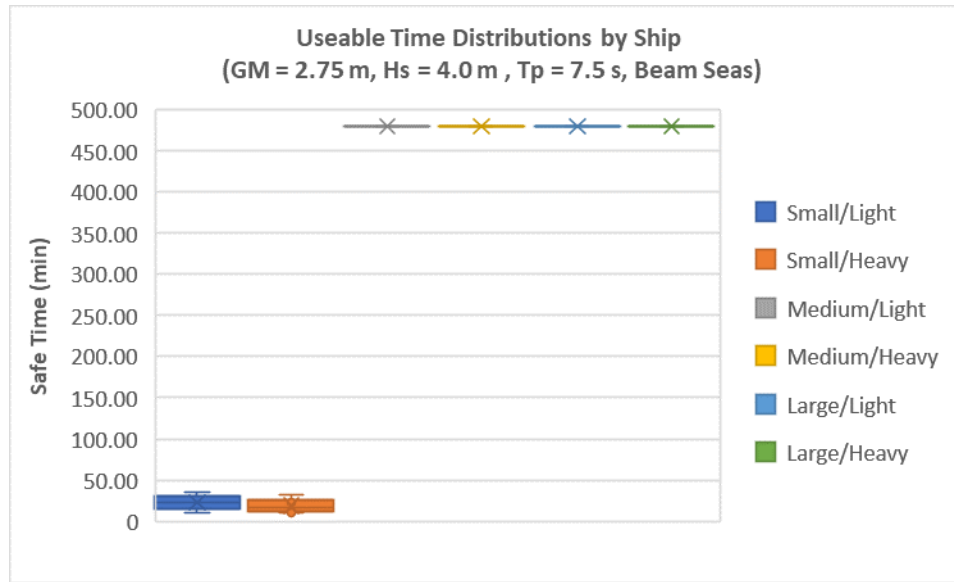
Figure 3-80: Useable Time Distributions, GM=2.75 m, Hs=4.0 m, Tp=7.5 s, Beam Seas

Combining the results from the 2 simulated peak periods above yields the following results for a combined 16 hour (960 minute) simulation.

Table 3-22: Safe Time Results, GM=2.75 m, Hs=4.0 m, Tp=6.0,7.5 s, Beam Seas

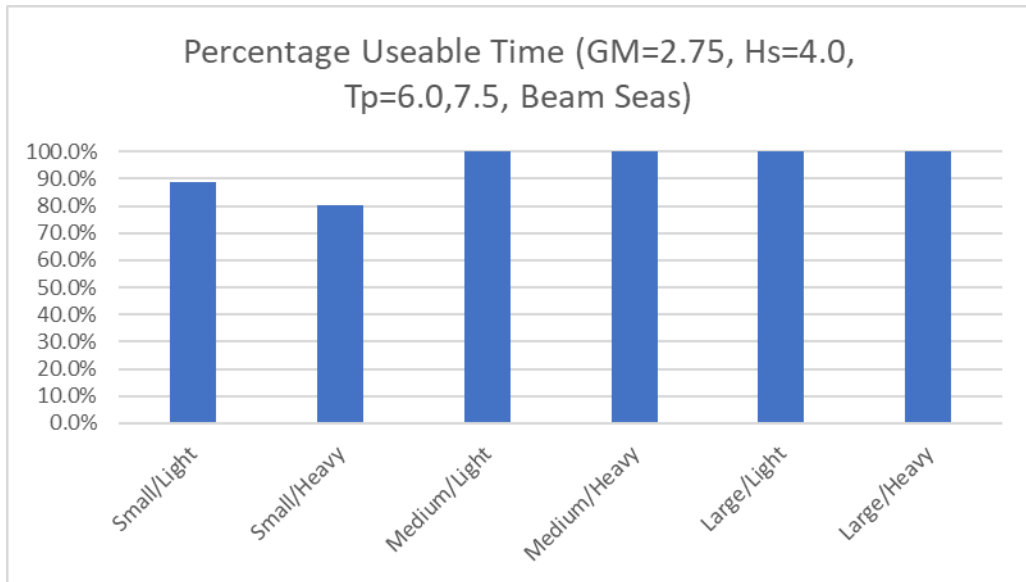| Ship	Total Number of Limit Exceedances	Mean Safe Time (min)	Total Safe Time (min)	Safe Time Standard Deviation (min)	Number of Useable Times	Mean Useable Time (min)	Total Useable Time (min)	Percentage of Useable Time
Small/Light	59	15.73	959.52	17.29	30	28.45	853	88.9%
Small/Heavy	102	9.22	958.99	12.21	33	23.30	769	80.1%
Medium/Light	0	480.00	960.00	N/A	2	480.00	960	100.0%
Medium/Heavy	0	480.00	960.00	N/A	2	480.00	960	100.0%
Large/Light	0	480.00	960.00	N/A	2	480.00	960	100.0%
Large/Heavy	0	480.00	960.00	N/A	2	480.00	960	100.0%

Figure 3-81: Percentage Useable Time, GM=2.75 m, Hs=4.0 m, Tp=6.0,7.5 s, Beam Seas

Distributions of both the "safe time" and "useable time" for the results shown in Table 3-22 are presented graphically through box and whisker plots in Figure 3-82 and Figure 3-83, respectively.

Figure 3-82: Safe Time Distributions, GM=2.75 m, Hs=4.0 m, Tp=6.0,7.5 s, Beam

Seas

Figure 3-83: Useable Time Distributions, GM=2.75 m, Hs=4.0 m, Tp=6.0,7.5 s, Beam

Seas

3.3.2.7 'Safe Time' Results – GM=2.75 m, Hs=5.0 m, Beam Seas

Individual summary results for each peak period are presented in Table 3-23 through

Table 3-25.

Table 3-23: Safe Time Results, GM=2.75 m, Hs=5.0 m, Tp=6.0 s, Beam Seas

Ship	Number of Limit Exceedances	Mean Safe Time (min)	Total Safe Time (min)	Safe Time Standard Deviation (min)	Number of Useable Times	Mean Useable Time (min)	Total Useable Time (min)	Percentage of Useable Time
Small/Light	223	2.13	477.38	2.97	7	13.11	91.74	19.1%
Small/Heavy	257	1.85	476.82	2.48	5	11.45	57.23	11.9%
Medium/Light	38	12.30	479.66	15.54	16	26.35	421.61	87.8%
Medium/Heavy	40	11.70	479.64	14.63	16	25.33	405.25	84.4%
Large/Light	0	480.00	480.00	N/A	1	480.00	480.00	100.0%
Large/Heavy	0	480.00	480.00	N/A	1	480.00	480.00	100.0%

Distributions of both the "safe time" and "useable time" for the results shown in Table

3-23 are presented graphically through box and whisker plots in Figure 3-84 and Figure
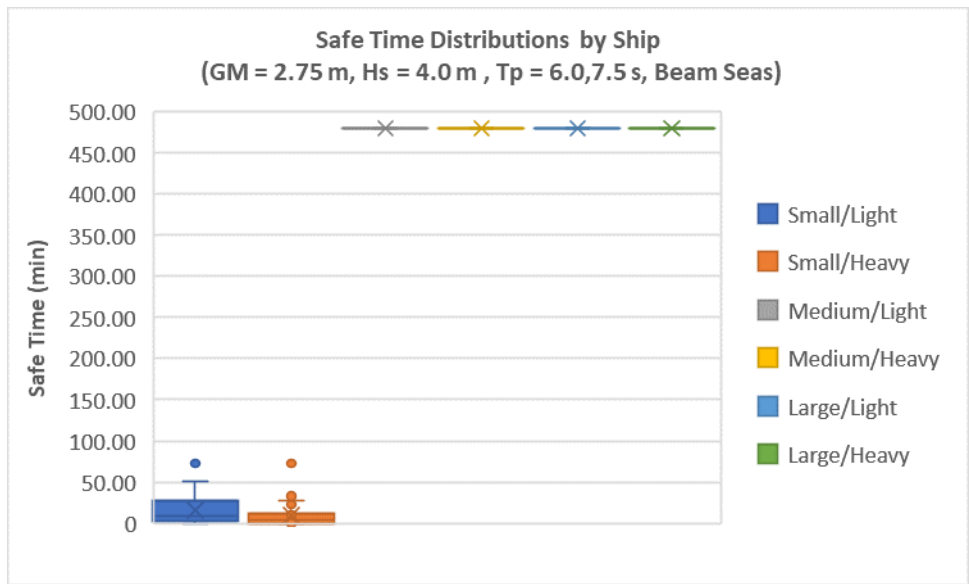
3-85, respectively.

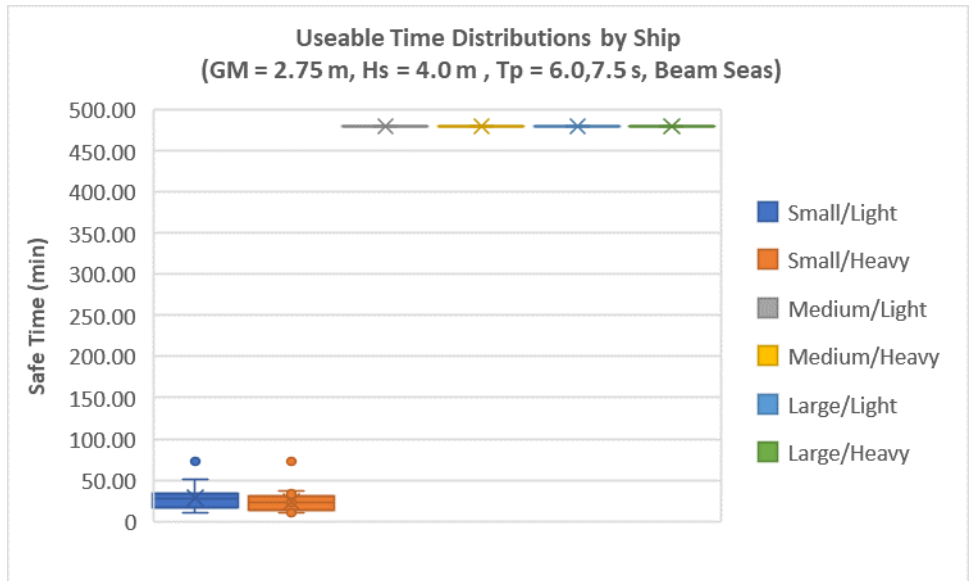**Figure 3-84: Safe Time Distributions, GM=2.75 m, Hs=5.0 m, Tp=6.0 s, Beam Seas**

Figure 3-85: Useable Time Distributions, GM=2.75 m, Hs=5.0 m, Tp=6.0 s, Beam Seas

Table 3-24: Safe Time Results, GM=2.75 m, Hs=5.0 m, Tp=7.5 s, Beam Seas

Ship	Number of Limit Exceedances	Mean Safe Time (min)	Total Safe Time (min)	Safe Time Standard Deviation (min)	Number of Useable Times	Mean Useable Time (min)	Total Useable Time (min)	Percentage of Useable Time
Small/Light	314	1.51	475.47	2.23	3	15.36	46.08	9.6%
Small/Heavy	469	1.01	472.85	1.46	1	11.11	11.11	2.3%
Medium/Light	104	4.56	478.62	5.89	16	15.32	245.16	51.1%
Medium/Heavy	139	3.42	478.11	4.70	12	15.04	180.49	37.6%
Large/Light	30	15.47	479.71	16.23	15	29.25	438.78	91.4%
Large/Heavy	39	11.99	479.61	14.09	16	27.11	433.70	90.4%

Distributions of both the "safe time" and "useable time" for the results shown in Table 3-24 are presented graphically through box and whisker plots in Figure 3-86 and Figure 3-87, respectively.
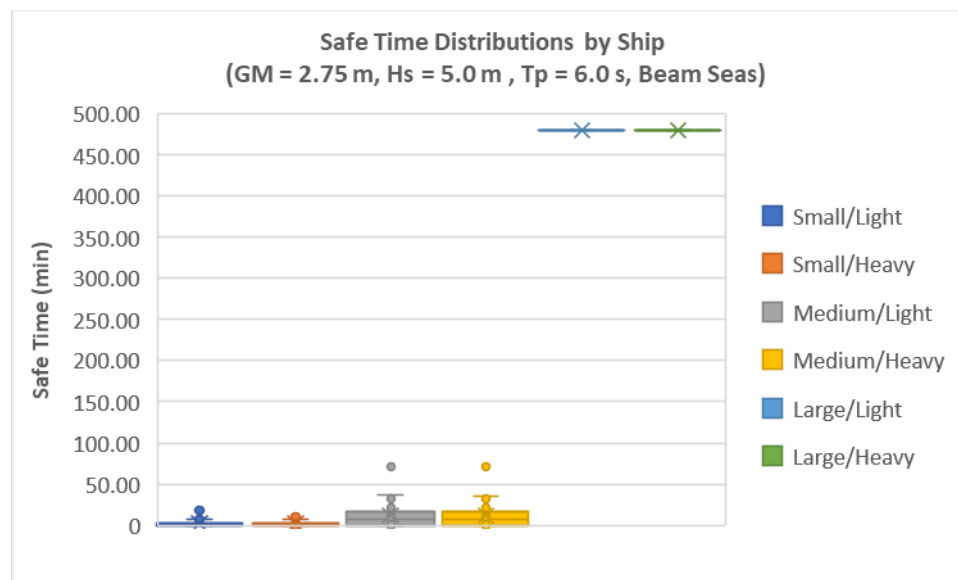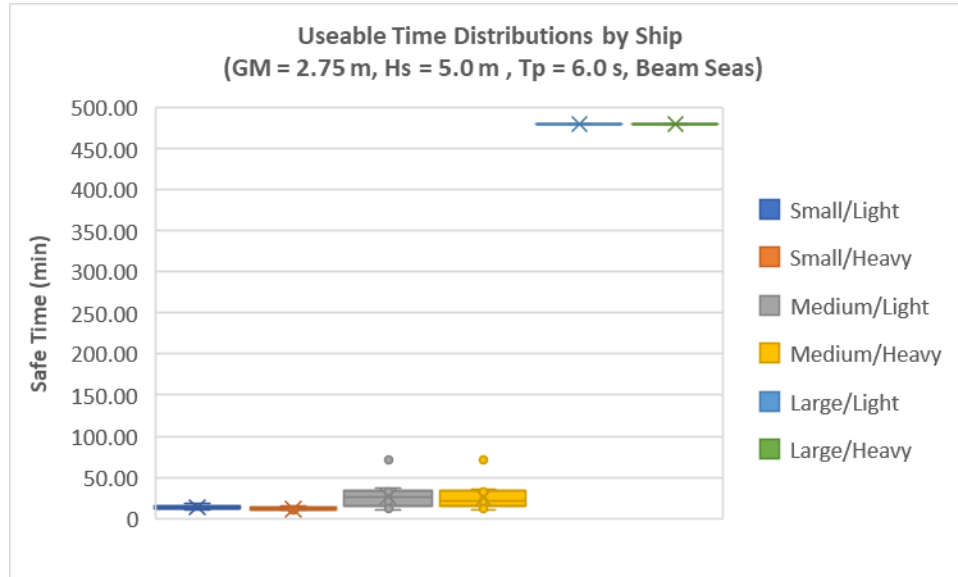
Figure 3-86: Safe Time Distributions, GM=2.75 m, Hs=5.0 m, Tp=7.5 s, Beam Seas

Figure 3-87: Useable Time Distributions, GM=2.75 m, Hs=5.0 m, Tp=7.5 s, Beam

Seas

Table 3-25: Safe Time Results, GM=2.75 m, Hs=5.0 m, Tp=11.5 s, Beam Seas

Ship	Number of Limit Exceedances	Mean Safe Time (min)	Total Safe Time (min)	Safe Time Standard Deviation (min)	Number of Useable Times	Mean Useable Time (min)	Total Useable Time (min)	Percentage of Useable Time
Small/Light	12	36.91	479.85	37.08	10	46.25	462.51	96.4%
Small/Heavy	13	34.27	479.85	31.26	10	46.18	461.80	96.2%
Medium/Light	6	68.56	479.93	63.64	6	78.92	473.51	98.6%
Medium/Heavy	6	68.56	479.93	63.58	6	78.92	473.51	98.6%
Large/Light	4	95.99	479.96	115.82	5	95.99	479.96	100.0%
Large/Heavy	4	95.99	479.96	57.57	5	95.99	479.96	100.0%

Distributions of both the "safe time" and "useable time" for the results shown in Table

3-25 are presented graphically through box and whisker plots in Figure 3-88 and Figure
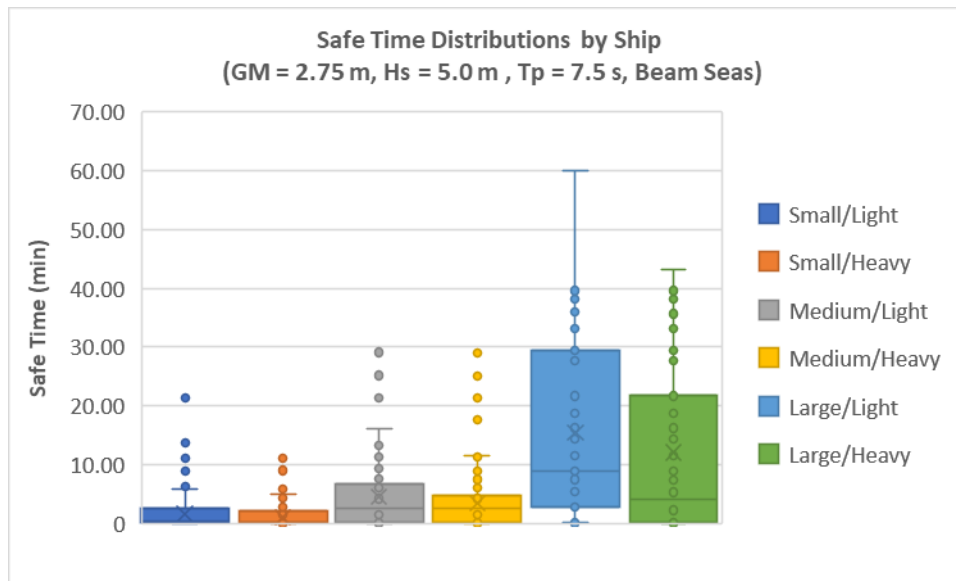
3-89, respectively.

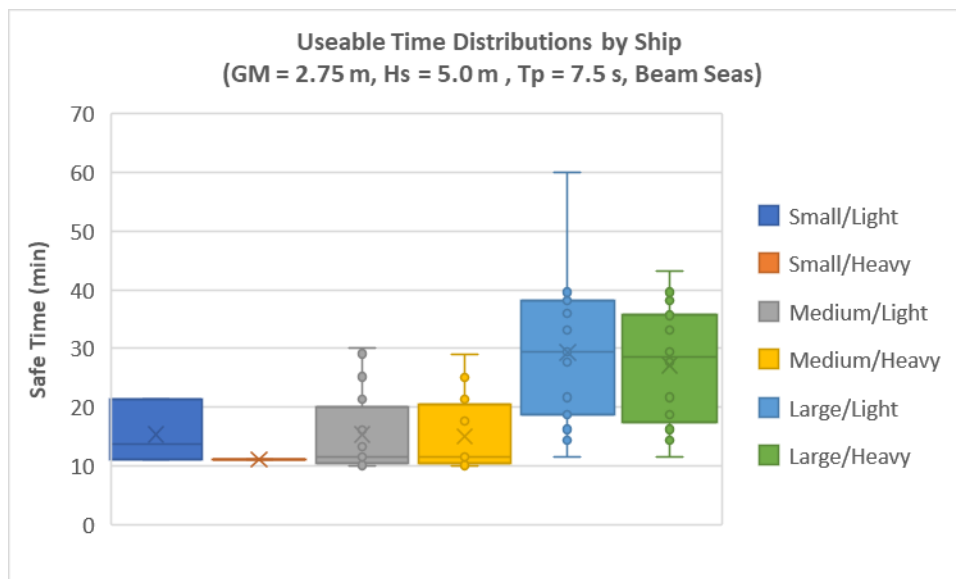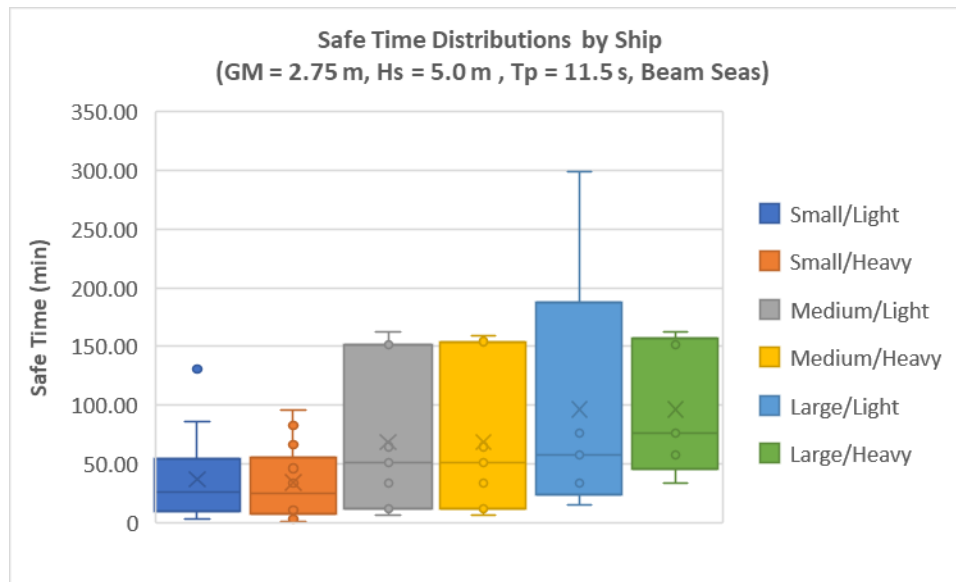**Figure 3-88: Safe Time Distributions, GM=2.75 m, Hs=5.0 m, Tp=11.5 s, Beam Seas**

Figure 3-89: Useable Time Distributions, GM=2.75 m, Hs=5.0 m, Tp=11.5 s, Beam Seas

Combining the results from the 3 simulated peak periods above yields the following results for a combined 24 hour (1440 minute) simulation.

Table 3-26: Safe Time Results, GM=2.75 m, Hs=5.0 m, Tp=6.0,7.5,11.5 s, Beam Seas

Ship	Total Number of Limit Exceedances	Mean Safe Time (min)	Total Safe Time (min)	Safe Time Standard Deviation (min)	Number of Useable Times	Mean Useable Time (min)	Total Useable Time (min)	Percentage of Useable Time
Small/Light	549	2.60	1432.70	8.06	20	30.02	600	41.7%
Small/Heavy	739	1.93	1429.52	6.40	16	33.13	530	36.8%
Medium/Light	148	9.52	1438.21	20.72	38	30.01	1140	79.2%
Medium/Heavy	185	7.65	1437.68	18.65	34	31.15	1059	73.6%
Large/Light	34	38.91	1439.67	89.67	21	66.61	1399	97.1%
Large/Heavy	43	31.30	1439.57	75.74	22	63.35	1394	96.8%
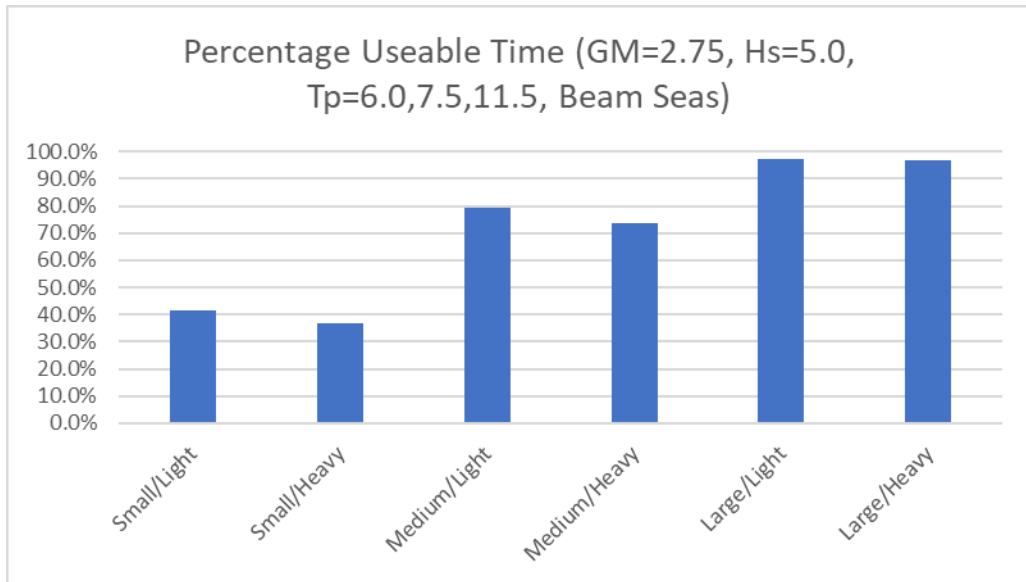
Figure 3-90: Percentage Useable Time, GM=2.75 m, Hs=5.0 m, Tp=6.0,7.5,11.5 s, Beam Seas

Distributions of both the "safe time" and "useable time" for the results shown in Table 3-26 are presented graphically through box and whisker plots in Figure 3-91 and Figure 3-92, respectively.

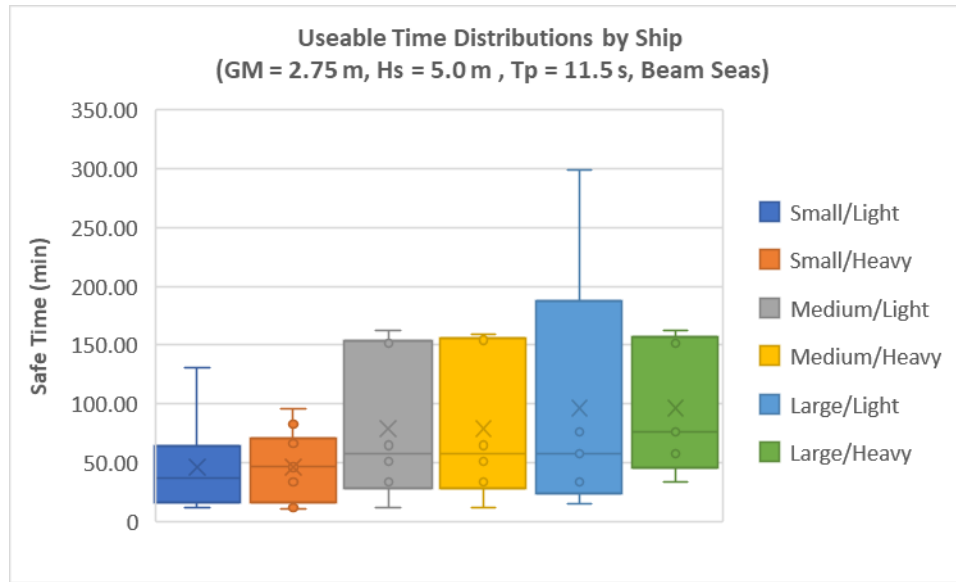**Figure 3-91: Safe Time Distributions, GM=2.75 m, Hs=5.0 m, Tp=6.0,7.5,11.5 s, Beam Seas**

Figure 3-92: Useable Time Distributions, GM=2.75 m, Hs=5.0 m, Tp=6.0,7.5,11.5 s, Beam Seas

3.3.2.8 'Safe Time' Results – GM=2.75 m, Hs=6.0 m, Beam Seas

Individual summary results for each peak period are presented in Table 3-27 through

Table 3-28.

Table 3-27: Safe Time Results, GM=2.75 m, Hs=6.0 m, Tp=11.5 s, Beam Seas

Ship	Number of Limit Exceedances	Mean Safe Time (min)	Total Safe Time (min)	Safe Time Standard Deviation (min)	Number of Useable Times	Mean Useable Time (min)	Total Useable Time (min)	Percentage of Useable Time
Small/Light	108	4.39	478.34	4.26	6	17.07	102.40	21.3%
Small/Heavy	113	4.19	478.21	4.08	9	14.44	129.99	27.1%
Medium/Light	69	6.84	478.81	8.05	13	19.01	247.16	51.5%
Medium/Heavy	74	6.38	478.74	8.44	9	22.86	205.74	42.9%
Large/Light	51	9.21	479.10	12.75	15	20.02	300.30	62.6%
Large/Heavy	55	8.56	479.11	12.38	14	20.20	282.78	58.9%

Distributions of both the "safe time" and "useable time" for the results shown in Table

3-27 are presented graphically through box and whisker plots in Figure 3-93 and Figure
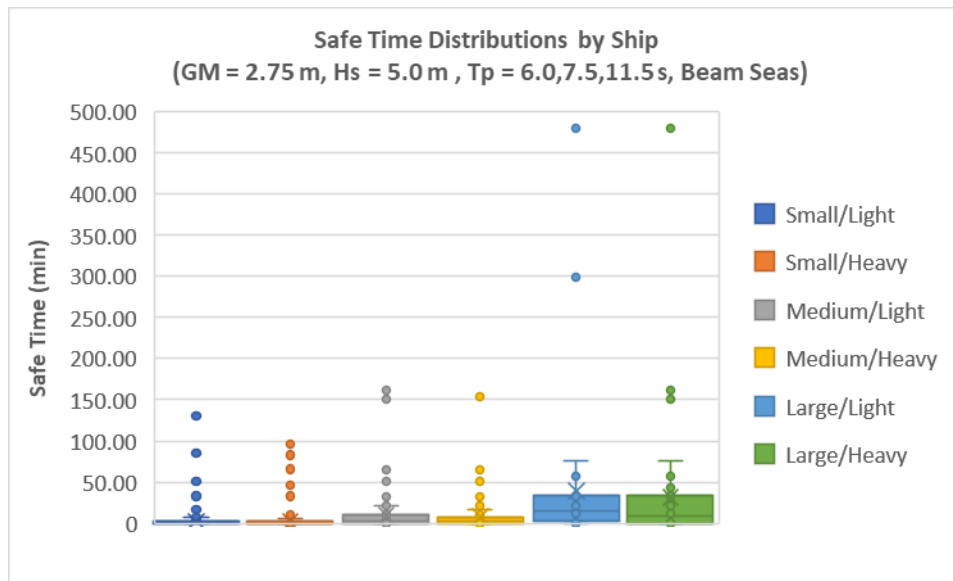
3-94, respectively.

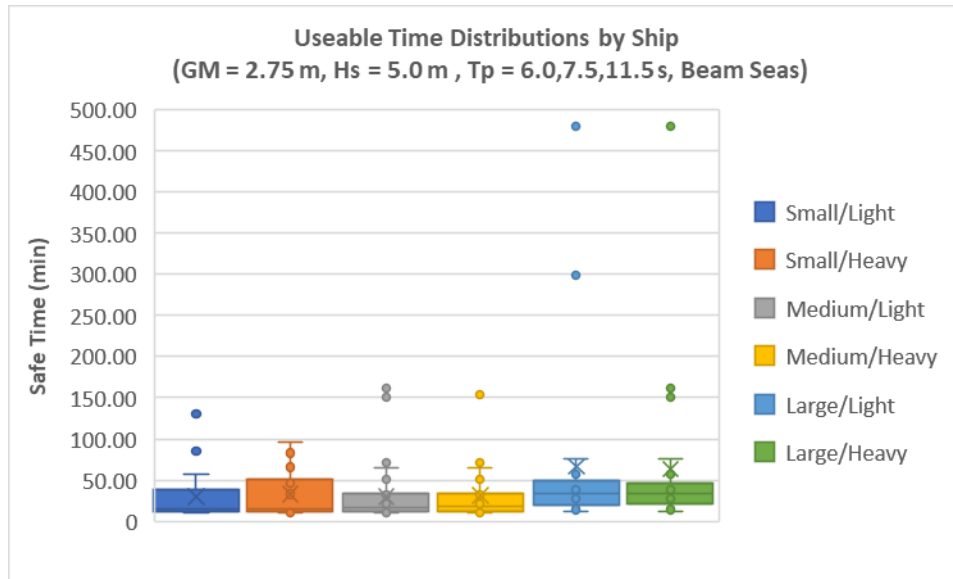**Figure 3-93: Safe Time Distributions, GM=2.75 m, Hs=6.0 m, Tp=11.5 s, Beam Seas**

Figure 3-94: Useable Time Distributions, GM=2.75 m, Hs=6.0 m, Tp=11.5 s, Beam Seas

Table 3-28: Safe Time Results, GM=2.75 m, Hs=6.0 m, Tp=15.5 s, Beam Seas

Ship	Number of Limit Exceedances	Mean Safe Time (min)	Total Safe Time (min)	Safe Time Standard Deviation (min)	Number of Useable Times	Mean Useable Time (min)	Total Useable Time (min)	Percentage of Useable Time
Small/Light	9	47.98	479.84	35.06	8	59.10	472.80	98.5%
Small/Heavy	11	39.99	479.84	28.13	10	47.28	472.79	98.5%
Medium/Light	7	59.99	479.90	60.94	6	78.81	472.85	98.5%
Medium/Heavy	8	53.32	479.89	58.55	7	67.55	472.84	98.5%
Large/Light	0	480.00	480.00	N/A	1	480.00	480.00	100.0%
Large/Heavy	0	480.00	480.00	N/A	1	480.00	480.00	100.0%

Distributions of both the "safe time" and "useable time" for the results shown in Table 3-28 are presented graphically through box and whisker plots in Figure 3-95 and Figure 3-96, respectively.
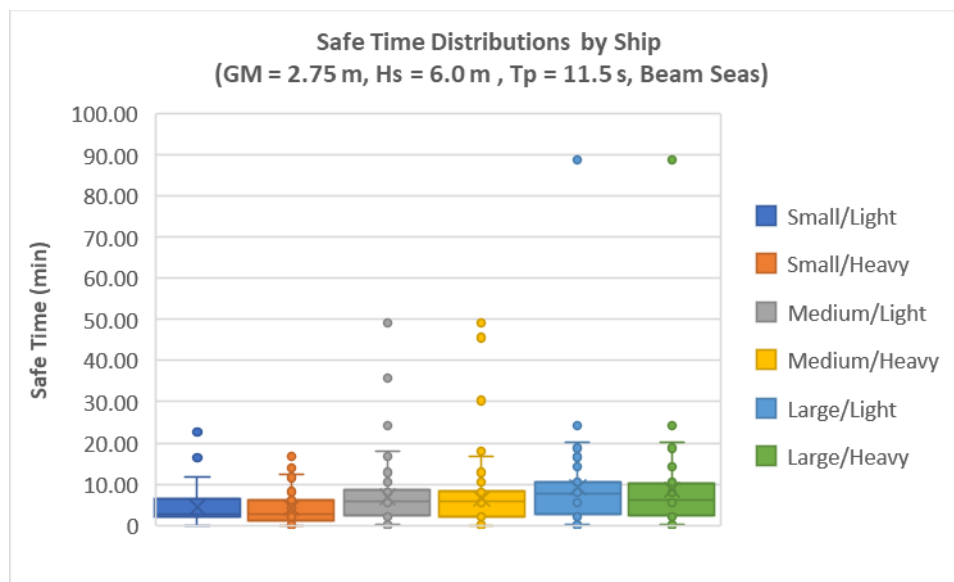
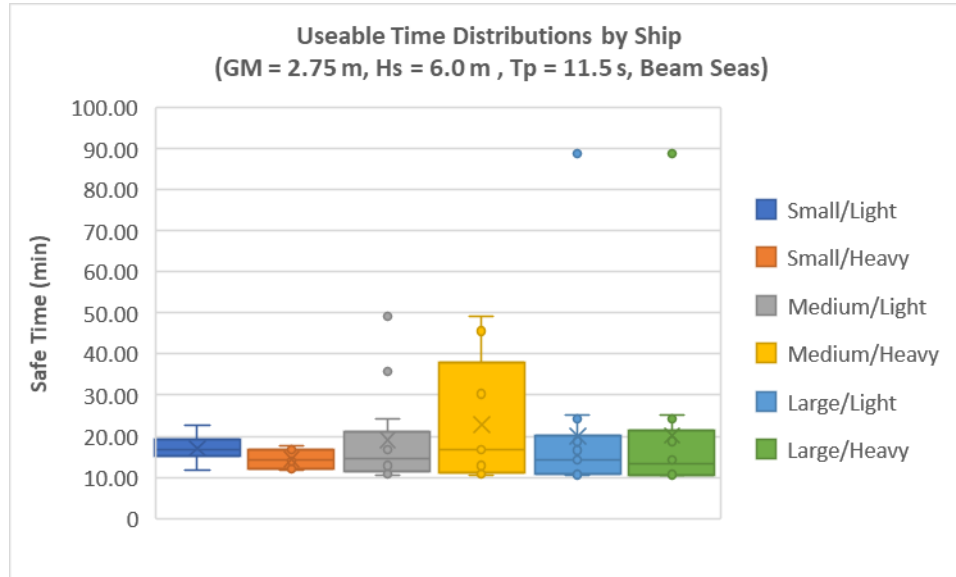**Figure 3-95: Safe Time Distributions, GM=2.75 m, Hs=6.0 m, Tp=15.5 s, Beam Seas**

Figure 3-96: Useable Time Distributions, GM=2.75 m, Hs=6.0 m, Tp=15.5 s, Beam

Seas

Combining the results from the 2 simulated peak periods above yields the following

results for a combined 16 hour (960 minute) simulation.

Table 3-29: Safe Time Results, GM=2.75 m, Hs=6.0 m, Tp=11.5,15.5 s, Beam Seas

Ship	Total Number of Limit Exceedances	Mean Safe Time (min)	Total Safe Time (min)	Safe Time Standard Deviation (min)	Number of Useable Times	Mean Useable Time (min)	Total Useable Time (min)	Percentage of Useable Time
Small/Light	117	8.05	958.18	16.06	14	41.09	575	59.9%
Small/Heavy	124	7.60	958.05	14.00	19	31.73	603	62.8%
Medium/Light	76	12.29	958.71	25.67	19	37.90	720	75.0%
Medium/Heavy	82	11.41	958.64	24.64	16	42.41	679	70.7%
Large/Light	51	18.10	959.10	65.89	16	48.77	780	81.3%
Large/Heavy	55	16.83	959.11	63.64	15	50.85	763	79.5%
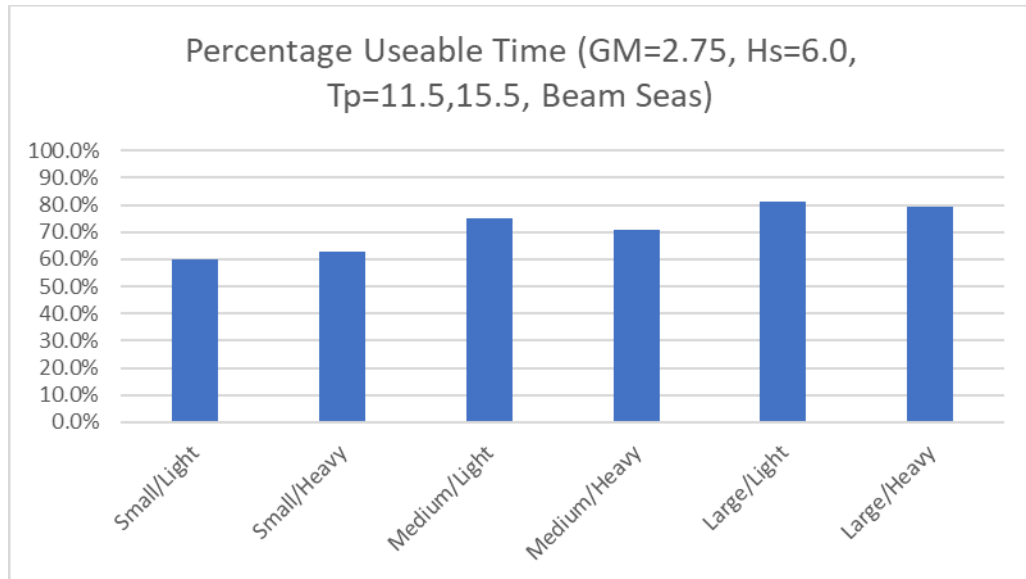
Figure 3-97: Percentage Useable Time, GM=2.75 m, Hs=6.0 m, Tp=11.5,15.5 s, Beam Seas

Distributions of both the "safe time" and "useable time" for the results shown in Table

3-29 are presented graphically through box and whisker plots in Figure 3-98 and Figure
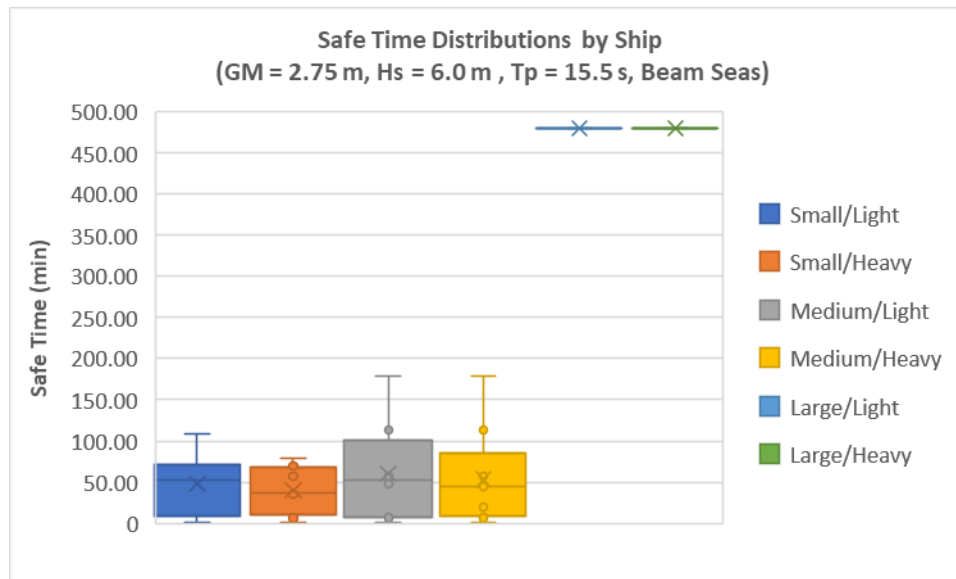
3-99, respectively.

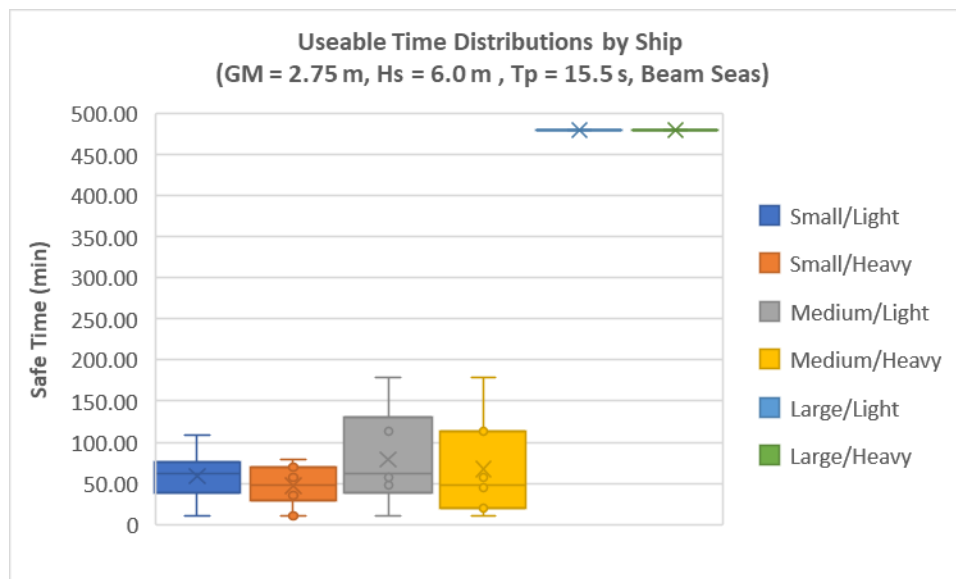**Figure 3-98: Safe Time Distributions, GM=2.75 m, Hs=6.0 m, Tp=11.5,15.5 s, Beam Seas**

Figure 3-99: Useable Time Distributions, GM=2.75 m, Hs=6.0 m, Tp=11.5,15.5 s, Beam Seas

3.3.2.9 'Safe Time' Results – GM=2.75 m, Hs=6.0 m, Bow

Quartering

Individual summary results for each peak period are presented in Table 3-30 through Table 3-31.

Table 3-30: Safe Time Results, GM=2.75 m, Hs=6.0 m, Tp=7.5 s, Bow Quartering

Ship	Number of Limit Exceedances	Mean Safe Time (min)	Total Safe Time (min)	Safe Time Standard Deviation (min)	Number of Useable Times	Mean Useable Time (min)	Total Useable Time (min)	Percentage of Useable Time
Small/Light	12	36.92	479.90	38.92	8	59.61	476.91	99.4%
Small/Heavy	0	480.00	480.00	N/A	1	480.00	480.00	100.0%
Medium/Light	0	480.00	480.00	N/A	1	480.00	480.00	100.0%
Medium/Heavy	0	480.00	480.00	N/A	1	480.00	480.00	100.0%
Large/Light	0	480.00	480.00	N/A	1	480.00	480.00	100.0%
Large/Heavy	0	480.00	480.00	N/A	1	480.00	480.00	100.0%

Distributions of both the "safe time" and "useable time" for the results shown in Table 3-30 are presented graphically through box and whisker plots in Figure 3-100 and Figure 3-101, respectively.

Figure 3-100: Safe Time Distributions, GM=2.75 m, Hs=6.0 m, Tp=7.5 s, Bow Quartering

Figure 3-101: Useable Time Distributions, GM=2.75 m, Hs=6.0 m, Tp=7.5 s, Bow Quartering

Table 3-31: Safe Time Results, GM=2.75 m, Hs=6.0 m, Tp=11.5 s, Bow Quartering

Ship	Number of Limit Exceedances	Mean Safe Time (min)	Total Safe Time (min)	Safe Time Standard Deviation (min)	Number of Useable Times	Mean Useable Time (min)	Total Useable Time (min)	Percentage of Useable Time
Small/Light	15	29.99	479.80	34.70	13	35.76	464.85	96.8%
Small/Heavy	0	480.00	480.00	N/A	1	480.00	480.00	100.0%
Medium/Light	0	480.00	480.00	N/A	1	480.00	480.00	100.0%
Medium/Heavy	0	480.00	480.00	N/A	1	480.00	480.00	100.0%
Large/Light	0	480.00	480.00	N/A	1	480.00	480.00	100.0%
Large/Heavy	0	480.00	480.00	N/A	1	480.00	480.00	100.0%

Distributions of both the "safe time" and "useable time" for the results shown in Table 3-31 are presented graphically through box and whisker plots in Figure 3-102 and Figure 3-103, respectively.
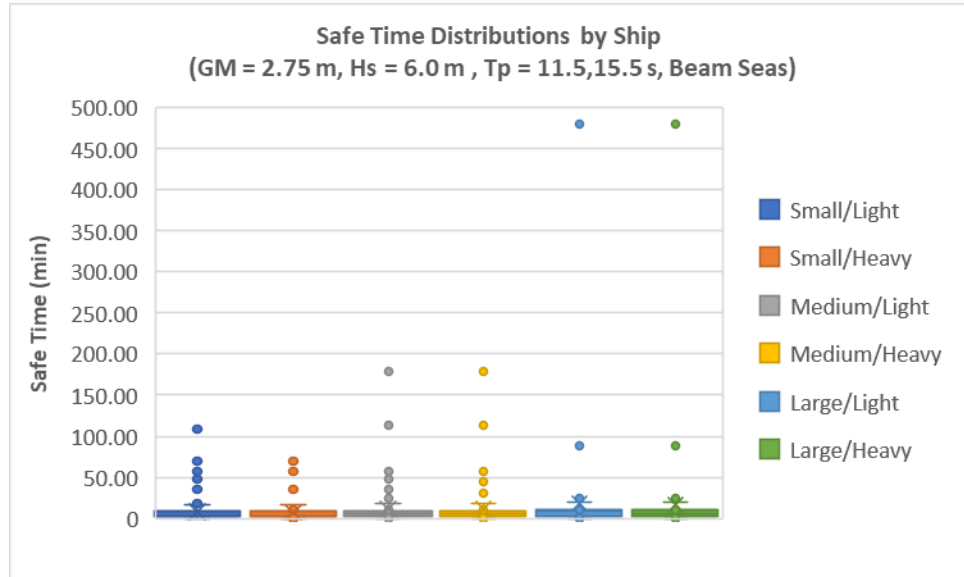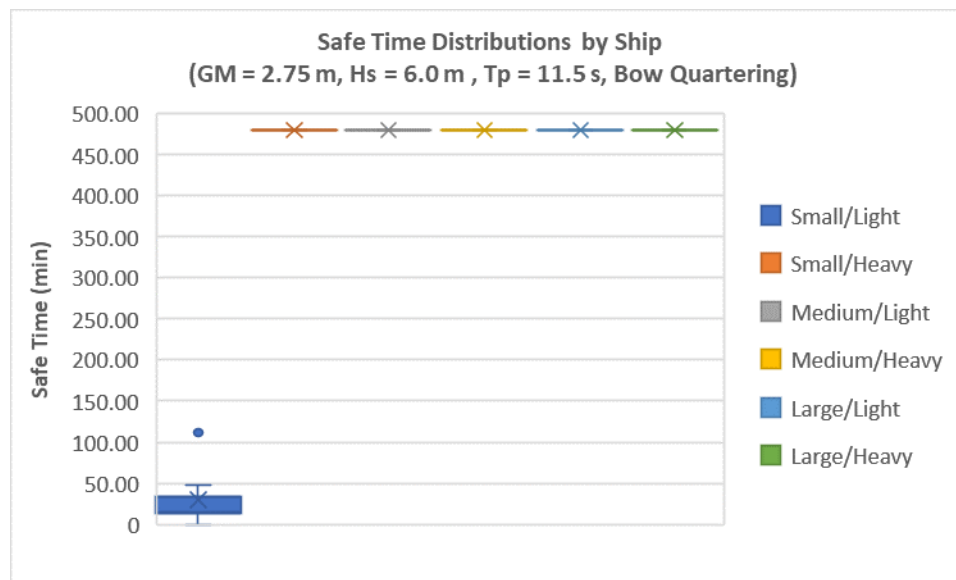

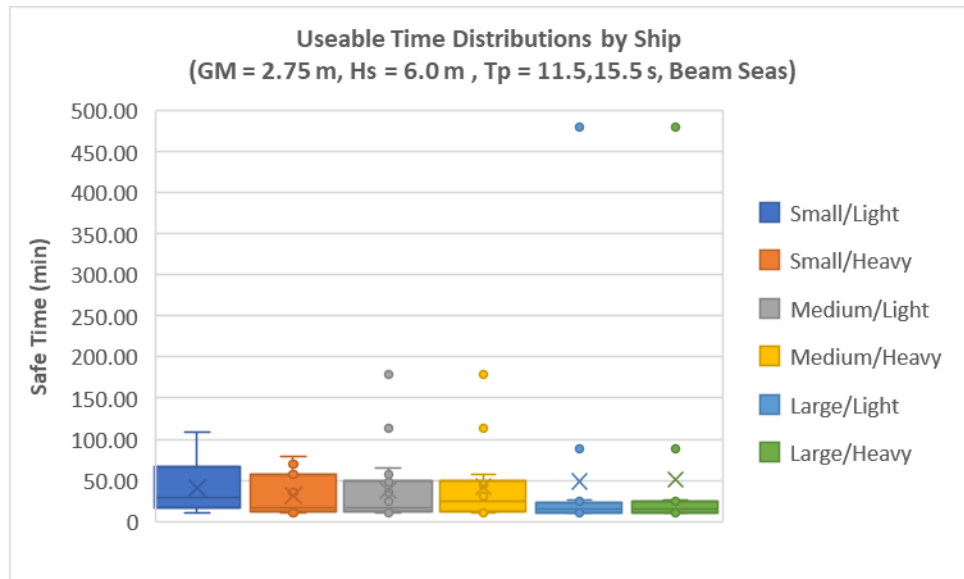**Figure 3-102: Safe Time Distributions, GM=2.75 m, Hs=6.0 m, Tp=11.5 s, Bow Quartering**

Figure 3-103: Useable Time Distributions, GM=2.75 m, Hs=6.0 m, Tp=11.5 s, Bow Quartering

Combining the results from the 2 simulated peak periods above yields the following results for a combined 16 hour (960 minute) simulation.

Table 3-32: Safe Time Results, GM=2.75 m, Hs=6.0 m, Tp=7.5,11.5 s, Bow Quartering

Ship	Total Number of Limit Exceedances	Mean Safe Time (min)	Total Safe Time (min)	Safe Time Standard Deviation (min)	Number of Useable Times	Mean Useable Time (min)	Total Useable Time (min)	Percentage of Useable Time
Small/Light	27	33.09	959.70	36.14	21	44.85	942	98.1%
Small/Heavy	0	480.00	960.00	N/A	2	480.00	960	100.0%
Medium/Light	0	480.00	960.00	N/A	2	480.00	960	100.0%
Medium/Heavy	0	480.00	960.00	N/A	2	480.00	960	100.0%
Large/Light	0	480.00	960.00	N/A	2	480.00	960	100.0%
Large/Heavy	0	480.00	960.00	N/A	2	480.00	960	100.0%

Figure 3-104: Percentage Useable Time, GM=2.75 m, Hs=6.0 m, Tp=7.5,11.5 s, Bow Quartering

Distributions of both the "safe time" and "useable time" for the results shown in Table 3-32 are presented graphically through box and whisker plots in Figure 3-105 and Figure 3-106, respectively.
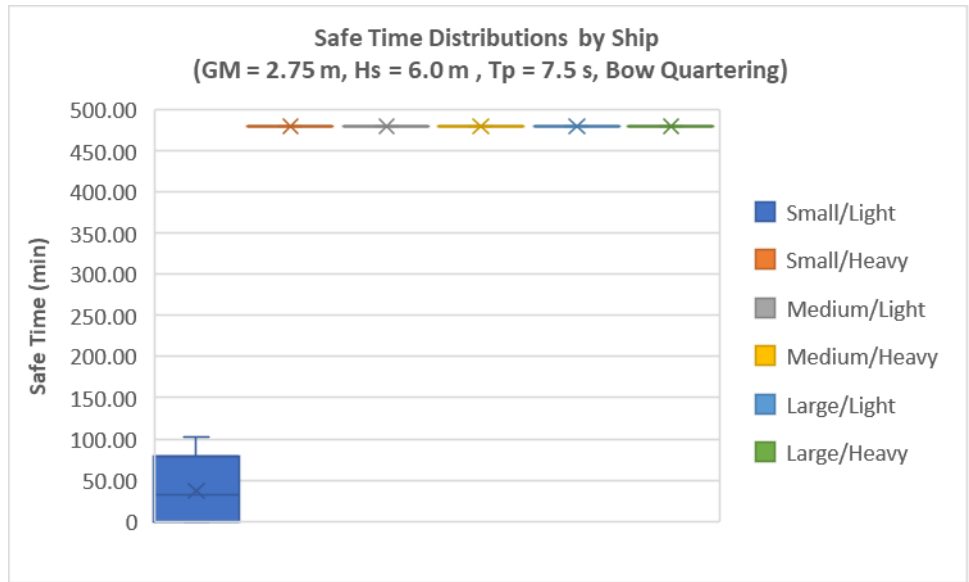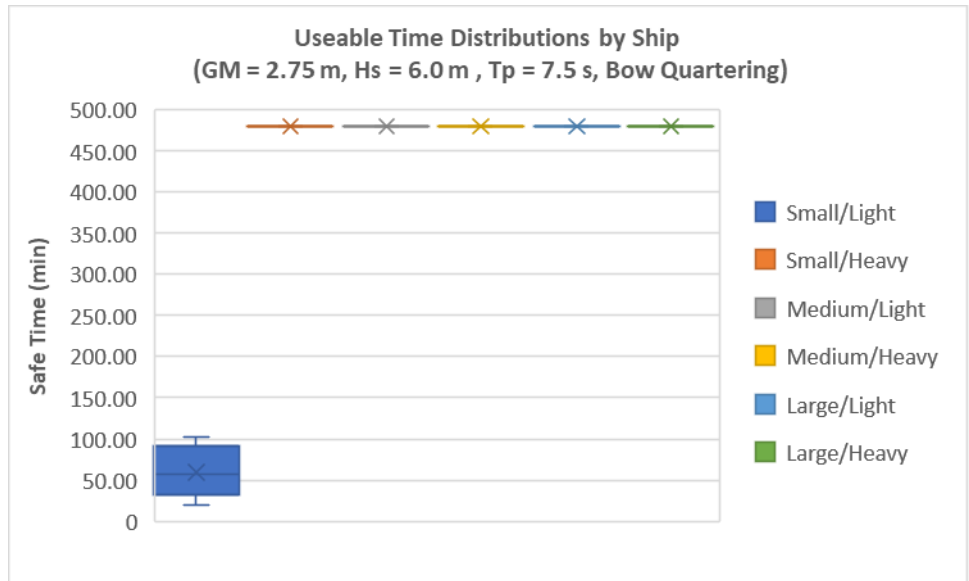
116

Figure 3-105: Safe Time Distributions, GM=2.75 m, Hs=6.0 m, Tp=7.5,11.5 s, Bow Quartering

Figure 3-106: Useable Time Distributions, GM=2.75 m, Hs=6.0 m, Tp=7.5,11.5 s, Bow Quartering

3.3.2.10 'Safe Time' Results – GM=2.75 m, Hs=8.0 m, Head Seas

Table 3-33: Safe Time Results, GM=2.75 m, Hs=8.0 m, Tp=12.5 s, Head Seas

Ship	Number of Limit Exceedances	Mean Safe Time (min)	Total Safe Time (min)	Safe Time Standard Deviation (min)	Number of Useable Times	Mean Useable Time (min)	Total Useable Time (min)	Percentage of Useable Time
Small/Light	97	4.88	478.01	4.92	17	12.83	218.05	45.4%
Small/Heavy	35	13.32	479.36	12.59	18	22.81	410.61	85.5%
Medium/Light	54	8.71	479.04	8.80	21	17.01	357.16	74.4%
Medium/Heavy	12	36.91	479.84	34.68	10	47.06	470.59	98.0%
Large/Light	21	21.80	479.62	23.86	15	30.39	455.88	95.0%
Large/Heavy	2	159.99	479.97	193.26	2	239.95	479.90	100.0%
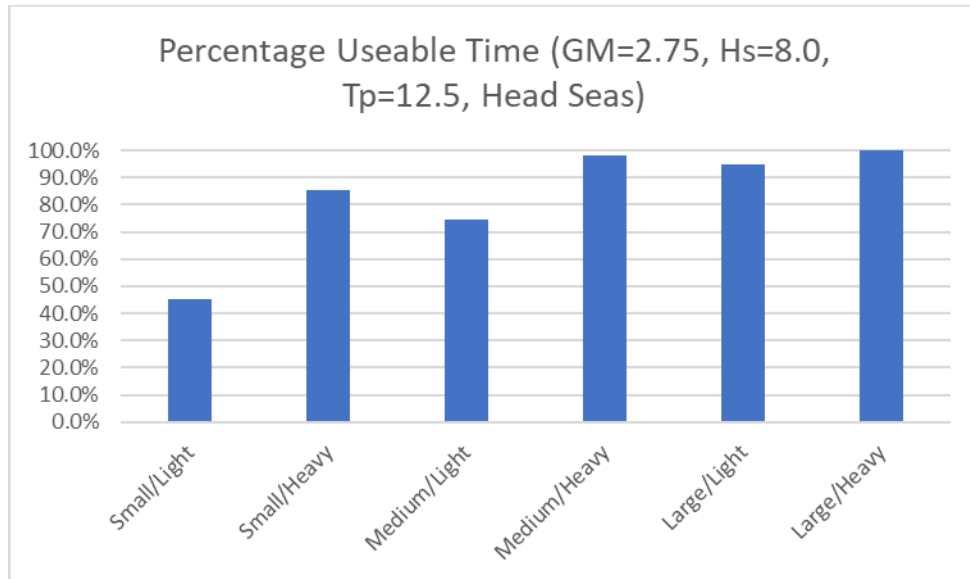
Figure 3-107: Percentage Useable Time, GM=2.75 m, Hs=8.0 m, Tp=12.5 s, Head Seas

Distributions of both the "safe time" and "useable time" for the results shown in Table 3-33 are presented graphically through box and whisker plots in Figure 3-108 and Figure 3-109, respectively.

118
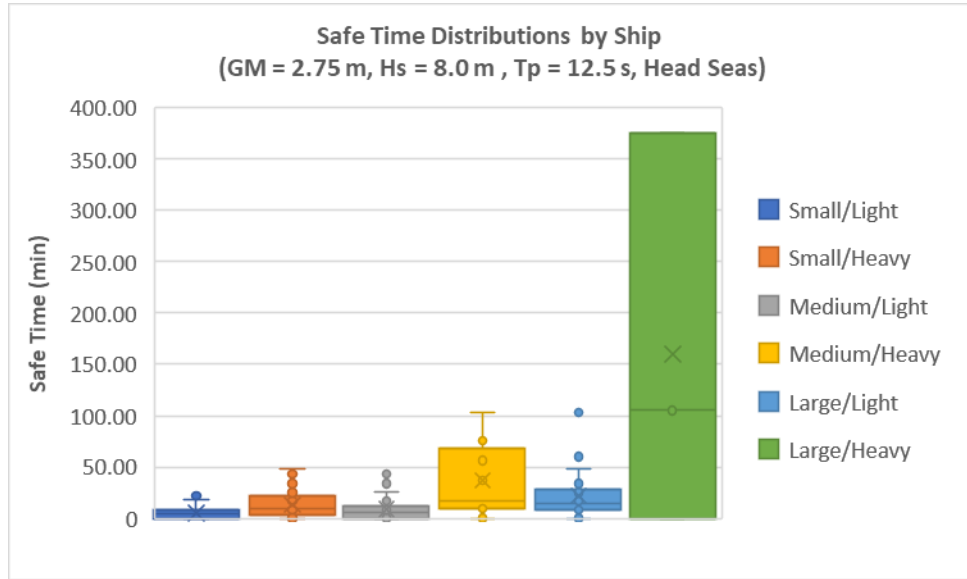
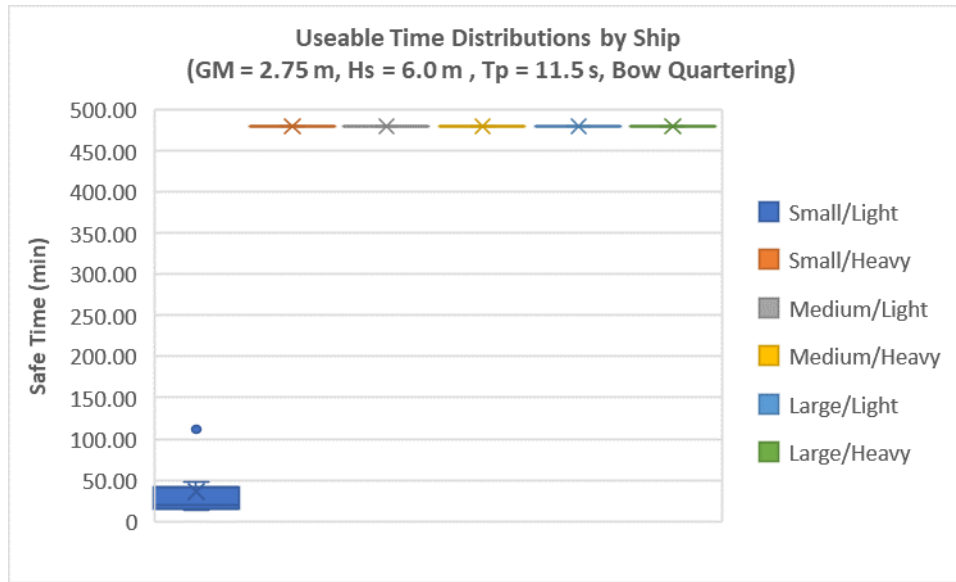**Figure 3-108: Safe Time Distributions, GM=2.75 m, Hs=8.0 m, Tp=12.5 s, Head Seas**
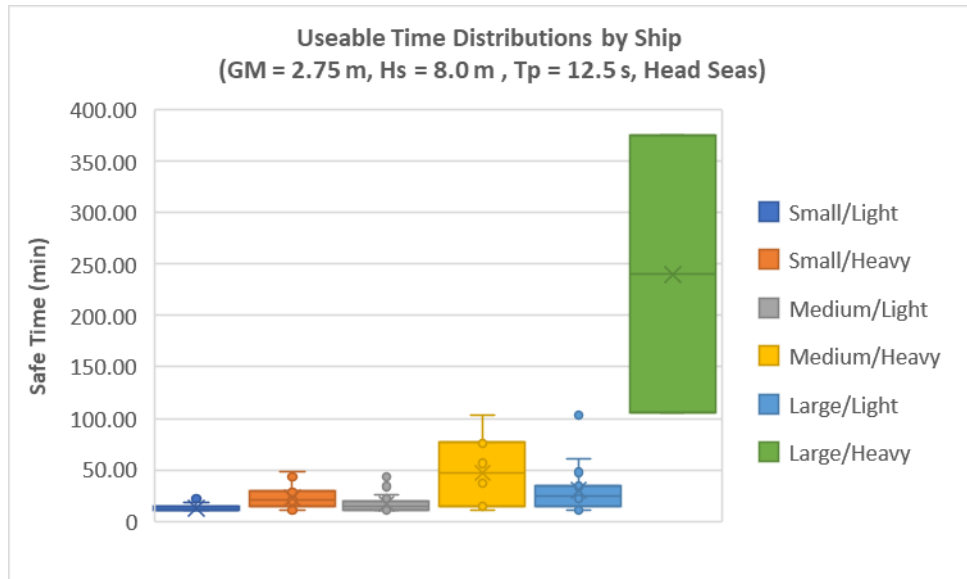
Figure 3-109: Useable Time Distributions, GM=2.75 m, Hs=8.0 m, Tp=12.5 s, Head

Seas

Table 3-34: Safe Time Results, GM=2.75 m, Hs=8.0 m, Tp=12.5 s, Bow Quartering

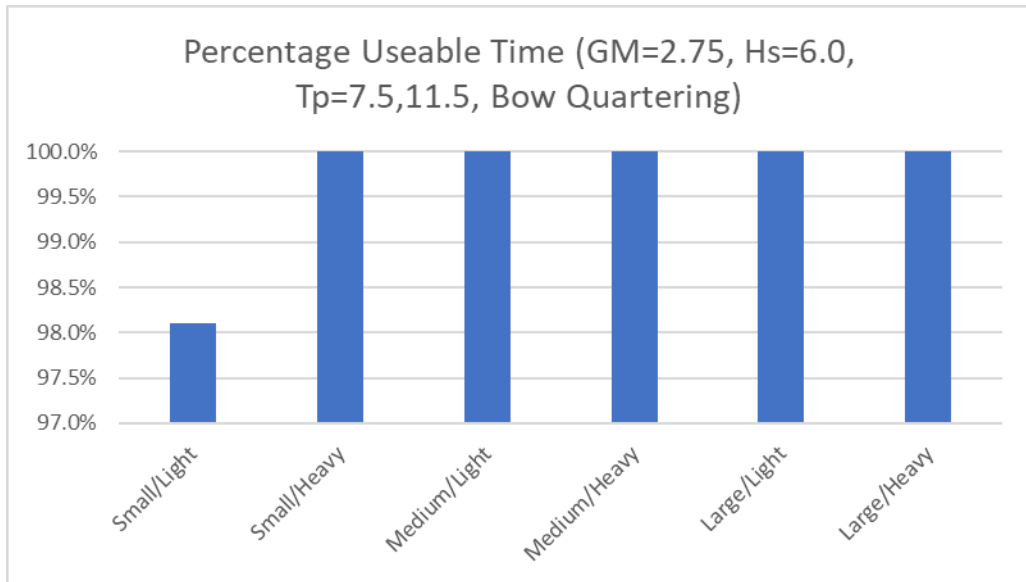| Ship	Number of Limit Exceedances	Mean Safe Time (min)	Total Safe Time (min)	Safe Time Standard Deviation (min)	Number of Useable Times	Mean Useable Time (min)	Total Useable Time (min)	Percentage of Useable Time
Small/Light	190	2.49	475.89	2.71	3	12.00	35.99	7.5%
Small/Heavy	118	4.01	477.56	3.90	10	12.63	126.30	26.3%
Medium/Light	134	3.53	477.01	4.40	11	13.95	153.44	32.0%
Medium/Heavy	79	5.98	478.44	6.28	17	15.53	264.03	55.0%
Large/Light	96	4.93	477.97	4.93	18	12.80	230.36	48.0%
Large/Heavy	43	10.89	479.16	11.49	18	21.54	387.71	80.8%
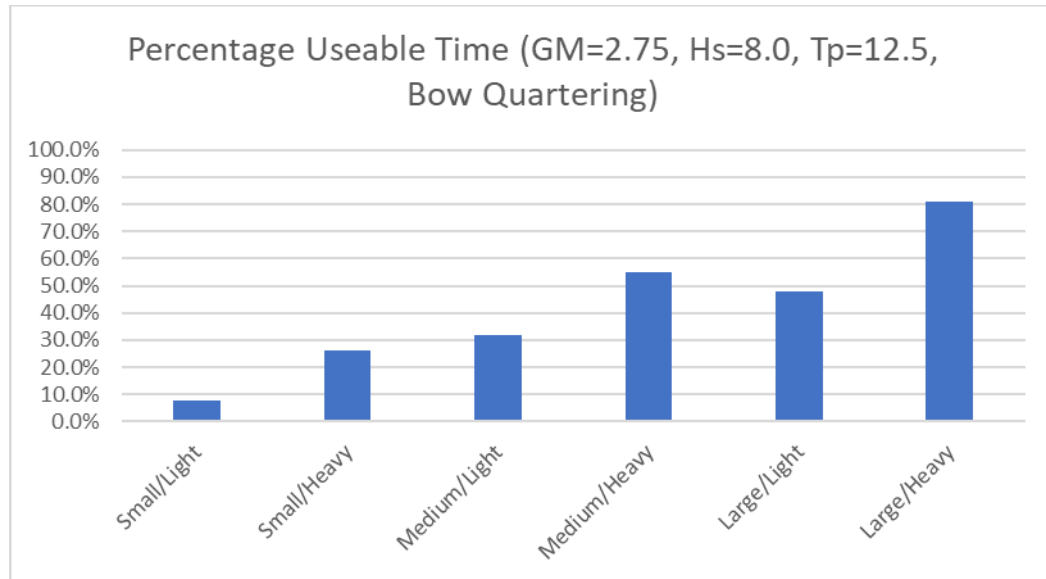
Figure 3-110: Percentage Useable Time, GM=2.75 m, Hs=8.0 m, Tp=12.5 s, Bow Quartering

Distributions of both the "safe time" and "useable time" for the results shown in Table 3-34 are presented graphically through box and whisker plots in Figure 3-111 and Figure 3-112, respectively.
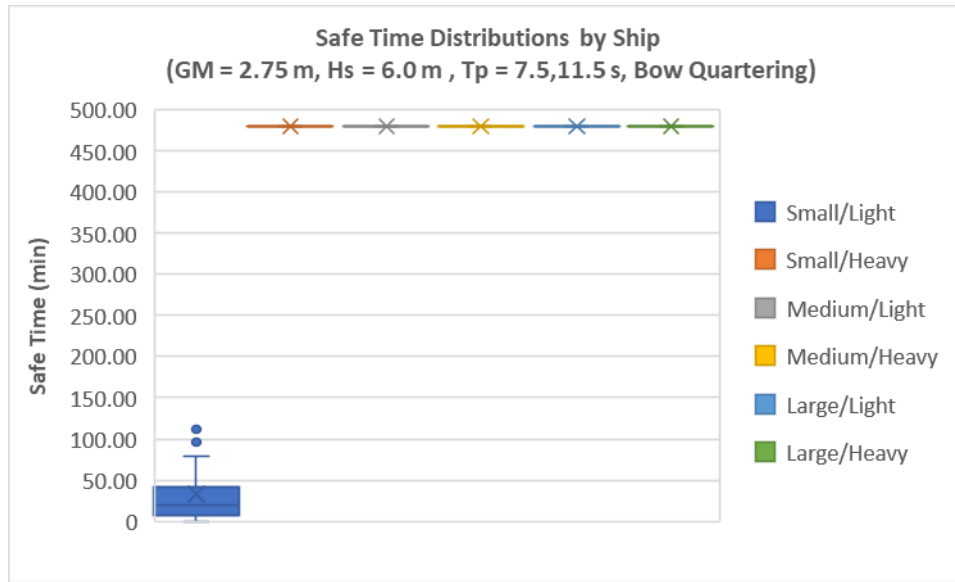
120
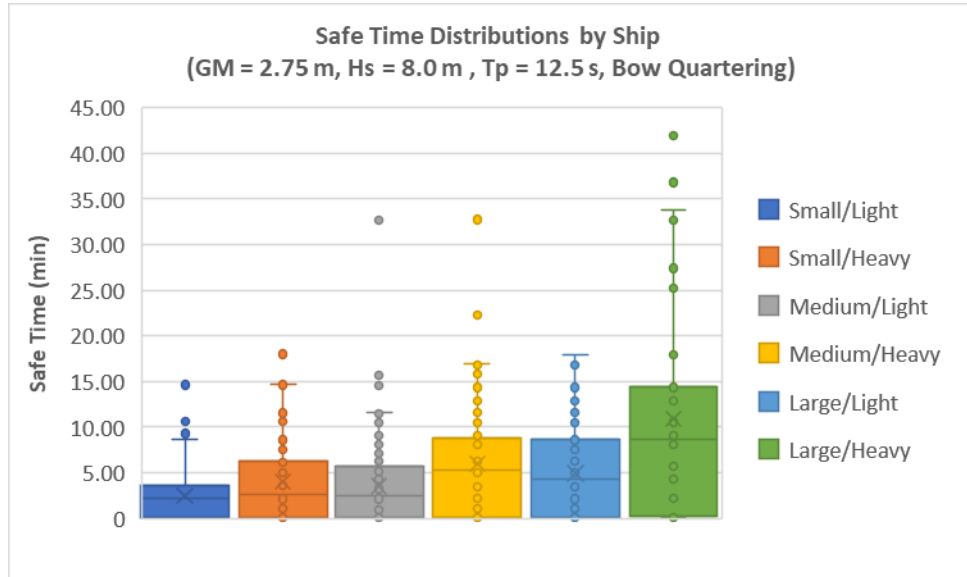
Figure 3-111: Safe Time Distributions, GM=2.75 m, Hs=8.0 m, Tp=12.5 s, Bow
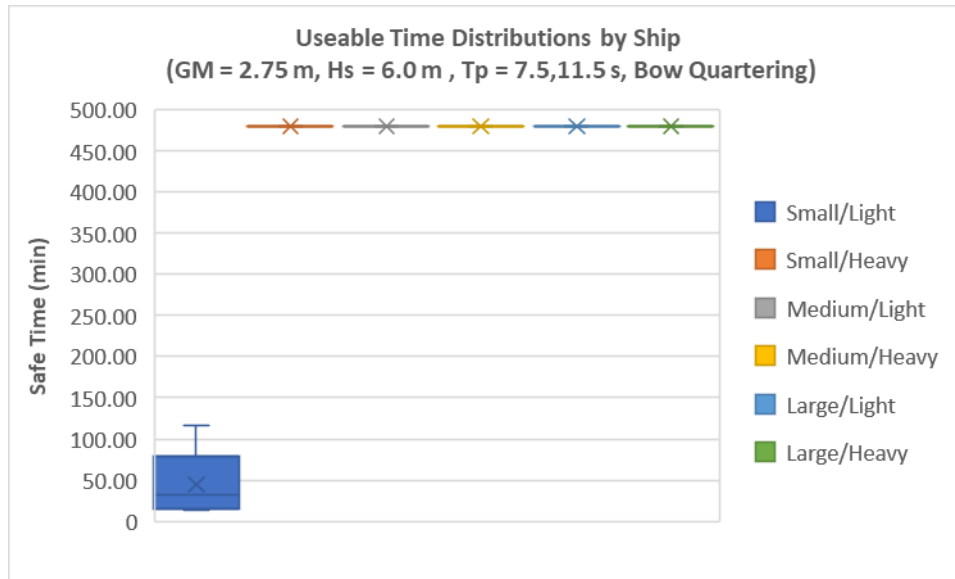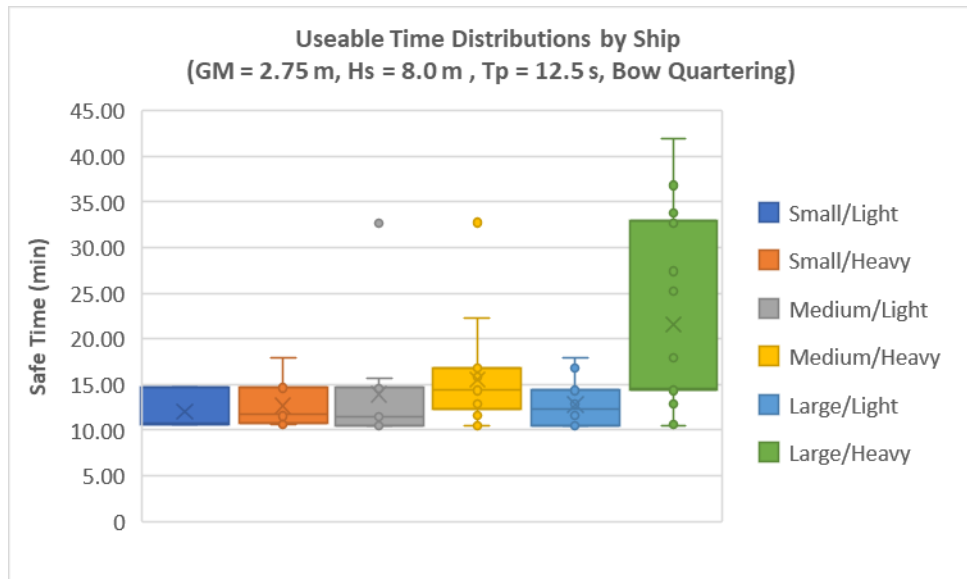
Quartering

Figure 3-112: Useable Time Distributions, GM=2.75 m, Hs=8.0 m, Tp=12.5 s, Bow

Quartering

The results presented in Section 3.3.2 illustrate the point that even in extreme weather conditions, there is a significant amount of time where the OSV motions are benign. As discussed in Section 2.2, the concept of "useable time" is defined as a continuous time period of at least 10 minutes where the deck velocities do not exceed the relative velocity limits for the FROG-6 capsule. Through comparison of the "safe time" and "useable time" distributions above, it is evident that not all of the safe time is useable, in fact, there is generally a very large difference between the two measures. Especially in higher sea-states, there are many deck velocity limit exceedances, but they are brief events. This results in a large percentage of "safe time" in almost all simulations, but with a much smaller fraction of useable time. As such, it is important to filter out the short duration safe times and focus on the useable time plots. In general the box plot of the distribution of useable time becomes taller with an increase in vessel size, which represents longer windows of useable time. Up to an H_s of 5 m in beam seas, every simulation that was analyzed had at least one window of useable time. For bow quartering and head seas, this is true up to an H_s of 8.0 m.

Another evident trend is in-line with the conclusions made based on the operability contours: switching to a larger OSV generally results in more useable time for a given seastate and heading. For a set block coefficient, switching to a larger OSV always results in an increase in the total useable time based on the simulation results. There are cases where the OSV with the larger block coefficient sees a lower total useable time than the corresponding "light" OSV of equivalent length. For example, as shown in Table 3-10,

for GM=2.0 m, H_s=5.0 m, T_p=7.5 s, Beam Seas, the small/light OSV seas a percentage useable time of 24.7%, compared to 18.9% for the small/heavy OSV. This result is only shown in the beam seas cases, and in general the trend of switching to a larger OSV does result in more useable time. Since the beam seas motions are dominated by roll, this points to a need for further investigation of the OSV roll response, particularly the inclusion of viscous roll damping.

3.4   Wind Speed Statistics

The maximum recommended wind speed for the FROG-6 capsule is 40 kt *(20.58 m/s)* ([3], Table 2). To investigate the wind speed limits relative to the wave height limits, a study was completed on the environmental data presented in [5]. Within this historical data, there are 31471 data points with H_s between 5 m and 6 m. Since the maximum H_s considered in the operability contour analysis is 6 m, a comparison between significant wave height and corresponding wind speed for this range is presented in Table 3-35 below. The complete set of wind speed data is not included due to the shear amount of data used; it is available upon request.

Table 3-35: Wind Speed Summary for Hs = 5 m - 6 m

Hs (m)	Number of Data Points	Average Wind Speed (m/s)	# < 20.58	# > 20.58	% Within Limit	% Outside Limit
5 - 6	31471	14.58	31184	287	99.09%	0.91%

As shown above, when the significant wave height is between 5 and 6 m, the FROG-6 wind speed limit is exceeded less than 1% of the time. This validates the assumption that

the wind speed limit can be treated independent of the wave height up to a maximum H_s of 6 m, as the wind speed limit will hardly ever be exceeded at this wave heights.

A similar comparison is presented in Table 3-36 below for H_s in the range of 8.0 – 8.5 m, corresponding with the maximum analyzed seastates in presented in Section 3.3.2 above.

Table 3-36: Wind Speed Summary for Hs = 8.0 m - 8.5 m

Hs (m)	Number of Data Points	Average Wind Speed (m/s)	# < 20.58	# > 20.58	% Within Limit	% Outside Limit
8.0 - 8.5	2029	18.75	1592	437	78.46%	21.54%

For H_s in the range of 8.0 – 8.5 m, the FROG-6 wind speed limit is exceeded approximately 21.5% of the time. This means that at these wave heights, the wind and wave forcing should not realistically be considered independent. Further work must be completed to fully understand the relationship between the wind speed and wave height limitations for crew transfer using personnel capsules such as the FROG-6. Similar to the OSV motion response due to waves, it is likely that there is significant safe time in between wind speed limit exceedances *(gusts),* especially at the lower seastates. Unfortunately, there is no reason to assume the wind speed limit exceedances are in phase with the OSV motion limit exceedances. It is also worth noting that wind forcing is not applied in the ShipMo3D analysis, and may also exacerbate the OSV motions, and therefore increase deck velocities. This is especially true for OSV roll motions, due to the large projected area of the superstructure above the OSV centre of motion.

4.0   Conclusion and Recommendations

This thesis presents a justification for a re-working of the current limits for crew and cargo transfer in the offshore oil and gas industry. For a given offshore platform, current limits are based solely on wave height, when in reality OSV size, metacentric height, heading, and predominant wave period are all factors that should be considered. The results and discussion within suggest that improved operations in rough conditions can be achieved by a combination of specific analysis for vessel in expected sea conditions, real time motion monitoring, motion compensated cranes and real time wave forecasting can increase limits of operation for personnel transfer.

This work has shown that the difference in operational percentage between two different ships / loading conditions can be as high as 54.3% in the winter season. The analysis results show a clear benefit in terms of operable time when switching to a larger OSV. This study defined a quantification of the effect of OSV metacentric height (GM) on the deck velocities and therefore operable time for crew transfer. For example, switching from a 2.0 m GM to a 2.75 m GM can mean a decrease in operational fraction of approximately 4% (Table 3-6), or the difference between 17 and 7 safe transfer windows in a given 8 hour period (Table 3-9 vs. Table 3-23). It is understood that the parameters identified above have their drawbacks – larger OSVs will burn more fuel and therefore be less economically and environmentally efficient. While a lower GM results in less extreme motions as the ship is less 'stiff', it also reduces the ability of the OSV to right itself in extreme seas, resulting in a reduction in safety.

This thesis also investigates the concept of 'safe time' for crew and cargo transfer in a harsh offshore environment. While a given seastate/OSV/heading combination may periodically cause extreme motions that do not allow for safe crew transfer operations, these limit exceedances are generally extremely brief, and there is a lot of useable time for transfer operations, even in very rough conditions. Using wave monitoring technologies and real-time OSV motion prediction systems, crew and cargo transfer operations can be safely carried out in conditions that previously would not have been accepted. This increase in operational efficiency is absolutely essential in the current high-efficiency mindset associated with the energy transition. As OSVs are continuously heading to and from offshore installations for various tasks, it is possible that a significant cost/carbon footprint reduction is achieved through marine crew transfer compared to dedicated trips in a helicopter. A complete cost-benefit analysis of the various transfer methods is needed to determine the actual savings, which could be investigated as a future work.

A statistical analysis is also completed to determine the effects of wind speed on crew transfer operations using the FROG-6 capsule. It is determined that for a given seastate (up to 6 m H_s), the wave-induced OSV motions cause limit exceedances before the wind speed limit is met, over 99% of the time. Based on this, the wind speed and wave loading are considered independent for this study. Note that this does not directly consider the OSV motions caused due to wind forcing.

Since this paper is based on analysis using a potential flow panel code seakeeping simulation, viscosity effects have not been included. Also, effects from dynamic positioning systems, multidirectional wave spectra, and onboard machinery have not been directly considered. These facts, along with the assumptions made and the inherent uncertainties associated with probabilistic analysis highlights the need for model tests, full scale trials and/or Computational Fluid Dynamics (CFD) modeling to further verify and refine these results.

It is noted that the concept of an 8 hour seastate that remains constant is not particularly realistic. In reality, the seastate will generally be growing or declining over this timeframe. The 8 hour simulations are considered to be mathematical constructs generated to determine statistics on a set of individual "snapshots" of a constant seastate. When combined with real time vessel motion prediction systems, the near-term peaks and lulls in vessel response are more relevant for attempting a crew transfer operation than the longer-term behaviour of the seastate. That being said, further analysis on the stationarity of the seastate would certainly have an effect on the percentages of safe time that are available within a given 8 hour window.

Generally, operators are risk-averse and would prefer to conduct crew transfers in benign conditions. But this is not always an option. One barrier to acceptance is that in a seastate with significant wave height of 6 m, we can expect maximum waves approximately double that size, i.e. 12 m high. Since this is a relatively extreme seastate, it is perhaps not realistic to expect operators to conduct routine operations in these conditions. However,

the principle of "useable time" shows that in an emergency situation, there are plenty of safe transfer windows, even in very extreme seas.

Historically, standard cranes have been typically used for crew and cargo transfers offshore. There are many emerging and improving technologies in the area of motion compensated cranes and other such systems, which if applied appropriately could theoretically raise wave height limits much higher. If combined with seakeeping analyses, a mathematical model of smart-crane technology would help to assess the feasibility of such approaches.

Cargo and crew transfer in rough environments is a continuously evolving practice. With the looming threat of climate change, and in the context of energy security, the offshore energy industry needs to be as efficient as possible. As the industry progresses into rougher and deeper waters with increasingly complicated technology, the need for more detailed operational limits becomes apparent. The work presented within this thesis is a launching pad for the definition of more specific operational limits for marine crew transfer using a rigid capsule system. Further work is required to rigidly define such limits, but the concepts of ship-specific limits and useable time within extreme seastates will be extremely valuable in the efficiency-driven operations in the coming years.

Reference List

[1] Molyneux, D., Boyd, N., 2016, *Scheduling of Offshore Support Vessels on the Grand Banks,* 35th International Conference on Ocean, Offshore and Arctic Engineering (OMAE2016), Busan, Korea, June 19 – 24, 2016, OMAE2016-54544

[2] Maersk Supply Service, 2013, *Fleet List – Offshore Support Vessels.*

[3] Reflex Marine, 2014, *FROG-6 User Manual – Rev 05,* November 24, 2014

[4] American Petroleum Institute, 2012, *Offshore Pedestal-mounted Cranes ,* API Specification 2C – Seventh Edition, March 2012

[5] C-CORE, Nalcor Energy Oil and Gas, 2015, *MetOcean Climate Study Offshore Newfoundland & Labrador – Cell Report – Cell # 33,* May 2015

[6] Boyd, N., Molyneux, D., 2016, *Analysis of Variance to Determine the Effect of Hull Form Parameters on Resistance and Seakeeping Performance for PSV Hulls,* 35th International Conference on Ocean, Offshore and Arctic Engineering (OMAE2016), Busan, Korea, June 19 – 24, 2016, OMAE2016-54542

[7] DNVGL, June 2014, *Risks of Marine Transfer of Personnel Offshore*

[8] Strong, P. - Reflex Marine Ltd., 2007, *Reducing Incidents in Marine Personnel Transfer,* SPE E&P Environmental and Safety Conference 2007, SPE 106794

[9] Brittan, D. – Reflex Marine, Douglas, S. – Seacor Marine LLC, 2009, *Offshore Crew Supply – Modern Marine Options Challenge Helicopters*, 2009 SPE Offshore Europe Oil & Gas Conference, SPE 123889

[10] Naaijen, P., Oosten, K., Roozen, K., Veer R., 2018, *Validation of a Deterministic Wave and Ship Motion Prediction System,* 37th International Conference on Ocean, Offshore and Arctic Engineering (OMAE2018), Madrid, Spain, June 17 – 22, 2018, OMAE2018-78037

[11] Anderson, M., Molyneux, D., 2018, *Assessment of Current Offshore Supply Vessel Capabilities for Crew Transfer Operations in the Flemish Pass,* 37th International Conference on Ocean, Offshore and Arctic Engineering (OMAE2018), Madrid, Spain, June 17 – 22, 2018, OMAE2018-78014

[12] ITTC, 2021, *Recommended Procedures and Guidelines – Seakeeping Experiments, Revision 7*

[13] Gustch, M., Sprenger, F. & Steen, S., 2017, *Design Parameters for Increased Operability of Offshore Crane Vessels*, 36th International Conference on Ocean, Offshore and Arctic Engineering (OMAE2017), Trondheim, Norway, June 25 – 30, 2017, OMAE2017-62307

[14] IMCA, June 2014, *Guidance on the Transfer of Personnel to and from Offshore Vessels and Structures,* IMCA SEL 025 Rev. 1, IMCA M 202 Rev. 1

[15] Tsujimoto, M. & Orihara, H., 2018, *Performance Prediction of Full-Scale Ship and Analysis by Means of on-board Monitoring (Part 1 Ship Performance Prediction in Actual Seas),,* Journal of Marine Science and Technology, January 2018

[16] Transport Canada, *CADORS Report 2009A0212 – Cougar Helicopters Inc. (4791)*. Retrieved 12

May 2024 (https://wwwapps.tc.gc.ca/Saf-Sec-Sur/2/cadors-

screaq/rd.aspx?cno%3d2009A0212%26dtef%3d%26dtet%3d%26otp%3d-

1%26ftop%3d%253e%253d%26ftno%3d0%26ijop%3d%253e%253d%26ijno%3d0%26olc%3d%

26prv%3d-1%26rgn%3d-1%26tsbno%3d%26tsbi%3d-

1%26arno%3d%26ocatno%3d%26ocatop%3d1%26oevtno%3d%26oevtop%3d1%26evtacoc%3d3

%26fltno%3d%26fltr%3d-1%26cars%3d-1%26acat%3d-1%26nar%3d%26aiddl%3d-

1%26aidxt%3d%26optdl%3d-1%26optxt%3d%26mkdl%3d-1%26mkxt%3d%26mdldl%3d-

1%26mdlxt%3d%26rt%3dQR%26hypl%3dy%26cnum%3d2009A0212)

[17] Ljunggren, D. - Reuters, 13 March 2009, *Update 2-No more survivors in Canada chopper crash, 17

dead*.

[18] Offshore Engineer, 3 February 2023, *Uptime's Gangway's for Pelagic Wind Services CSOVs*.

Retrieved 12 May 2024 (https://www.oedigital.com/news/502644-uptime-s-gangway-s-for-

pelagic-wind-services-csovs)

[19] Ships and Oil, 2015, *A Swing Rope Accident.* Retrieved 12 May 2024

(https://www.shipsandoil.co.uk/a-swing-rope-accident)

[20] Reflex Marine, May 2016, *Offshore Personnel Transfer by Crane – Best Practice Guidelines for

Routine and Emergency Operations*, Marine Transfer Forum, May 2016

Appendix A – Matlab Scripts

Script for Operability Contours "Transformation.m"

```matlab
% This script calculates deck velocities in the 3 principle directions
% (in translating ship axes) for a given point, using input of the 6 DOF
% motion about the vessel's CoG, and deck positions relative to the CoG.
% Author: Mitchell Anderson - 201127370

% Initialize Variables
Point = zeros(8,3);

% User Input - For each ship (SmallLight = 1, LargeHeavy = 6)
ship = 6;
% Adjusts Zmax
GM = 3.5;

if ship == 1
    X1 = -34.21;
    X2 = -8.66;
    X4 = 16.90;
    Yaft = 7.82;
    Ymax = 8.50;
    Zmax = 1.81;
elseif ship == 2
    X1 = -33.13;
    X2 = -7.13;
    X4 = 18.87;
    Yaft = 7.82;
    Ymax = 8.50;
    Zmax = 2.11;
elseif ship == 3
    X1 = -39.10;
    X2 = -9.89;
    X4 = 19.31;
    Yaft = 8.96;
    Ymax = 9.75;
    Zmax = 1.74;
elseif ship == 4
    X1 = -37.86;
    X2 = -8.15;
    X4 = 21.57;
    Yaft = 8.96;
    Ymax = 9.75;
    Zmax = 2.12;
elseif ship == 5
    X1 = -43.98;
    X2 = -11.13;
    X4 = 21.72;
    Yaft = 10.11;
```

```
        Ymax = 11.00;
        Zmax = 1.68;
elseif ship == 6
        X1 = -42.60;
        X2 = -9.16;
        X4 = 24.27;
        Yaft = 10.11;
        Ymax = 11.00;
        Zmax = 2.03;
end

Zmax = Zmax + (GM - 2.0);

% Deck Positions
Point(1,:) = [X1 Yaft Zmax];
Point(2,:) = [X1 0 Zmax];
Point(3,:) = [X2 Ymax Zmax];
Point(4,:) = [X2 0 Zmax];
Point(5,:) = [0 Ymax Zmax];
Point(6,:) = [0 0 Zmax];
Point(7,:) = [X4 Ymax Zmax];
Point(8,:) = [X4 0 Zmax];

for j = 1:8
    Point_Velocity = zeros(12001,3);
    Lat_Magnitude = zeros(12001,1);
    Velocity_Magnitude = zeros(12001,1);

    for i = 1:12001

    % Get radii for rotational motions
    R_Roll = sqrt((Point(j,2).^2) + (Point(j,3).^2));
    R_Pitch = sqrt((Point(j,1).^2) + (Point(j,3).^2));
    R_Yaw = sqrt((Point(j,1).^2) + (Point(j,2).^2));


    % Convert Degrees to Radians
    T_Rollvel = degtorad(Rollvel(i));
    T_Pitchvel = degtorad(Pitchvel(i));
    T_Headingvel = degtorad(Headingvel(i));
    T_Roll = degtorad(Roll(i));
    T_Pitch = degtorad(Pitch(i));
    T_Heading = degtorad(Heading(i));

    % Rotation Matrices
    Rx_phi = [1 0 0; 0 cos(-T_Roll) -sin(-T_Roll); 0 sin(-T_Roll) cos(-T_Roll)];

    Ry_theta = [cos(T_Pitch) 0 sin(T_Pitch); 0 1 0; -sin(T_Pitch) 0 cos(T_Pitch)];

    R_Total = Ry_theta * Rx_phi;
```

```matlab
% Coordinates in Global Frame
Xn = R_Total * transpose(Point(j,:));

% Angles of Deck Position Vector with Respect to Calm Water Surface
if Xn(1) == 0.0 && Xn(3) > 0.0
    Phi = pi / 2;
elseif Xn(1) == 0.0 && Xn(3) < 0.0
    Phi = 3 .* pi / 2;
elseif Xn(1) > 0.0 && Xn(3) == 0.0
    Phi = 0.0;
elseif Xn(1) > 0.0 && Xn(3) > 0.0
    Phi = atan(Xn(3)/Xn(1));
elseif Xn(1) > 0.0 && Xn(3) < 0.0
    Phi = -atan(-Xn(3)/Xn(1));
elseif Xn(1) < 0.0 && Xn(3) == 0.0
    Phi = pi;
elseif Xn(1) < 0.0 && Xn(3) > 0.0
    Phi = pi - atan(Xn(3)/-Xn(1));
elseif Xn(1) < 0.0 && Xn(3) < 0.0
    Phi = pi + atan(-Xn(3)/-Xn(1));
elseif Xn(1) == 0.0 && Xn(3) == 0.0
    Phi = 0.0;
end

if Xn(2) == 0.0 && Xn(3) > 0.0
    Theta = pi / 2;
elseif Xn(2) == 0.0 && Xn(3) < 0.0
    Theta = 3 .* pi / 2;
elseif Xn(2) > 0.0 && Xn(3) == 0.0
    Theta = 0.0;
elseif Xn(2) > 0.0 && Xn(3) > 0.0
    Theta = atan(Xn(3)/Xn(2));
elseif Xn(2) > 0.0 && Xn(3) < 0.0
    Theta = -atan(-Xn(3)/Xn(2));
elseif Xn(2) < 0.0 && Xn(3) == 0.0
    Theta = pi;
elseif Xn(2) < 0.0 && Xn(3) > 0.0
    Theta = pi - atan(Xn(3)/-Xn(2));
elseif Xn(2) < 0.0 && Xn(3) < 0.0
    Theta = pi + atan(-Xn(3)/-Xn(2));
elseif Xn(2) == 0.0 && Xn(3) == 0.0
    Theta = 0.0;
end

if Xn(1) == 0.0 && Xn(2) == 0.0
    Psi = 0.0;
elseif Xn(1) == 0.0 && Xn(2) > 0.0
    Psi = pi / 2;
elseif Xn(1) == 0.0 && Xn(2) < 0.0
    Psi = 3 .* pi / 2;
elseif Xn(1) > 0.0 && Xn(2) == 0.0
    Psi = 0.0;
elseif Xn(1) > 0.0 && Xn(2) > 0.0
```

```matlab
        Psi = atan(Xn(2)/Xn(1));
    elseif Xn(1) > 0.0 && Xn(2) < 0.0
        Psi = (2 .* pi) - atan(-Xn(2)/Xn(1));
    elseif Xn(1) < 0.0 && Xn(2) == 0.0
        Psi = pi;
    elseif Xn(1) < 0.0 && Xn(2) > 0.0
        Psi = pi - atan(Xn(2)/-Xn(1));
    elseif Xn(1) < 0.0 && Xn(2) < 0.0
        Psi = pi + atan(-Xn(2)/-Xn(1));
    end

    % Get translational components of surge and sway
    Surge = (xfvel(i) .* cos(T_Heading)) + (yfvel(i) .* sin(T_Heading));
    Sway = (-xfvel(i) .* sin(T_Heading)) + (yfvel(i) .* cos(T_Heading));

    Point_Velocity(i,1) = Surge + (T_Pitchvel .* R_Pitch .* sin(Phi)) - (T_Headingvel .* R_Yaw .* sin(Psi));
    Point_Velocity(i,2) = Sway + (T_Rollvel .* R_Roll .* sin(Theta)) + (T_Headingvel .* R_Yaw .* cos(Psi));
    Point_Velocity(i,3) = Heavevel(i) - (T_Rollvel .* R_Roll .* cos(Theta)) - (T_Pitchvel .* R_Pitch .* cos(Phi));

    Lat_Magnitude(i) = sqrt((Point_Velocity(i,1).^2) + (Point_Velocity(i,2).^2));
    Velocity_Magnitude(i) = norm(Point_Velocity(i,:));
    end

    if j == 1
        Output11 = zeros(12001,5);
        Output11(:,1) = Point_Velocity(:,1);
        Output11(:,2) = Point_Velocity(:,2);
        Output11(:,3) = Point_Velocity(:,3);
        Output11(:,4) = Lat_Magnitude(:);
        Output11(:,5) = Velocity_Magnitude(:);
    elseif j == 2
        Output12 = zeros(12001,5);
        Output12(:,1) = Point_Velocity(:,1);
        Output12(:,2) = Point_Velocity(:,2);
        Output12(:,3) = Point_Velocity(:,3);
        Output12(:,4) = Lat_Magnitude(:);
        Output12(:,5) = Velocity_Magnitude(:);
    elseif j == 3
        Output21 = zeros(12001,5);
        Output21(:,1) = Point_Velocity(:,1);
        Output21(:,2) = Point_Velocity(:,2);
        Output21(:,3) = Point_Velocity(:,3);
        Output21(:,4) = Lat_Magnitude(:);
        Output21(:,5) = Velocity_Magnitude(:);
    elseif j == 4
        Output22 = zeros(12001,5);
        Output22(:,1) = Point_Velocity(:,1);
        Output22(:,2) = Point_Velocity(:,2);
        Output22(:,3) = Point_Velocity(:,3);
        Output22(:,4) = Lat_Magnitude(:);
        Output22(:,5) = Velocity_Magnitude(:);
```

```matlab
    elseif j == 5
        Output31 = zeros(12001,5);
        Output31(:,1) = Point_Velocity(:,1);
        Output31(:,2) = Point_Velocity(:,2);
        Output31(:,3) = Point_Velocity(:,3);
        Output31(:,4) = Lat_Magnitude(:);
        Output31(:,5) = Velocity_Magnitude(:);
    elseif j == 6
        Output32 = zeros(12001,5);
        Output32(:,1) = Point_Velocity(:,1);
        Output32(:,2) = Point_Velocity(:,2);
        Output32(:,3) = Point_Velocity(:,3);
        Output32(:,4) = Lat_Magnitude(:);
        Output32(:,5) = Velocity_Magnitude(:);
    elseif j == 7
        Output41 = zeros(12001,5);
        Output41(:,1) = Point_Velocity(:,1);
        Output41(:,2) = Point_Velocity(:,2);
        Output41(:,3) = Point_Velocity(:,3);
        Output41(:,4) = Lat_Magnitude(:);
        Output41(:,5) = Velocity_Magnitude(:);
    elseif j == 8
        Output42 = zeros(12001,5);
        Output42(:,1) = Point_Velocity(:,1);
        Output42(:,2) = Point_Velocity(:,2);
        Output42(:,3) = Point_Velocity(:,3);
        Output42(:,4) = Lat_Magnitude(:);
        Output42(:,5) = Velocity_Magnitude(:);
    end
end
% Condensed Output for Easy Export
Output = zeros(12001,40);
Output(:,1) = Output11(:,1);
Output(:,2) = Output11(:,2);
Output(:,3) = Output11(:,3);
Output(:,4) = Output11(:,4);
Output(:,5) = Output11(:,5);

Output(:,6) = Output12(:,1);
Output(:,7) = Output12(:,2);
Output(:,8) = Output12(:,3);
Output(:,9) = Output12(:,4);
Output(:,10) = Output12(:,5);

Output(:,11) = Output21(:,1);
Output(:,12) = Output21(:,2);
Output(:,13) = Output21(:,3);
Output(:,14) = Output21(:,4);
Output(:,15) = Output21(:,5);

Output(:,16) = Output22(:,1);
Output(:,17) = Output22(:,2);
Output(:,18) = Output22(:,3);
```

```matlab
Output(:,19) = Output22(:,4);
Output(:,20) = Output22(:,5);

Output(:,21) = Output31(:,1);
Output(:,22) = Output31(:,2);
Output(:,23) = Output31(:,3);
Output(:,24) = Output31(:,4);
Output(:,25) = Output31(:,5);

Output(:,26) = Output32(:,1);
Output(:,27) = Output32(:,2);
Output(:,28) = Output32(:,3);
Output(:,29) = Output32(:,4);
Output(:,30) = Output32(:,5);

Output(:,31) = Output41(:,1);
Output(:,32) = Output41(:,2);
Output(:,33) = Output41(:,3);
Output(:,34) = Output41(:,4);
Output(:,35) = Output41(:,5);

Output(:,36) = Output42(:,1);
Output(:,37) = Output42(:,2);
Output(:,38) = Output42(:,3);
Output(:,39) = Output42(:,4);
Output(:,40) = Output42(:,5);
```

Script for Safe Time Analysis "Transformation_LongTime.m"

```matlab
% This script calculates deck velocities in the 3 principle directions
% (in translating ship axes) for a given point, using input of the 6 DOF
% motion about the vessel's CoG, and deck positions relative to the CoG.
% Author: Mitchell Anderson - 201127370

% Initialize Variables
Point = zeros(8,3);

% User Input - For each ship (SmallLight = 1, LargeHeavy = 6)
ship = 6;
% Adjusts Zmax
GM = 2.75;

% Output File

if ship == 1
    X1 = -34.21;
    X2 = -8.66;
    X4 = 16.90;
    Yaft = 7.82;
    Ymax = 8.50;
    Zmax = 1.81;
```

```matlab
elseif ship == 2
    X1 = -33.13;
    X2 = -7.13;
    X4 = 18.87;
    Yaft = 7.82;
    Ymax = 8.50;
    Zmax = 2.11;
elseif ship == 3
    X1 = -39.10;
    X2 = -9.89;
    X4 = 19.31;
    Yaft = 8.96;
    Ymax = 9.75;
    Zmax = 1.74;
elseif ship == 4
    X1 = -37.86;
    X2 = -8.15;
    X4 = 21.57;
    Yaft = 8.96;
    Ymax = 9.75;
    Zmax = 2.12;
elseif ship == 5
    X1 = -43.98;
    X2 = -11.13;
    X4 = 21.72;
    Yaft = 10.11;
    Ymax = 11.00;
    Zmax = 1.68;
elseif ship == 6
    X1 = -42.60;
    X2 = -9.16;
    X4 = 24.27;
    Yaft = 10.11;
    Ymax = 11.00;
    Zmax = 2.03;
end

Zmax = Zmax + (GM - 2.0);

% Deck Positions
Point(1,:) = [X1 Yaft Zmax];
Point(2,:) = [X1 0 Zmax];
Point(3,:) = [X2 Ymax Zmax];
Point(4,:) = [X2 0 Zmax];
Point(5,:) = [0 Ymax Zmax];
Point(6,:) = [0 0 Zmax];
Point(7,:) = [X4 Ymax Zmax];
Point(8,:) = [X4 0 Zmax];

for j = 4:6
    Point_Velocity = zeros(288001,3);
    Lat_Magnitude = zeros(288001,1);
    Velocity_Magnitude = zeros(288001,1);
```

```matlab
for i = 1:288001

    % Get radii for rotational motions
    R_Roll = sqrt((Point(j,2).^2) + (Point(j,3).^2));
    R_Pitch = sqrt((Point(j,1).^2) + (Point(j,3).^2));
    R_Yaw = sqrt((Point(j,1).^2) + (Point(j,2).^2));


    % Convert Degrees to Radians
    T_Rollvel = degtorad(Rollvel(i));
    T_Pitchvel = degtorad(Pitchvel(i));
    T_Headingvel = degtorad(Headingvel(i));
    T_Roll = degtorad(Roll(i));
    T_Pitch = degtorad(Pitch(i));
    T_Heading = degtorad(Heading(i));

    % Rotation Matrices
    Rx_phi = [1 0 0; 0 cos(-T_Roll) -sin(-T_Roll); 0 sin(-T_Roll) cos(-T_Roll)];

    Ry_theta = [cos(T_Pitch) 0 sin(T_Pitch); 0 1 0; -sin(T_Pitch) 0 cos(T_Pitch)];

    R_Total = Ry_theta * Rx_phi;

    % Coordinates in Global Frame
    Xn = R_Total * transpose(Point(j,:));

    % Angles of Deck Position Vector with Respect to Calm Water Surface
    if Xn(1) == 0.0 && Xn(3) > 0.0
        Phi = pi / 2;
    elseif Xn(1) == 0.0 && Xn(3) < 0.0
        Phi = 3 .* pi / 2;
    elseif Xn(1) > 0.0 && Xn(3) == 0.0
        Phi = 0.0;
    elseif Xn(1) > 0.0 && Xn(3) > 0.0
        Phi = atan(Xn(3)/Xn(1));
    elseif Xn(1) > 0.0 && Xn(3) < 0.0
        Phi = -atan(-Xn(3)/Xn(1));
    elseif Xn(1) < 0.0 && Xn(3) == 0.0
        Phi = pi;
    elseif Xn(1) < 0.0 && Xn(3) > 0.0
        Phi = pi - atan(Xn(3)/-Xn(1));
    elseif Xn(1) < 0.0 && Xn(3) < 0.0
        Phi = pi + atan(-Xn(3)/-Xn(1));
    elseif Xn(1) == 0.0 && Xn(3) == 0.0
        Phi = 0.0;
    end

    if Xn(2) == 0.0 && Xn(3) > 0.0
        Theta = pi / 2;
    elseif Xn(2) == 0.0 && Xn(3) < 0.0
        Theta = 3 .* pi / 2;
```

```matlab
    elseif Xn(2) > 0.0 && Xn(3) == 0.0
        Theta = 0.0;
    elseif Xn(2) > 0.0 && Xn(3) > 0.0
        Theta = atan(Xn(3)/Xn(2));
    elseif Xn(2) > 0.0 && Xn(3) < 0.0
        Theta = -atan(-Xn(3)/Xn(2));
    elseif Xn(2) < 0.0 && Xn(3) == 0.0
        Theta = pi;
    elseif Xn(2) < 0.0 && Xn(3) > 0.0
        Theta = pi - atan(Xn(3)/-Xn(2));
    elseif Xn(2) < 0.0 && Xn(3) < 0.0
        Theta = pi + atan(-Xn(3)/-Xn(2));
    elseif Xn(2) == 0.0 && Xn(3) == 0.0
        Theta = 0.0;
    end

    if Xn(1) == 0.0 && Xn(2) == 0.0
        Psi = 0.0;
    elseif Xn(1) == 0.0 && Xn(2) > 0.0
        Psi = pi / 2;
    elseif Xn(1) == 0.0 && Xn(2) < 0.0
        Psi = 3 .* pi / 2;
    elseif Xn(1) > 0.0 && Xn(2) == 0.0
        Psi = 0.0;
    elseif Xn(1) > 0.0 && Xn(2) > 0.0
        Psi = atan(Xn(2)/Xn(1));
    elseif Xn(1) > 0.0 && Xn(2) < 0.0
        Psi = (2 .* pi) - atan(-Xn(2)/Xn(1));
    elseif Xn(1) < 0.0 && Xn(2) == 0.0
        Psi = pi;
    elseif Xn(1) < 0.0 && Xn(2) > 0.0
        Psi = pi - atan(Xn(2)/-Xn(1));
    elseif Xn(1) < 0.0 && Xn(2) < 0.0
        Psi = pi + atan(-Xn(2)/-Xn(1));
    end

    % Get translational components of surge and sway
    Surge = (xfvel(i) .* cos(T_Heading)) + (yfvel(i) .* sin(T_Heading));
    Sway = (-xfvel(i) .* sin(T_Heading)) + (yfvel(i) .* cos(T_Heading));

    Point_Velocity(i,1) = Surge + (T_Pitchvel .* R_Pitch .* sin(Phi)) - (T_Headingvel .* R_Yaw .* sin(Psi));
    Point_Velocity(i,2) = Sway + (T_Rollvel .* R_Roll .* sin(Theta)) + (T_Headingvel .* R_Yaw .* cos(Psi));
    Point_Velocity(i,3) = Heavevel(i) - (T_Rollvel .* R_Roll .* cos(Theta)) - (T_Pitchvel .* R_Pitch .* cos(Phi));

    Lat_Magnitude(i) = sqrt((Point_Velocity(i,1).^2) + (Point_Velocity(i,2).^2));
    Velocity_Magnitude(i) = norm(Point_Velocity(i,:));
    end

    if j == 1
        Output11 = zeros(288001,5);
        Output11(:,1) = Point_Velocity(:,1);
```

```matlab
        Output11(:,2) = Point_Velocity(:,2);
        Output11(:,3) = Point_Velocity(:,3);
        Output11(:,4) = Lat_Magnitude(:);
        Output11(:,5) = Velocity_Magnitude(:);
    elseif j == 2
        Output12 = zeros(288001,5);
        Output12(:,1) = Point_Velocity(:,1);
        Output12(:,2) = Point_Velocity(:,2);
        Output12(:,3) = Point_Velocity(:,3);
        Output12(:,4) = Lat_Magnitude(:);
        Output12(:,5) = Velocity_Magnitude(:);
    elseif j == 3
        Output21 = zeros(288001,5);
        Output21(:,1) = Point_Velocity(:,1);
        Output21(:,2) = Point_Velocity(:,2);
        Output21(:,3) = Point_Velocity(:,3);
        Output21(:,4) = Lat_Magnitude(:);
        Output21(:,5) = Velocity_Magnitude(:);
    elseif j == 4
        Output22 = zeros(288001,5);
        Output22(:,1) = Point_Velocity(:,1);
        Output22(:,2) = Point_Velocity(:,2);
        Output22(:,3) = Point_Velocity(:,3);
        Output22(:,4) = Lat_Magnitude(:);
        Output22(:,5) = Velocity_Magnitude(:);
    elseif j == 5
        Output31 = zeros(288001,5);
        Output31(:,1) = Point_Velocity(:,1);
        Output31(:,2) = Point_Velocity(:,2);
        Output31(:,3) = Point_Velocity(:,3);
        Output31(:,4) = Lat_Magnitude(:);
        Output31(:,5) = Velocity_Magnitude(:);
    elseif j == 6
        Output32 = zeros(288001,5);
        Output32(:,1) = Point_Velocity(:,1);
        Output32(:,2) = Point_Velocity(:,2);
        Output32(:,3) = Point_Velocity(:,3);
        Output32(:,4) = Lat_Magnitude(:);
        Output32(:,5) = Velocity_Magnitude(:);
    elseif j == 7
        Output41 = zeros(288001,5);
        Output41(:,1) = Point_Velocity(:,1);
        Output41(:,2) = Point_Velocity(:,2);
        Output41(:,3) = Point_Velocity(:,3);
        Output41(:,4) = Lat_Magnitude(:);
        Output41(:,5) = Velocity_Magnitude(:);
    elseif j == 8
        Output42 = zeros(288001,5);
        Output42(:,1) = Point_Velocity(:,1);
        Output42(:,2) = Point_Velocity(:,2);
        Output42(:,3) = Point_Velocity(:,3);
        Output42(:,4) = Lat_Magnitude(:);
        Output42(:,5) = Velocity_Magnitude(:);
    end
```

```matlab
end

% Crossing Times
Periods_TL = 0;
Starts_TL = zeros(500,1);
Times_TL = zeros(500,1);
Ends_TL = zeros(500,1);
Periods_MS = 0;
Starts_MS = zeros(500,1);
Times_MS = zeros(500,1);
Ends_MS = zeros(500,1);

% Mode  = 1 if exceeding velocity limit, 0 if not.
Mode_TL = 0;
LastMode_TL = 1;
Mode_MS = 0;
LastMode_MS = 1;

for i = 1:288001
    % Target Landing Limits
    if abs(Output22(i,4)) >= 2.0 || abs(Output22(i,3)) >= 4.0;
        Mode_TL = 1;
    else
        Mode_TL = 0;
    end

    if Mode_TL == 0
        if LastMode_TL == 1
            Periods_TL = Periods_TL + 1;
            Starts_TL(Periods_TL) = i/10;
            Times_TL(Periods_TL) = Times_TL(Periods_TL) + 0.1;
        else
            Times_TL(Periods_TL) = Times_TL(Periods_TL) + 0.1;
        end
    end
    LastMode_TL = Mode_TL;

    % Midship Limits
    if abs(Output32(i,4)) >= 2.0 || abs(Output32(i,3)) >= 4.0;
        Mode_MS = 1;
    else
        Mode_MS = 0;
    end

    if Mode_MS == 0
        if LastMode_MS == 1
            Periods_MS = Periods_MS + 1;
            Starts_MS(Periods_MS) = i/10;
            Times_MS(Periods_MS) = Times_MS(Periods_MS) + 0.1;
        else
            Times_MS(Periods_MS) = Times_MS(Periods_MS) + 0.1;
        end
```

```matlab
        end
        LastMode_MS = Mode_MS;

    end

    for j = 1:500
        Ends_TL(j) = Starts_TL(j) + Times_TL(j);
        Ends_MS(j) = Starts_MS(j) + Times_MS(j);

        Times_TL(j) = Times_TL(j) / 60;
        Times_MS(j) = Times_MS(j) / 60;
    end

    Output = zeros(500,6);
    Output(:,1) = Starts_TL(:);
    Output(:,2) = Ends_TL(:);
    Output(:,3) = Times_TL(:);
    Output(:,4) = Starts_MS(:);
    Output(:,5) = Ends_MS(:);
    Output(:,6) = Times_MS(:);
```

Appendix B – Environmental Data

Cell: 337 (48.25°N, 46.5°W)		Significant Wave Height and Period - Joint Probability Distribution for Winter Months																
		Significant Wave Height (m)																
		0.5	1.5	2.5	3.5	4.5	5.5	6.5	7.5	8.5	9.5	10.5	11.5	12.5	13.5	14.5	15.5	16.5
		0-1	1-2	2-3	3-4	4-5	5-6	6-7	7-8	8-9	9-10	10-11	11-12	12-13	13-14	14-15	15-16	16-17
0.5	0-1	0	0	0	0	0	0	0	0	0	0	0	0	0	0	0	0	0
1.5	1-2	0	0	0	0	0	0	0	0	0	0	0	0	0	0	0	0	0
2.5	2-3	0	0	0	0	0	0	0	0	0	0	0	0	0	0	0	0	0
3.5	3-4	0	0	0	0	0	0	0	0	0	0	0	0	0	0	0	0	0
4.5	4-5	0.005	0.0085	0	0	0	0	0	0	0	0	0	0	0	0	0	0	0
5.5	5-6	0	0.01175	0.03125	0.001	0	0	0	0	0	0	0	0	0	0	0	0	0
6.5	6-7	0	0.0185	0.45425	0.12975	0.001	0	0	0	0	0	0	0	0	0	0	0	0
7.5	7-8	0	0.08275	1.146	1.98925	0.286	0.0035	0	0	0	0	0	0	0	0	0	0	0
8.5	8-9	0	0.18275	1.615	3.15875	3.0675	0.242	0.002	0	0	0	0	0	0	0	0	0	0
9.5	9-10	0	0.129	2.51125	3.79725	5.38025	2.67625	0.18325	0.0005	0	0	0	0	0	0	0	0	0
10.5	10-11	0	0.1165	2.48575	5.481	4.69475	5.21725	1.92875	0.14375	0.00675	0	0	0	0	0	0	0	0
11.5	11-12	0	0.02425	1.29725	5.7355	5.09425	3.546	3.59275	1.48975	0.21625	0.0075	0	0	0	0	0	0	0
12.5	12-13	0	0.045	0.844	2.59625	3.03775	1.95	1.62475	1.9135	1.13175	0.529	0.056	0.0005	0	0	0	0	0
13.5	13-14	0	0.0105	0.3005	1.6075	2.3585	1.74375	1.16225	0.725	0.68925	0.877	0.718	0.189	0.009	0	0	0	0
14.5	14-15	0	0.0035	0.06825	0.6625	1.6475	1.40425	0.749	0.396	0.2095	0.23375	0.312	0.384	0.215	0.023	0	0	0
15.5	15-16	0	0	0.001	0.03625	0.10325	0.245	0.177	0.07425	0.0415	0.013	0.019	0.03075	0.107	0.096	0.009	0	0
16.5	16-17	0	0	0.0165	0.04325	0.115	0.08175	0.02025	0.0115	0.0045	0	0.0005	0.00475	0.001	0.03025	0.0235	0.00925	0
17.5	17-18	0	0	0	0.00225	0.02575	0.024	0.00475	0.0025	0	0	0	0	0	0	0.0005	0.00375	0
18.5	18-19	0	0	0	0	0	0	0	0	0	0	0	0	0	0	0	0	0
19.5	19-20	0	0	0	0	0	0	0	0	0	0	0	0	0	0	0	0	0

(Left axis: Wave Period (s))

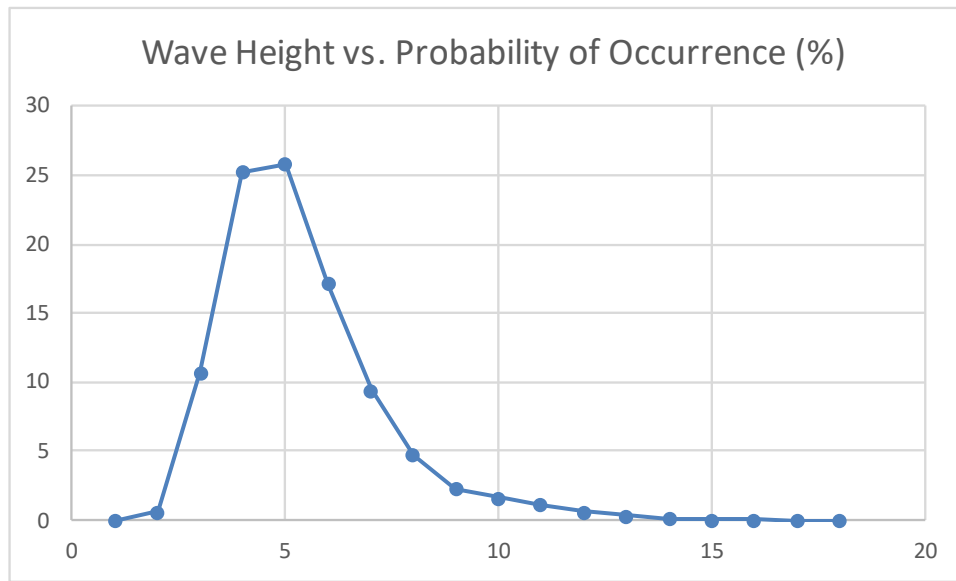**Figure B-1: Joint Probability Distribution for Winter Months**

Figure B-2: Wave Height vs. Probability of Occurrence (Winter Months)

| Cell: 337 (48.25°N, 46.5°W) | Significant Wave Height and Period - Joint Probability Distribution for Summer Months | | | | | | | | | | | | | | | | |
| | Significant Wave Height (m) | | | | | | | | | | | | | | | | |
Wave Period (s)	0-1	1-2	2-3	3-4	4-5	5-6	6-7	7-8	8-9	9-10	10-11	11-12	12-13	13-14	14-15	15-16	16-17
0-1	0	0	0	0	0	0	0	0	0	0	0	0	0	0	0	0	0
1-2	0	0	0	0	0	0	0	0	0	0	0	0	0	0	0	0	0
2-3	0	0	0	0	0	0	0	0	0	0	0	0	0	0	0	0	0
3-4	0	0	0	0	0	0	0	0	0	0	0	0	0	0	0	0	0
4-5	0	0.03125	0.0015	0	0	0	0	0	0	0	0	0	0	0	0	0	0
5-6	0	1.0155	0.436	0	0	0	0	0	0	0	0	0	0	0	0	0	0
6-7	0	2.69325	5.26325	0.077	0	0	0	0	0	0	0	0	0	0	0	0	0
7-8	0	9.64375	12.27675	3.4155	0.01625	0	0	0	0	0	0	0	0	0	0	0	0
8-9	0	7.06275	10.05125	5.6885	0.77025	0.00325	0	0	0	0	0	0	0	0	0	0	0
9-10	0	3.47925	12.21225	3.69525	2.0235	0.24325	0.002	0	0	0	0	0	0	0	0	0	0
10-11	0	1.426	5.282	2.224	0.9585	0.7245	0.108	0.00375	0	0	0	0	0	0	0	0	0
11-12	0	0.2125	1.2275	1.18125	0.49125	0.3325	0.2595	0.055	0.00675	0	0	0	0	0	0	0	0
12-13	0	0.1905	1.053	0.703	0.21375	0.12225	0.08475	0.06775	0.02525	0.005	0.0005	0	0	0	0	0	0
13-14	0	0.553	0.971	0.264	0.107	0.026	0.0225	0.01725	0.01025	0.014	0.00975	0.0005	0	0	0	0	0
14-15	0	0.0975	0.22	0.09075	0.05	0.02525	0.0195	0.006	0.001	0.001	0.003	0.00675	0.00225	0	0	0	0
15-16	0	0.021	0.077	0.013	0.0045	0.00325	0	0	0	0	0	0	0	0	0	0	0
16-17	0	0.06125	0.075	0.0255	0	0	0	0	0	0	0	0	0	0	0	0	0
17-18	0	0.0425	0.04875	0.0345	0.0005	0	0	0	0	0	0	0	0	0	0	0	0
18-19	0	0	0.00275	0.0005	0	0	0	0	0	0	0	0	0	0	0	0	0
19-20	0	0	0	0	0	0	0	0	0	0	0	0	0	0	0	0	0
20-21	0	0	0	0	0	0	0	0	0	0	0	0	0	0	0	0	0
21-22	0	0.00525	0.00225	0	0	0	0	0	0	0	0	0	0	0	0	0	0

Figure B-3: Joint Probability Distribution for Summer Months